Identification of EMCV Leader protein's cellular partners for inhibition of nucleocytoplasmic trafficking

by

Jessica J. Ciomperlik

A dissertation submitted in partial fulfillment of the requirements for the degree of

Doctor of Philosophy

(Cellular and Molecular Biology)

at the

University of Wisconsin – Madison

2015

Date of final oral examination: 8/10/2015

The dissertation is approved by the following members of the Final Oral Committee:
      Ann C. Palmenberg, Professor, Molecular Virology, Biochemistry
      Paul D. Friesen, Professor, Molecular Virology and Biochemistry
      Paul G. Ahlquist, Professor, Molecular Virology and Oncology
      Nathan M. Sherer, Virology and Oncology Assistant Professor, Molecular
      Kristen A. Bernard, Associate Professor, Virology and Pathobiological Sciences

Acknowledgements

Dr. Ann Palmenberg, for her tremendous support, encouragement, patience, and being an excellent role model in science and life

Dr. Nate Sherer, for his advice, mentoring, help with various reagents and technologies, and galvanizing enthusiasm

Drs. Paul Ahlquist, Kristen Bernard, Paul Bertics, James Dahlberg and Paul Friesen for their many suggestions and guidance through my graduate career

Marchel Hill, for her support, advice, and being a general blessing

Drs. Kelly Watters and Holly Basta (and other Palmenberg lab members) for being noteworthy co-workers, and sharing their time, good humor and reagents

Members of the Sherer, Friesen and Ahlquist labs, for being great colleagues

My friends, for joy, calories, adventures on foot and by bike, etc., and sharing their lives with me

My parents and siblings, and rest of my family, for continuous love, encouragement, laughter and always being there (in person, by phone, or online)

And Divine support - thank You.

Abstract

Identification of EMCV Leader protein's cellular partners for inhibition of nucleocytoplasmic trafficking

Jessica J. Ciomperlik

Under the supervision of Professor Ann C. Palmenberg

At the University of Wisconsin - Madison

Nucleocytoplasmic trafficking is a frequent target of viral manipulation, particularly for RNA viruses. Inhibition of this cellular process constrains cellular defenses and protein production, and can release necessary replication-enhancing factors into the cytoplasm for viral use. Enteroviruses use viral proteases to excise nuclear pore proteins (Nups) and thus prevent macromolecules from translocating through the pores, but Cardioviruses direct cellular kinases to phosphorylate these Nups instead. The only necessary Cardiovirus protein required for this trafficking inhibition is the Leader (L) protein. Experiments presented herein determined which multiple trafficking pathways are inhibited, established cellular export proteins CRM1 and CAS as L-binding partners, and identified specific kinases used by L.

While it was known that Nups 214, 153, and 62 become phosphorylated in Cardiovirus infections to prevent nucleocytoplasmic translocation, we demonstrate that Nup98 is an additional phosphorylation substrate for L-directed kinases, though Nup50 is not. Recombinant Nups and native cytosolic Nups (not inserted into nuclear pores) are not phosphorylatable, indicating a critical Nup localization aspect. The use of mCherry-tagged proteins containing nuclear localization signals (NLS) and an nuclear export signal (NES) indicated that all cardiovirus Ls are able to shut down 4 different nuclear import and export pathways, and in the case of Encephalomyocarditis virus (EMCV) infection, this occurs as quickly as 3 hours post-infection.

Additional L binding partners from HeLa cytosol were identified by Orbi-trap mass spectrometry. Although L binds RanGTPase (Ran) in stoichiometric amounts, not enough of

this protein is bound to L at the time of trafficking shut down to be the sole binding partner for such an efficient inhibition, nor would Ran necessarily hold L at the pores. Cellular exportins CRM1 (exportin 1) and CAS (exportin 2) were demonstrated to be cellular binding partners of L. CRM1:L binding was independent of Ran and withstood up to 500 mM NaCl, indicating a strong interaction. Phosphorylation on Thr47 of L enhanced CRM1:L binding, and CRM1:L:Ran formed a high molecular weight complex in eluates from gel filtration chromatography, suggesting a trimeric complex. shRNA-mediated knockdown of CRM1 decreased L-directed Nup phosphorylation to 11%, and EMCV replication to 30% of that seen of CRM1-expressing cells. CRM1 cargo-binding inhibitor Leptopmycin B was not sufficient to prevent association of CRM1:L and suggests that L binds to a separate region of CRM1. Moreover, inclusion of LMB in infections did not have any impact on Nup phosphorylation in an EMCV infection, suggesting that L's activities might preclude the action of this drug inhibitor. Prior studies with chemical inhibitors by F. Porter in the Palmenberg lab narrowed the candidate pool of potential L-directed kinases to those in the MAPK family. In HeLa cells, siRNAs were used to knock down specific kinases prior to infection with EMCV. L-facilitated Nup phosphorylation was decreased with the knockdown of ERK1/2, p38α/β or RSK2/3. A cell-free system comprised of recombinant kinases, GST-L and fractionated nuclei was used to further demonstrate that these specific kinases were able to phosphorylate Nups in the presence of L, though not with either L or the recombinant kinases alone. Moreover, GST-tagged cardiovirus Ls were able bind endogenous kinases present in HeLa cytosol, which confirmed an L:kinase association.

Major findings of this thesis include determination of specific nucleocytoplasmic trafficking pathways inhibited during a cardiovirus infection, the association of L with exportins CRM1 and CAS, and identification of ERK2 and RSK2/3 as kinases used by L to phosphorylate Nups. The model suggested by this data and other recent studies follows that L binds to the viral protein 2A once released from the polyprotein, and travels to the nucleus via 2A's NLS. At the nucleus, L becomes phosphorylated, and 2A is supplanted by Ran and CRM1. This L:CRM1:Ran complex associates with ERK2 (or RSK2/3) to effect Nup phosphorylation and

preclude nucleocytoplasmic trafficking. These studies extend our knowledge of virus host

interactions in the picornavirus field, and are important to parallel studies in cellular

nucleocytoplasmic trafficking regulation.

Table of Contents

List of Figures

List of Tables

List of Abbreviations

2Apro - 2A protease

3Cpro, 3CDpro - viral protein 3C or 3CD protease

aa - amino acids

Akt - protein kinase B

AMPK - AMP activating kinase

ATP - adenosine triphosphate

BeAn - demyelinating strain of TMEV

BP1 - Ran binding protein 1

CAS - exportin 2 (from Cellular Apoptosis Susceptibility Protein)

cdc42 - Cell division control protein 42 homolog, a GTPase

CDK1 - cyclin dependent kinase 1

cDNA - complementary DNA

CHYSEL - cis-acting hydrolase element

CRE- cis-replication element

Crm1 - exportin 1 (from Chromosomal region maintenance 1)

DA - demyelinating strain of TMEV

DAPI - 4',6-diamidino-2-phenylindole, florescent DNA stain

D-domain - docking domain

DEF - Docking site for ERK, FXFP

DEJL - for ERK and JNK, LXL docking motif

DLK - Mitogen-activated protein kinase kinase kinase 12

dsRNA - double stranded RNA

DUSP - dual specificity phosphatases

EGF - epidermal growth factor

eIF4G, eIF4b and eIF3 - translation elongation initiation factors 4G, 4b, and 3, respectively

EMCV - Encephalomyocarditis virus

ER - endoplasmic reticulum

ERK - extracellular signal-related kinases

FG - phenylalanine-glycine

FMDV - Foot-and-mouth-disease-virus

GDP - guanidine diphosphate

GFP – green fluorescent protein

GPCR - G-protein coupled receptors

GST - Glutathione S-transferases, common protein tag

GTP - guanidine triphosphate

HCV - Hepatitis C Virus

HEAT - protein domain/structural motif, from Huntington elongation factor 3, regulatory subunit A of protein phosphatase A, and TOR1

HIV - Human immunodeficiency virus

hnRNPA1 - Heterogeneous nuclear ribonucleoprotein A1

hr - hour

HT- Halotag

Ig - immunoglobulin

IL-1 - interlukin1

IP - immunoprecipitation

IRES - internal ribosomal entry site

ITAF - IRES trans-acting factors

JNK - c-Jun N-terminal kinase

Kap - karyopherin

K_D - equilibrium dissociation constant

kDa - kiloDalton

L - Leader protein

L_E - EMCV L protein

L_M - Leader from Mengo strain of EMCV

LMB – Leptomycin B, a CRM1 cargo-binding inhibitor

L_S - Saffold virus L protein

L_T - TMEV L protein

M9 – motif on hnRNPA1 used for nuclear import

mAB - monoclonal antibody

MAPK - mitogen activated protein kinase

MAPKAP - MAPK activating protein kinase

MAPKAPK - MAPKAKP kinase

MAPKK - MAPK kinase

MAPKKK - MAPKK kinase

mCherry - monomeric red fluorophore

MEF2 - myocyte enhancer complex

MEK - mitogen-activated protein kinase kinase

min - minute

miRNA - microRNA

MK - MAPK kinase

MKK - MK kinase

MLK - Mitogen-Activated Protein Kinase Kinase Kinase 10

MNK - MAP kinase-interacting serine/threonine-protein kinase 1

MOI - multiplicity of infection

mRNA - messenger RNA

mRNP - messenger ribonucleoprotein

MSK - Mitogen and stress activated protein kinase

NES - nuclear export signal

NF-KB - nuclear factor kappa-light-chain-enhancer of activated B cells)

NIMA - 'never in mitosis A' denotes phenotype of kinase-deficient mutant

NLK - Nemo-like kinase

NLS- nuclear localization sequence

nm - nanometer

NMR - nuclear magnetic resonance

NTF2 - nuclear transport factor2

Nup - nuclear pore protein, or nucleoporin

OGlcNAc - O-linked N-acetylgucosamine

ORF - open reading frame

PAK - p21 activated kinase

PCB2 - poly(rC)-binding protein 2

PDGF - platelet-derived growth factor

PDK1 - phosphoinositide-dependent protein kinase 1

phosphor – phosphorylated

PI – post infections

PI3 - Phosphoinositide 3-kinase

PK - post knockdown

PKA - protein kinase A

PKI – PKA inhibitor

PP1 - protein phosphatase 1

PP2a - Protein phosphatase 2a

PTB - polypyrimidine tract-binding protein

Raf - serine/threonine kinase protein/family (from 'Rapidly Accelerated Fibrosarcoma')

RanBP2 - Ran binding protein 2 (also called Nup358)

RanGAP- RanGTPase activating protein

RCC1 - guanidine nucleotide exchange factor

rKinase - recombinant kinase

RNA - ribonucleic acid

RNAse - enzyme that degrades RNA

RSK - p90 Ribosomal s6 kinase

SafV - Saffold virus

SAPK - for stress activated protein kinase, p38

SR - serine arginine protein (transportin)

Src - proto-oncogene encoding a tyrosine kinase (from 'sarcoma')

STAT3 - Signal transducer and activator of transcription 3

SV40 - Simian vacuolating virus 40

T3- triangulation number of capsid

TAK - Cyclin-Dependent Kinase 9

Tao - serine-threonine kinase

TAP/NXF1 - RNA exportins

TBB - (4,5,6,7-tetrabromo-2-azabenzimidazole), a CK2 inhibitor

tet - tetracycline

TEY - Thr-Glu-Tyr activation domain

TGY - Thr-Gly-Tyr activation domain

TMEV - Theiler's murine encephalitis virus

TNFα - tumor necrosis factor alpha

TRAF - TNF receptor associated factors

tRNA - transfer RNA

UTR - untranslated region

VCAM-1 - Vascular Cell Adhesion Molecule 1

vEC9 - EMCV with truncated polyC

VHEV - Vilyuisk human encephalomyelitis virus

VPg - viral protein, genome-linked

TBCA - [(E)-3-(2,3,4,5-tetrabromophenyl) acrylic acid], a CK2 inhibitor

Chapter 1: Introduction

Picornavirus overview

Picornaviruses are as the name suggests; tiny ("pico"), positive (messenger) sense RNA viruses, in the virus taxonomy order Picornavirales. The picornaviridae currently comprise 29 genera with 50 species at present (http://www.picornaviridae.com/, Table 1.1). Several of those species are not yet assigned to a genus, and more picornaviruses are sure to be added with present sequencing technologies. The general guidelines for taxonomy of a picornaviridae genus are as follows, "(i) the leader, 2A, 2B and 3A polypeptides would normally be expected to be functionally homologous among members of a genus...; (ii) members of a genus should normally share a structurally homologous internal ribosomal entry site (IRES) (this rule may not apply if the first rule is true); and (iii) members of a genus should normally share phylogenetically related P1, P2, and P3 genome regions, each sharing >40%, >40%, and 50% amino acid identity, respectively" (1). The host range of Picornaviridae is staggering; these viruses infect mainly animals and birds, though picornaviruses which infect fish and insects (mainly the Dicistroviridae) have been described.

Capsids, receptors, and attachment

Picornaviruses are contained in non-enveloped virions composed of four proteins. These proteins make up roughly one third of the 5' open reading frame (ORF) of the viral polyprotein, in the P1 region. Once the polyprotein is produced, VP1 must fold before the region is cleaved by virus protease 3C (or active precursor 3CD), to produce VP0, VP1, and VP3. 60 copies of each of these associate by their termini, forming pentamer structures. The pentamers ultimately assemble into a semi-spherical capsid ranging from 27- 30 nm in diameter; RNA is enclosed and VP0 auto-catalytically cleaves to form the (N-terminal) VP4 and (C-terminal) VP2. This final

Table 1.1: Picornaviridae

Genus	Species	Number of type
Aphthovirus	Bovine rhinitis A virus	2
	Bovine Rhinitis B virus	1
	Equine rhinitis A virus	1
	Foot-and-mouth-disease virus	7
Aquamavirus	Aquamavirus A	1
Avihepatovirus	Avihepatovirus A	1
Avisivirus	Avisivirus A	1
Cardiovirus	Cardiovirus A (Encephalomyocarditis virus)	2
	Cardiovirus B (Theiler's murine encephalomyelitis virus, Saffold virus)	12
	Cardiovirus C	2
Cosavirus	Cosavirus A	1
Dicipivirus	Cadicivirus A	1
Enterovirus	Enterovirus A	25
	Enterovirus B (Coxsackie B)	63
	Enterovirus C (Poliovirus, Coxsackie A)	23
	Enterovirus D (Enterovirus-D68)	5
	Enterovirus E	4
	Enterovirus F	6
	Enterovirus G	11
	Enterovirus H	1
	Enterovirus J	6
	Rhinovirus A (Human rhinovirus A)	80
	Rhinovirus B (Human rhinovirus B)	32
	Rhinovirus C (Human rhinovirus C)	55
	unassigned	3
Erbovirus	Erbovirus A	1
Gallivirus	Gallivirus A *	1*
Hepatovirus	Hepatovirus A	1
Hunnivirus	Hunnivirus A	1
Kobuvirus	Aichivirus A	1
	Aichivirus B	2*
	Aichivirus C	1
Kunsagivirus	Kunsagivirus A	1
Megrivirus	Melegrivirus A*	1*
Meschivirus	Meschivirus A	1
Mosavirus	Mosavirus A	1
Oscivirus	Oschivirus A	1
Parechovirus	Parechovirus A	16
	Parechovirus B**	4**
Pasivirus	Pasivirus A	1
Passerivirus	Passerivirus A	1
Rosavirus	Rosavirus A	1
Sakobuvirus	Sakobuvirus A	1

Salivirus	Salivirus A	1
Sapelovirus	Sapelovirus A	6
	Sapelovirus B	3
	Avian Sapelovirus**	1
Senecavirus	Senecavirus A	1
Sicinivirus	Sicinivirus A	1
Teschovirus	Teschovirus A	1
Tremovirus	Tremovirus A	1
Proposed new genera	Limnipivirus	3
	Potamipivirus	1
Unassigned		22
Candidates	Fish picorna-like viruses	9?
	Amphibian picorna-like viruses	?
	Reptile picorna-like viruses	3?
	Avian picorna-like viruses	6?
	mammalian picorna-like viruses	3?

Reference www.picornaviridae.com, accessed 7/1/2015.

** indicates that more are currently being documented/added

step is known as maturation cleavage and it is thought to stabilize the structure (given that the VP0 intermediates are less resistant to ionic strength, detergents and heat). Maturation cleavage occurs in all of the picornaviruses except the kobuviruses and parechoviruses. Picornaviruses have "psuedo T3" icosahedron virion structures; the 60 trimers that make up the capsid are each split into smaller segments corresponding to VP2, VP1, or VP3. VP1 termini form pentamers, while VP2 and VP3 alternate around two- and three-fold axes. VP4 is located in the interior of the capsid, and becomes myristoylated on the N-terminus. The C-terminals of the other capsid proteins project from the outer surface, forming the variable chains that contribute to most of the antigenetic sites. Other notable features include a depression in the pentamer formed by VP1 around the 5-fold axis, called the canyon in rhinovirus (2), which serves as the receptor binding site (3). Other picornaviruses contain similar characteristics; in cardioviruses, there are in fact 5 separate depressions in the areas corresponding to the deepest canyon areas on rhinovirus capsids (4). It has also been shown that the bottom of the enterovirus canyon forms a hydrophobic pocket in which endogenous lipids referred to as 'pocket factors' bind. Pocket factors are necessary for a conformational change associated with viral uncoating to release RNA. Some antivirals (like the WIN compounds) displace natural pocket factors for rhinoviruses, partially preventing binding of the receptor, and blocking conformation change (5).

Specific cellular receptors vary between picornaviruses. This specificity usually determines each virus' preferred tissue or cell type (6). Upon attachment, receptor-mediated endocytosis occurs (7, 8), and when inside the cell, the virus capsid undergoes a structural rearrangement (sometimes referred to as 'uncoating') to release the genome into the cytoplasm (9).

Genomes and translation

Enclosed within the virion is a tightly packed RNA genome with a highly conserved characteristic structure conserved among picornaviruses (Figure 1.1; Picornavirus genome organization). It is a messenger (positive) sense RNA, covalently linked to a viral genome-

Picornavirus Replication Overview
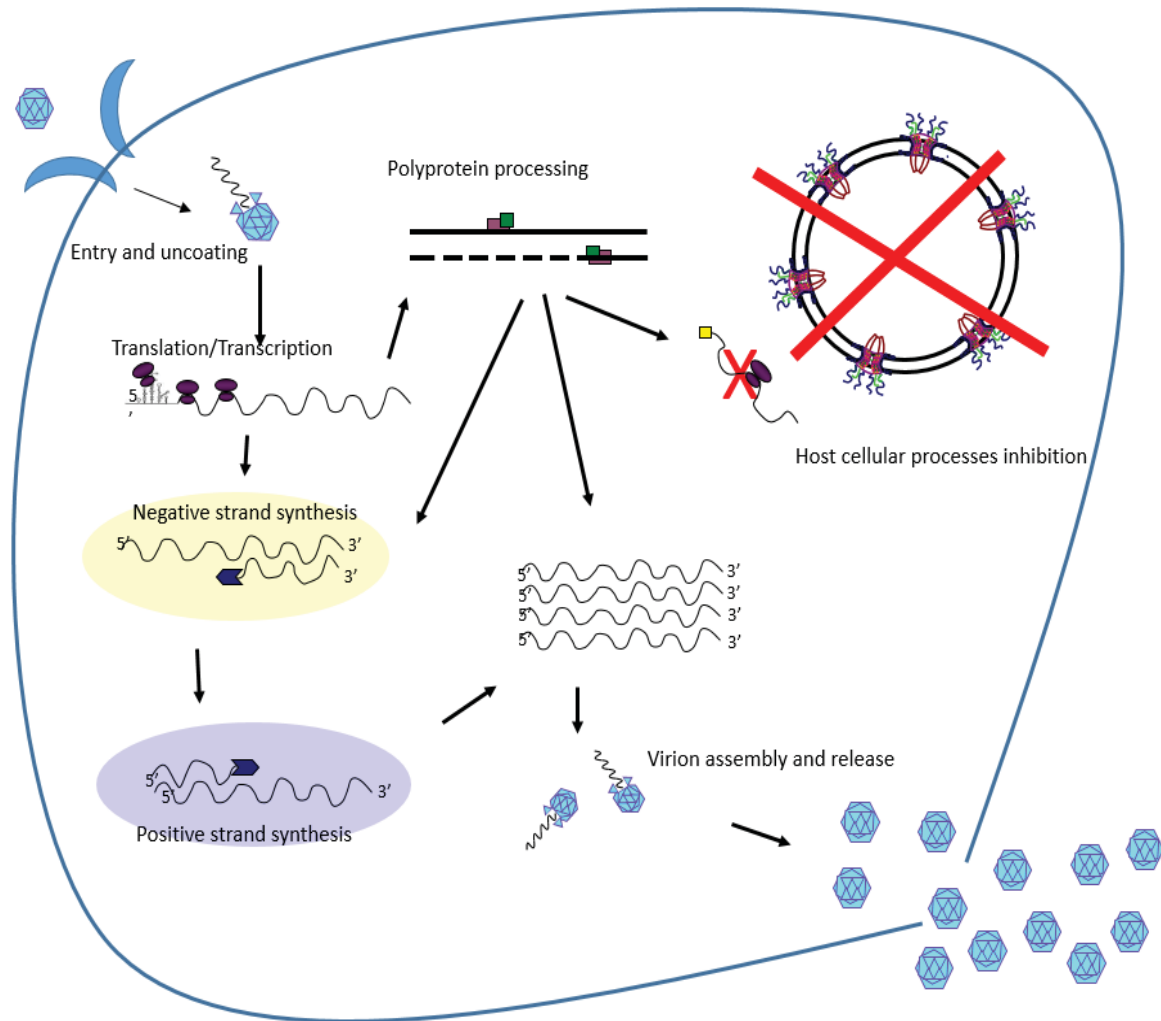
Figure 1.1 Picornavirus replication overview. Picornaviruses interact with specific cellular receptors that help define cellular trophism. Viral uncoating occurs upon entry into the cell, with release of positive sense RNAs. These are then translated using the viral IRES, yielding viral proteins whose functions include shut down of host defenses, inhibition of cellular mRNA translation, use as viral polymerases, and virion proteins. Replication likely occurs in virus-induced membrane-bound structures. Negative strands are produced for use as templates in positive strand synthesis. These positive sense RNAs are then packaged with a VPg protein in virions formed by 12 copies of viral capsid protein pentamers. These virions then undergo maturation cleavage.

linked protein (VPg), and the genomic mRNA can be immediately translated into a single polyprotein upon release into the cytoplasm. An overview of the picornavirus replication cycle is found in Fig. 1.1.

Picornavirus mRNA translation is cap-independent, reliant on a 5' structure called an internal ribosomal entry site (IRES) (10, 11). IRESes have subsequently been found in about 10% of cellular mRNAs (12), and allow binding of the ribosome. In picornaviruses, the IRES is about 5% of the viral genome, and consists of a highly structured region featuring variously branched RNA stemloops of which there are 4 different types (I-IV) throughout Picornavirdae. Type I belongs to the enteroviruses, including rhinoviruses, poliovirus, and coxsackievirus B3. Enterovirus IRESes use key stems II-IV to recruit the 43S ribosomal subunit, and a variable length spacer section is found between the mapped IRES and the AUG start sequence. The cardioviruses, aphthovirus (foot-and-mouth disease virus, FMDV), erbovirus, kobuvirus, parechovirus, avihepatoviruses use a type II.). The type II IRES is better defined, with the regions referred to as H to M are necessary for binding of the 43S ribosomal subunit. This type of IRES is notable in that it retains function even when removed from the viral genome, and thus is frequently used in various recombinant protein systems to drive protein translation. Type III IRES is used by Hepatitis A virus. This IRES type does not translate well in cell-free systems or cell culture, and subsequently little is known about particular elements. The type IV IRES is similar to that used by Hepatitis C Virus (HCV), a flavivirus. This IRES has two minimal structural elements (domains II and III). Generally, while some of the IRESes have long-distance interactions with portions of the 5' UTR that contribute to folding, the basic structure of the type II IRES seems to fold independently of the rest of the genome, as established with the FMDV IRES. It has also been shown that the type II IRES, type IV IRES, and within the 3' UTR of some plant RNA viruses, that there may be internal sites that can act as a tRNA-like signal when cleaved by RNAse P ribozyme (1).

IRESes act as sites for binding of both the ribosomal subunit as well as various regulatory factors, with both enhancing and adverse effects. For instance, necessary initiation factors eIF4G, eIF4b and eIF3 bind near the 3' end of the type II IRES, and likewise eIF4G binds to domain V of the type I IRES; mutations to these IRES sites preclude eIF4G association and IRES activity. Cellular proteins called IRES trans-acting factors (ITAFs) have been implicated as mediating viral IRES activity. These usually act to stimulate IRES activity, though in two cases to repress or downregulate activity. Picornaviruses with type I, II and III IRESes require polypyrimidine tract-binding protein (PTB), probably to stabilize folding of the IRES into a conformation recognizable by the translational machinery, and La autoantigen by use of that same cohort of IRESes. The poly(rC)-binding protein 2 (PCB2) has also been implicated for use by type I and type III IRESes (and possibly by the type II group). Type I IRESes have been shown to use the upstream of N-ras protein (unr) and SRp20, and various type II IRESes use Ebp1/ITAF. There are numerous accounts of other ITAFs (reviewed in (1, 13)). For the most part, these ITAFs serve to help assemble the translational ribonucleic complex, though PTB and PCBP2 have been shown as substrates for viral proteases, which might modify them for picornavirus use. However, Gemin5 has been shown to downregulate the type II IRES.

Ribosomal binding is further affected by the region between the IRES and the start codon, which contains different features between picornaviruses. This region is a 25 nucleotide stretch for the type II IRES group, and this distance is slightly longer for viruses in the type I IRES group. ATP and eIF4 are required for 43S complexes, likely to 'melt' the RNA structure and allow ribosome entry. For the start codon itself, most picornavirus genomes contain only one AUG, but bovine rhinovirus 2 and FMDV contain two in-frame start sites, the second of which (AUG2) is more commonly used and located in an A-rich, conserved stem loop region. Other type II IRESes have triplet out-of-frame AUGs, though the second of these (AUG10) is the

initiator triplet (14). The type IV IRES group has the AUG in the ribosomal entry site (reviewed in (1)).

Polyprotein processing and protein function

As the polyprotein is translated, it is processed in one of three ways that will be described in more detail below. The most common processing mechanism is by a viral protease that recognizes and cleaves the polyprotein at a specific amino acid motif. Another processing mechanism is ribosomal skipping, which occurs when a specific peptide in the nascent chain is not synthesized and yields a break in the polypeptide. A third processing method is the maturation step that occurs during viral RNA encapsidation, when the 1AB precursor is cleaved, though the mechanism behind this has not yet been determined in detail, and is not a step required by some picornaviruses.

Picornaviruses encode between 11 and 14 proteins (Fig. 1.2, Polyprotein processing). There are no picornavirus subgenomic mRNAs, though one of the cardioviruses (Theiler's murine encephalitis virus, TMEV) may produce an N-terminal protein out-of-frame with the primary ORF (15). The picornavirus proteins can be organized into 3 basic groups; the N-terminal P1 region consists of capsid proteins (VP0, VP1 and VP3), and the P2 and P3 regions yield the processing proteins (3Cpro, and 3CDpro) and replication proteins (2B, 2C, 3A, 3B (VPg), 3C, and 3Dpol). Many genera also have additional proteins in the P1 and P2 groups. Seven of the twelve genera, including cardioviruses and aphthoviruses (FMDV), encode the small Leader (L) protein before the P1 region. L functions as a viral protease for the aphtho- and erboviruses, with other 'security protein' functions for the cardioviruses that will be discussed in greater detail in later portions of this thesis. The 2A protein has varying functions. In the entero- and sapeloviruses, 2A is a protease, and notated as 2Apro in these instances (Figure 1.2, Polyprotein processing). For the aphtho-, avihepato-, cardio-, cosa-, erbo, seneca- and

Figure 1.2 Picornavirus genomes and polyprotein processing

adapted from [1]
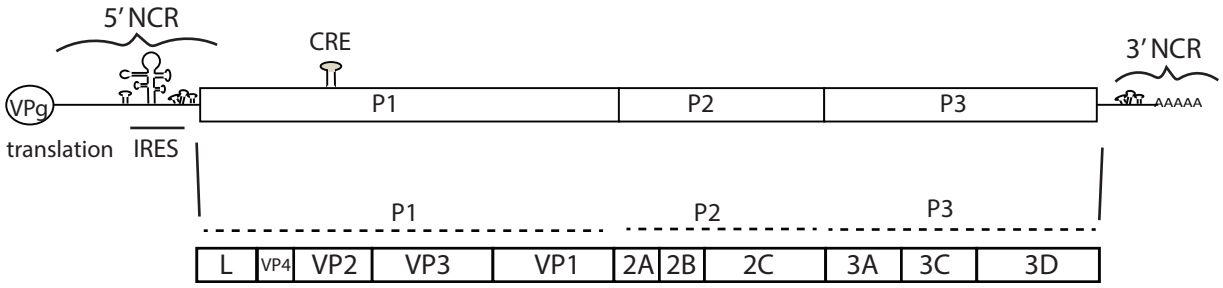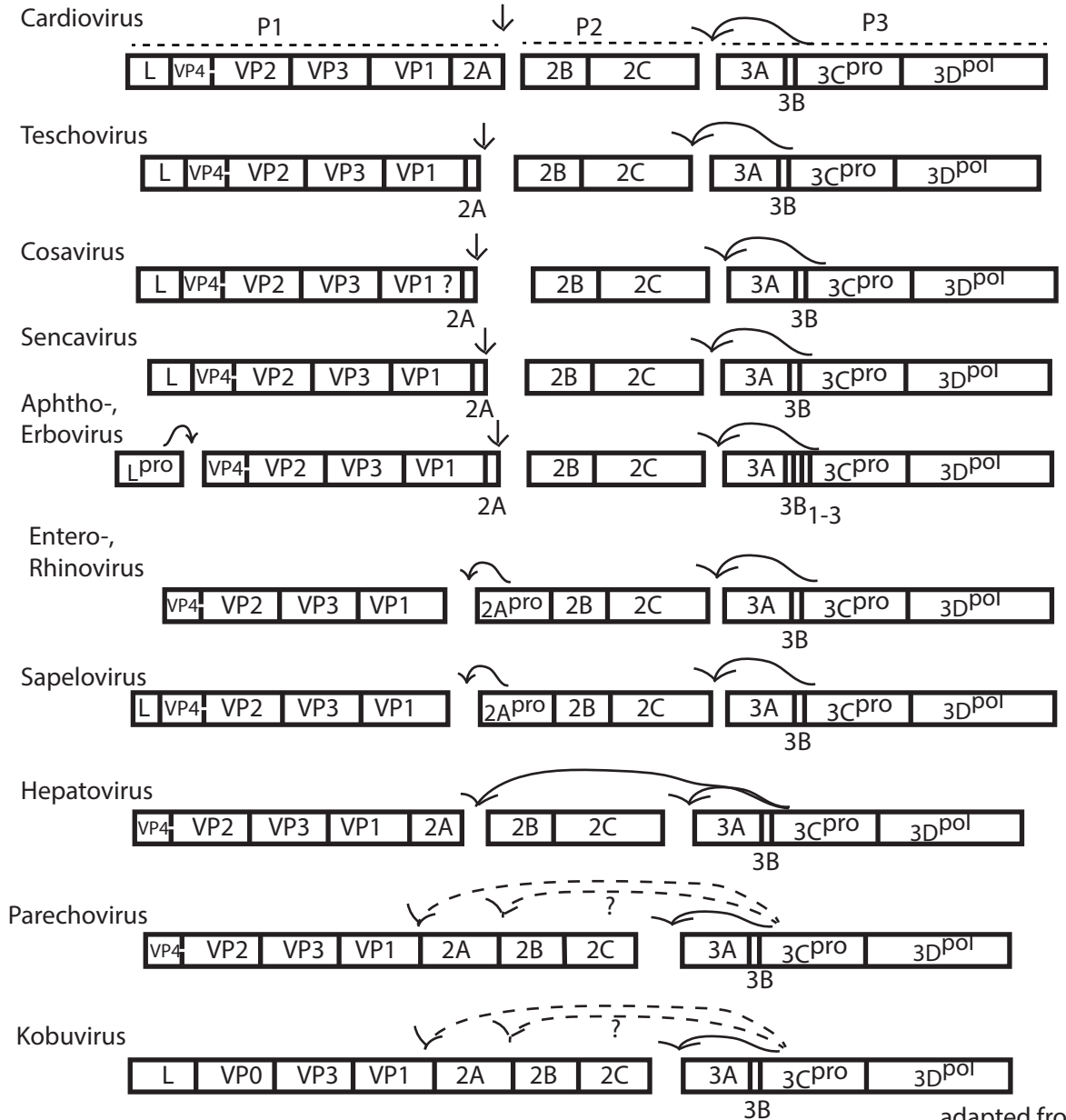
teschoviruses, 2A is an oligo-peptide responsible for ribosomal skipping (appearing as a longer protein in the cases of the cardioviruses), a parechovirus (Ljungan virus) and an avihepatovirus (duck hepatitis A virus). In the parecho- and hepatoviruses, 2A is not a protease nor causes the recoding ribosomal skipping translation event.

The proteases described above contribute to a two-step processing pattern (reviewed in (1, 16)). Once translated, a primary cis-acting processing event serves to release the viral proteases from the polyprotein, at sites denoted by an arrow in Figure 1.2. For many genera with a 2A-mediated translational recoding event, this event releases the N-terminal P1 precursor. As a protease, 2A performs a cis-cleavage at its N-terminus. For the hepatoviruses, this precursor is released in a manner akin to the 3C protease's action at the C-terminus of 2A (reviewed in (1)). For all picornaviruses, 3C also catalyzes a cleavage between itself and the C-terminus of the 2C protein (Fig. 1. 2, indicated by an arrow). For those viruses in which L acts as protease, this cleaves between the C-terminal of L and the N-terminal of 1A. Once the primary processing step occurs, these precursors are then further processed into intermediate forms. Typically, a form of the 3Cprotease (3Cpro) then cleaves between 1B, 1C and 1D; for entero- and rhinoviruses, this is done by 3CDprotease (3CDpro), whereas aphthoviruses use 3CDpro (preferred) or 3Cpro, and cardioviruses and hepatoviruses can use either 3C- or 3CDpro. The P3 protein is usually processed by 2Aprotease (reviewed in (16)).

The structure of the 3Cpro utilizes a chymotrypsin-like fold. Active sites for these proteases have been determined via comparison of known products; enteroviruses have the most conserved site preferences of cleavage between a glutamine and glycine amino acid motif. The 2A protease of sapelo- and enteroviruses use a different sequence; for instance, Poliovirus cleaves between tyrosine and glycine (Y-G), but this is variable with other enteroviruses, tolerating (A/V/H/Y/T/I/L/F-G) (17, 18). These proteases function through an active site

containing a catalytic triad consisting of an amino acid like a histidine acting as a general acid/base proton transporter, an acidic residue acting to orient the histidine's imidazole ring, and a nucleophilic cysteine/sulfhydryl group or serine/hydroxyl group. Variation at the catalytic triad correlate to different substrate preferences. Rhinovirus 2Aproteases (2Apro) feature a zinc ion to stabilize the triad (19). Other picornaviruses, including cardio-, aphtho-, and enteroviruses use a 2A-directed ribosomal skipping mechanism, a cis-acting hydrolase element (CHYSEL) which recognizes a specific sequence (DxExNPGP) and effectively prevents a peptide bond formation due to a 'tight turn' constraint as the prolyl-tRNA leaves the ribosome exit tunnel (20).

RNA replication

 Once the polyprotein is processed, transcription can proceed. Viral genomes cannot be used simultaneously for translation and negative strand transcription. A few studies have shown that when enough of the polyprotein builds up, elements like 3CD accumulate and alter the association of cellular factors that support replication, like the ITAF PCBP2, and subsequently stimulate replication (21, 22). Furthermore, replication occurs in the cytosol and there is evidence for the negative strand of the RNA being transcribed in viral protein-induced small membrane-bound structures. To induce these, the 2B protein forms complexes with itself and 2C, shown to associate with membranes (23, 24). 2B additionally shuts down cellular secretory transport and induces membrane rearrangement (25, 26). Structures formed by these rearranged membranes are thought to offer some protection from detection of host innate defenses by sequestering viral replication. Viral protein 3D is a RNA-dependent RNA polymerase (27, 28), and negative sense RNA templates are made first to act as positive sense RNA templates (29). It has been found that there are 20-50 fold more positive sense RNAs than negative templates present during replication, but the mechanism driving this difference has not yet been determined (30, 31). The RNA genome has an associated VPg protein (viral protein

3B) covalently linked via the third amino acid at the N-terminus. This protein is uridylated, and serves as a primer for positive and negative strand transcription (32, 33). Uridylation is the post-translational addition of uridine at the cis-replication element (CRE), a stem-loop structure in the protein coding region, usually at VP2. The CRE allows a nascent VPg to be uridylated by 3Dpol, which then acts as a primer for viral replication (34, 35).

Cardioviruses and the L protein

There are three species of the cardiovirus genus, Cardiovirus A (formerly called Encephalomyocarditis virus, or EMCV), of which there are 2 serotypes (36). The Cardiovirus B species (formerly called Theilovirus), contains titular virus Theiler's murine encephalomyelitis virus (TMEV), Saffold virus 1-11 (SAFV-1/2/3/4/5/6/7/8/9/10/11) and Vilyuisk human encephalomyelitis virus (VHEV), both of which infect humans, Thera virus (found in rats), and Genet fecal theilovirus (37). The Cardiovirus C species is comprised of Boone's cardioviruses A and B, which were very recently isolated at the University of Missouri from Brown rats (*rattus norvegicus*) (Gohndrone, J.D. and Riley, L.K. Identification of a novel cardiovirus in laboratory rats. Unpublished).

Early mentions of cardioviruses are twice found in the literature. These were isolated in 1939 as Columbia-SK, and in 1942 as 'MM' during attempts to adapt human poliovirus into monkeys by inoculation with the brain tissue from dead lab mice. The recovered neurological agent caused hind leg paralysis and death upon reinfection of mice, and was determined to be a non-poliovirus viral agent. The first description of Cardiovirus A (EMCV) was isolated from the pleural fluids of a gibbon and a chimpanzee in Miami, who died from pulmonary edema and myocarditis. This unknown virus was later determined to be caused by a virus denoted 'EMC'. The EMCV strain Mengo virus was isolated from a captive rhesus monkey with paralyzed lower

limbs by researchers in the Mengo district of Uganda, and was found to have serological cross-reactivity to the Columbia-SK, MM, and EMC viruses (38, 39). While EMCV is not described as a human pathogen, it can infect all mammals, and can cause economic losses in affected domesticated swine populations, captive primate colonies, and zoos (39). There is an effective vaccine consisting of a deletion mutant strain where the poly-C tract of Mengo has been truncated (40). EMCV, SAFV and TMEV share about 50% identity (reviewed in (38)), with the greatest divergence seen between the L and 2A proteins, which have been described as virulence factors or 'security proteins' (41).

Cardiovirus replication cycle

Cardioviruses use the sialoglycoprotein receptor Vascular Cell Adhesion Molecule 1 (VCAM-1) for targeting and entry into murine vascular endothelial cells as well as other 70 kDA sialoglycoproteins in HeLa and K562 cells (42, 43); there may be other saialglycoproteins that serve as the main receptor (followed by the usual receptor-mediated endocytosis).

The cardiovirus capsid is 30 nm (4), containing a single-stranded RNA of 7.6 - 8 kb and an associated viral VPg protein. Cardiovirus genomes have a particularly long 5' untranslated region (UTR) featuring a 5' proximal polyC tract. Depending on the strain, this region ranges from 60 residues ($C_{44}UC_{10}$, for Mengo, a strain of cardiovirus As) to 420 residues ($C_{125}UCUC_3UC_{10}$, for EMCV-R). The cardiovirus B species members lack polyC regions. While the polyC tract is single-stranded, it is immediately followed by some structured psuedoknots, then the well conserved, highly structured type II IRES featuring 5 structural domains H-L (Figure 1.1. picornavirus genome). Translation produces the polyprotein, processed as delineated in the main picornavirus section (L-VP4231-2ABC-3ABCD, Figure 1.1. polyprotein processing). Specifically, cardioviruses are self-cleaved at the Asn-Pro-Gly-Pro (NPG[P]) sequence during translation (44) and a secondary processing step occurs via 3Cprotease at

usually Gly-Gly, Gln-Ser (though other sequences are also recognized). Polyprotein products P3, 3ABC, and 3CD are all active proteases.

Cardiovirus viral proteins have functions conserved by all picornavirus. The P1 region is composed of four proteins, VP1, VP2, VP3, and VP4, of which 60 copies (12 of each) make up the capsid. The P2 region is processed into 2A, 2B, and 2C. EMCV 2A (17 kDA) has a putative nuclear localization sequence (NLS) and an eIF4E binding site (45). It is thought that 2A triggers the hypo-phosphorylation of protein 4E-BP1, and causes eIF4E sequestration (46). Direct binding of eIF4E and 2A via amino acids 126-134 prevent eIF4E binding to eIF4G and hinder the initiation of cap-dependent translation. Additionally, 2A localizes to the nucleolus and interacts there with the 40S ribosomal subunit, possibly to induce a preference for EMCV's IRES (47). It is thought that immediately upon release from the polyprotein, 2A and Leader (L) protein associate and utilize 2A's NLS to traffic to the nuclear pore (48). Finally, when 115 amino acids are deleted from 2A, infected cells undergo apoptotic death with activation of caspase 3 (49), though this might also have something to do with L's kinase-stimulating activities (50). The functions of viral protein 2B are not yet well described; it contains 2 or more hydrophobic regions, and while 2B decreases the calcium levels in the cell's endoplasmic reticulum (ER), this effect does not extend to the Golgi. Protein 3B, also called VPg, serves as a primer for the 3D RNA-dependent RNA-polymerase in viral replication. Again, 3C serves as the viral protease.

Cardiovirus L protein

The functions of the Cardiovirus A virus EMCV Leader protein (EMCV L or L_E) are the focus of this thesis. This protein is 67 amino acids with a PI of 3.7 for this species, and 71-76 amino acids in the Cardiovirus B species (Figure 1. 3, Cardiovirus Leaders). L has not yet been studied in any detail in the Cardiovirus C species. L_E has two domains, an N-terminal novel zinc finger from amino acids 10-22 (51, 52), and a C-terminal acidic domain at amino acids 37-52. These
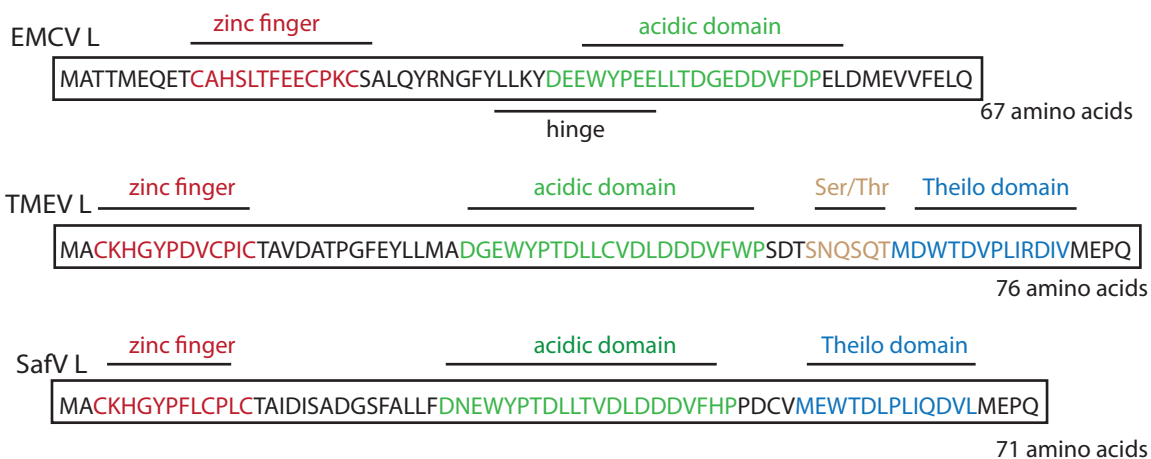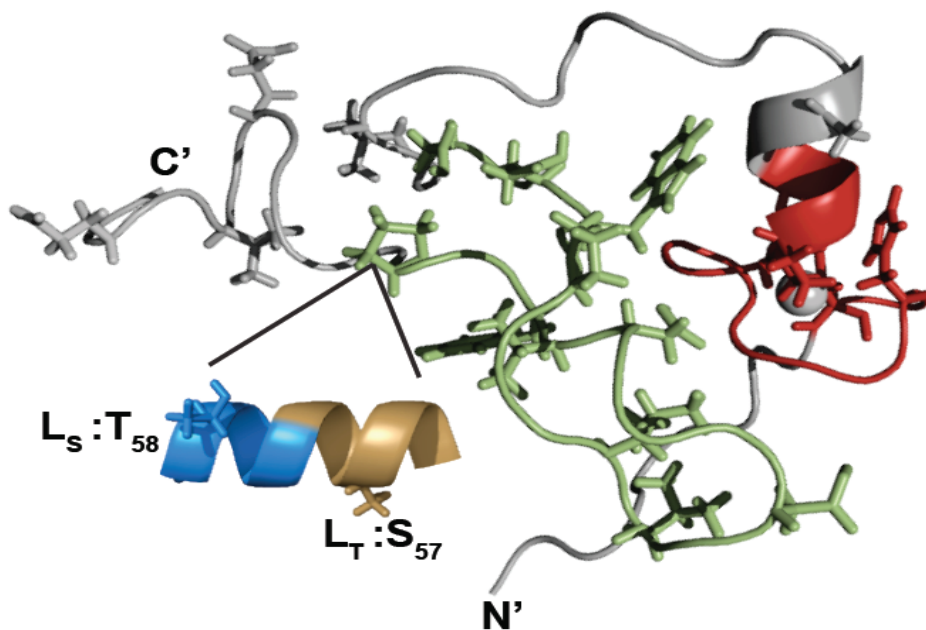
Figure 1.3 Cardiovirus Leader proteins (A) and structure with theilo domain model (B). Colors correspond to domains between the amino acid sequences (A) and structure/model (B).

two domains are necessary for its various anti-host functions. Additionally, there is a region between the zinc finger and the acidic domain, the 'hinge' region, at amino acids 35-44, which binds RanGTPase (53). In the Cardiovirus B group, a third domain consisting of a serine/threonine-rich region is referred to as the theilo domain, which proceeds the acidic domain (Fig. 1.3). TMEV strains BeAn and DA are known to cause persistent infections and chronic demyelinating disease in mice despite a strong, specific immune response (54, 55). Because of this, infections resulting from these strains are considered a model for multiple sclerosis. Early studies reported that TMEV L (or L_T) prevented an interferon response in infected cells by blocking transcription (56), as does EMCV/Mengo L, possibly by preventing activation of NF-κB by enhancing ferritin production (57). L has also been shown to inhibit protein synthesis (58) and modulate IRES activity (59). While cardioviruses are infectious when L is deleted from the genome, resulting plaques are greatly reduced in size when compared to wildtype infections (52). Additionally, assays for translation of EMCV L-deletion mutants RNA transcripts decreased protein synthesis to 67%, while deletion templates lacking the L zinc finger region decreased viral protein synthesis to 79% and deleting the acidic region decreased viral protein expression to 71% (52). There are also early reports that cardiovirus L changes the nucleocytoplasmic distribution of various cellular proteins, including PTB and interferon regulatory factor 3 (60, 61).

L proteins have phosphorylation sites. Phosphotyrosine antibodies detected a phosphor-site in the acidic domain (52), as well as phosphorylation of Threonine47 as necessary for anti-host functions (58). These phosphorylation events are sequential, and the responsible kinases have been determined for EMCV. First, Casein Kinase 2 has been shown to phosphorylate Threonine47 *in vitro* as well as by kinase inhibitor studies (62, 63), and then Spleen Tyrosine kinase phosphorylates Tyrosine41 (63). While L_T and L_S also become phosphorylated, the theilo domain insertion alters these phosphorylation sites. L_T becomes phosphorylated on Serine57

within the Ser/Thr domain, and L_S has a phospho-site at Threonine58 in the theilo domain, both of which can be phosphorylated by AMP-activated protein kinase (AMPK) (64). These sites are equivalent to the EMCV Thr47 phosphorylation site.

Chimeric cardioviruses made by swapping the L proteins between species demonstrate that cardiovirus Ls can be functionally substituted, though this alters the kinetics of an infection (61) – Mengo L altered nucleocytoplasmic protein distribution more quickly than L_T, but displayed a decreased viral replication. This 'redistribution' of nucleocytoplasmic trafficking was later determined to be the inhibition of nucleocytoplasmic trafficking via phosphorylation of nuclear pore proteins (nucleoporins, or Nups). While other picornaviruses inhibit transport of factors through the nuclear pores (65-67), these viruses do so through a different mechanism: proteolytic release of Nups from the pores. For instance, rhinoviruses use the 2A protease to target amino acid motifs on Phe-Gly (FG) repeat Nups in a species-specific fashion (68, 69), preventing all active transport and promoting a release of various nuclear factors like ITAFS PTB and La autoantigen required for picornavirus replication. Cardioviruses also hinder nucleocytoplasmic trafficking, but the Nups remain inserted in native context of the pore ((70-72), and Chapter 2 of this thesis). It has been shown that nuclear pore proteins (Nups) 62, 214, 153 and now Nup98 become phosphorylated by L_E ((73) and Chapter 2), to prevent (either by charge or by sterics) binding of various karyopherins/transportins. Additionally, L_T can direct Nup phosphorylation, as demonstrated for Nup98 (71). Active transport is inhibited, as illustrated by efflux of proteins tagged with a NLS but small enough for passive transport (70, 74). This inhibition is caused by L alone, and requires a fully intact, phosphorylated L; mutations which remove the zinc finger domain (70), acidic domain (74), hinge region (53), or phosphorylation sites (63, 70) prevent L-directed Nup phosphorylation. L does not have any known enzymatic activity and acts through cellular kinases, specifically those in extracellular signal-related kinases (ERK)1/2 and p38 pathways ((74, 75) and Chapter 4), shown by

requirements of cytosolic factors as well as use of broad spectrum kinases inhibitors. Determining the exact parameters and kinases involved were a major aim of this work.

L_E localizes to the nuclear envelope (74), though TMEV L* might also localize to the mitochondrial membrane (76). Recent work shows that L_E binds to the 2A protein with an equilibrium dissociation constant (K_D) of 1.5 μM affinity (77). 2A has a pI of 9.67 and contains an NLS similar to that of used by importin 7 (45). It is hypothesized that soon after excision from the polyprotein, 2A and L associate and are transported to the nucleus, where they dissociate when L binds to other proteins like RanGTPase (Ran). The L:Ran association has a 1:1 stoichiometry (74) with a very tight K_D of approximately 3nM that is facilitated by the guanidine nucleotide exchange factor RCC1 (77). This interaction is through the 'hinge' region of L; mutations to L_E sites K35, D37 and W40 decrease this interaction (53). L:Ran binding is not affected by the phosphorylation status of L (53). However, at the time of nucleocytoplasmic trafficking inhibition, only very small amounts of L are produced. Ran is a very abundant cellular protein, and these small amounts of L are not capable of titrating out all usable Ran (53). The NMR crystal structure for L:Ran was solved recently, showing that L binds to Ran *sans* nucleotide, but locks Ran into a conformation similar to that of a Ran bound to GTP (78). This orientation allows for association of additional factors. As described in (78) and Chapter 3 of this thesis, Ran:L can bind the transportins CRM1 and CAS. The lack of nucleotide associated with Ran implies that this complex cannot be dissociated by common methods.

Other activities associated with L contribute to its status as a 'security protein', or one used by the virus to interfere with host antiviral functions (79). Cardiovirus L proteins have been shown to prevent stress granule formation, which are cellular aggregates of stalled preinitiation complexes and mRNAs formed in stressed cells. Cells infected with L-deletion mutants form stress granules, but the L proteins of TMEV and Mengo inhibit these during wildtype infections, as well as in non-infected, chemically stressed cells (80). Moreover, TMEV L*, produced

through an alternative ORF, has been described as contributing to the establishment of persistent CNS infections(51, 81). L* has been shown to associate with the outer mitochondrial membrane, potentially targeted there by HSP70 (76), and upon infection of cells with cardiovirus L-deletion mutants, cytochrome C is released from the mitochondria, activating caspases and effecting eventual apoptosis (79).

Nucleocytoplasmic trafficking overview

Nuclear pore architecture and trafficking

This thesis focuses on inhibition of nucleocytoplasmic trafficking by a viral protein, and this activity is located at nuclear pores. There are approximately 2800 nuclear pores fenestrating each vertebrate nucleus (82). Each pore is an estimated 125 megaDaltons, with varying copies of about 30 nuclear pore proteins (nucleoporins or Nups), arranged in octagonal radial symmetry. The pores are organized into several main regions (Fig. 1.4); the fibril-like proteins that extend into the cytoplasm, the nuclear plug which serves as a channel of 30 nm in diameter and ~50 nm long through the envelope, and the nuclear basket that extends into the nucleus. There are also integral membrane Nups that anchor the pore in nuclear envelope (83).

The structural/scaffolding Nups make up about half of the mass of each pore, and contribute to the shape and strength of the pores. These proteins typically have α-solenoid, β-propeller or a mixed N-terminal β-propeller, C-terminal α-solenoid protein structure (84), and share elements to those that comprise clathrin-coated vesicles (85). The cytoplasmic fibril Nups include Nup358 and Nup214, and the nuclear basket Nups include Nup153 and Nup50. Nup98 has also been observed within both the basket and the nuclear plug. These external Nups serve as docking regions for cargos and their karyopherin transportin proteins. The Nups within the nuclear plug
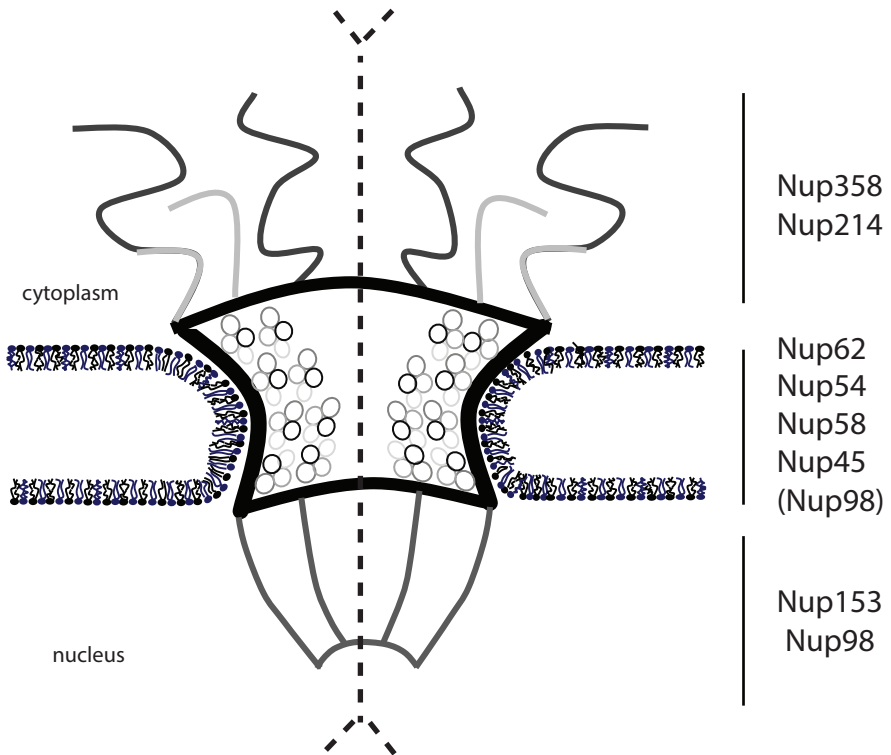
Figure 1.4 Nuclear pore complex. The nuclear pores are 125 MDa structures comprised of about 30 proteins arranged in octagonal symmetry around an inner channel (indicated by dotted line). Nups extending into the cytoplasm include Nup358 and Nup214, and contain binding sites that serve as staging areas for karyopherin:cargo complexes entering and exiting the pores. The portion of the nuclear pore that sits in the nuclear envelope contains Nup62, Nup45, Nup58, and Nup54, found in multiple groups of these 4 proteins. These have primarily uncoiled secondary structure, and form a barrier that prevents diffusion of macromolecules larger than 40 kDa. This region also contains hydrophobic Nups that are inserted into the nuclear envelope to provide anchoring and structure. The nuclear basket is composed of Nup153 and Nup98, and extends into the nucleus to allow docking of complexes on the nuclear side of the pores. All Nups lining the inner channel contain FG-repeats, with which karypherins interact in a transient, 'stepping stone' like fashion for active transport of macromolecules.

are Nups 62, 58, 54, 45, and sometimes 98. These Nups are usually said to form sub-groupings of one of each the main 4 proteins, and are generally an unfolded protein conformation. While the exact mechanism of cargo translocation remains undetermined, various Nups are associated with specific pathways determined by the traversing karyopherin (see table one, trafficking chapter). These pathways are either for import or export, and rely on transient interactions of the karyopherins/transportins with phenylalanine-glycine (Phe-Gly, or FG) repeats comprising motifs on the Nups lining the inner channel of the pores. These characteristic sequences are highly hydrophobic, may also consist of Gly-Leu-Phe-Gly (GLFG) or Phe-X-Phe-Gly (FXFG) repeats, and tend to be further modified with O-linked N-acetylgucosamine (OGlcNAc). Glycosylation may serve as a binding site for lectins (86). The FG repeat proteins also contain coiled-coiled domains that provide protein-protein interactions that hold them within the central channel of the pore (84).

Active (facilitated) transport is required for macromolecules too big to diffuse across the pores, generally considered to be molecules greater than 40 kDA. The lower threshold for active transport is around 5nm, or a sphere of about 30-40 kDa (87, 88). With pore flexibility, the upper limit for facilitated transport is 39 nm, or the size of ribosomal subunits and some viral capsids (89). There have been reports of even larger transported macromolecules, but these generally rearrange themselves to fit the dimensions of the pores, as demonstrated by mRNPs (90). Generally, macromolecules which require active transport either directly interact with the FG Nups themselves, or, more likely, use adaptor proteins that interact with the FG Nups instead.

Proteins which act as adaptors, carrying cargos and interacting with FG-Nups, are karyopherins (Kaps, from *karyo*- 'kernal' + *phero*- 'in'), also called variously transportins, importins (specifically those which bear cargo into the nucleus) and exportins (specifically to those bearing cargos out of the nucleus). These proteins belong to the importin α/β protein family, and usually consist of about 20 HEAT domain repeats (from Huntington elongation factor 3, regulatory subunit A of

protein phosphatase A, and TOR1 (91)) arranged in a flexible helical structure (92, 93). This is illustrated in Fig. 1.5, a nucleocytoplasmic trafficking overview. Karyopherins generally function by recognizing and binding to specific amino acid motifs on their cargos, then binding to RanGTPase and translocating across the nuclear pore. RanGTPase is a binary 'switch', toggling between GTP- and GDP- bound forms. The predominant nucleotide bound to Ran varies due to localization: RanGTP is found primarily in the nucleus, and RanGDP is mainly in the cytoplasm. This distinction drives nucleocytoplasmic trafficking, as cargos exiting the nucleus typically require a RanGTP bound, and the complex dissociates on the cytoplasmic face upon hydrolysis of RanGTP into GDP by the activity of RanGTPase activating protein (RanGAP). Ran guanine nucleotide exchange factor RCC1 is found in the nucleus, and exchanges Ran GDP for GTP there (94). For the classical transport pathway, mediated by importins α/β, importin α binds to a cargo in the cytoplasm, associates with importin β and crosses into the nucleus. On the other side, RanGTP binds to the complex, dissociating the cargos and preventing reverse translocation. The RanGTP:importins then recycle back across the pore, where RanGTP is hydrolyzed to GDP by RanGAP with the help of RanBP1 and BP2(Nup358) (95-97); the importins and cargo dissociate (98, 99). For export of cargos out of the nucleus, the exportin binds cargos and then RanGTP is preloaded, traverses the pore, and the hydrolysis of RanGTP dissociates the exportin complex (100, 101). Nuclear transport factor 2 (NTF2) binds to RanGDP to take it back into the nucleus, for the RCC1-mediated exchange of GDP for GTP.

Karyopherins and translocation

There are over 20 karyopherins in higher vertebrates (reviewed in (102)). These interact with their cargos via amino acid motifs as mentioned above; a nuclear localization signal (NLS) targets a macromolecule to the nucleus, and a nuclear export signal (NES) targets nuclear macromolecules to the cytoplasm. As outlined above, the most common import pathway is the classical pathway utilizing importins α and β, which recognizes mainly basic NLS typified by that
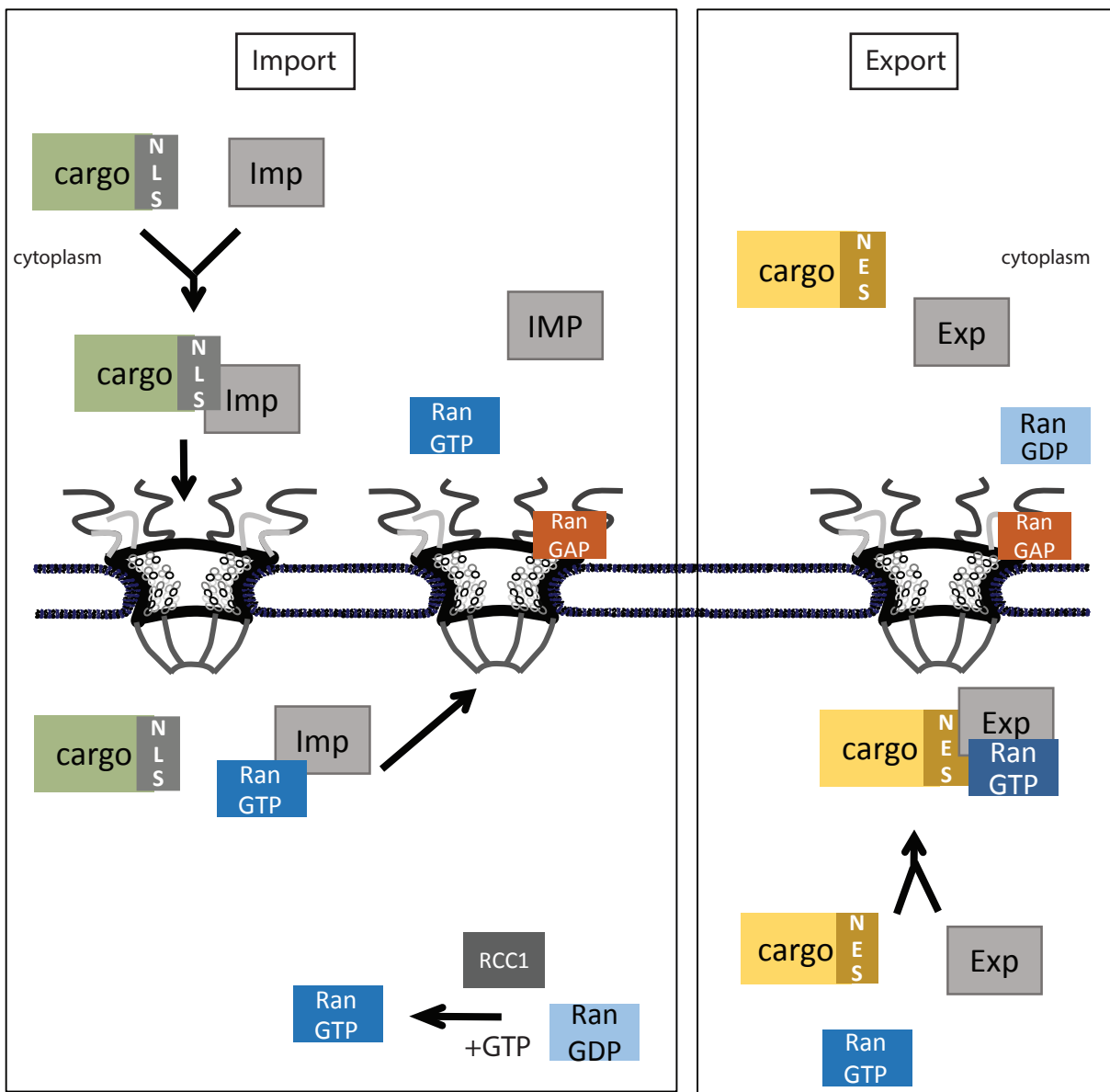
Figure 1.5 Nucleocytoplasmic trafficking. For import (left panel), cytoplasmic cargos containing nuclear localization signal motifs (NLS) associate with appropriate importin karyopherins (for instance, with importin α/β), and these complexes then traffic through when the karyopherins transiently bind to FG-repeat domains on nups lining the nuclear pores. Once inside, RanGTP associates with the importins, and the cargo is released. The importins:Ran then traverse back across the pore to the cytoplasm, where RanGAP hydrolyzes the GTP on Ran into GDP, which dissociates the importin to repeat the cycle. RanGDP is converted back to RanGTP in the presence of guaninine nucleotide exchange factor RCC1 in the nucleus.For export out of the nucleus, a cargo containing a nuclear export signal (NES) motif associates with an approriate exportin karyopherin (CRM1, for instance) and RanGTP, which then interact with FG-repeats on Nups lining the inner pore channel to the cytoplasm. There, RanGAP again hydrolyzes GTP to GDP, and the complex components dissociate.

found on SV40's Large T antigen. The classical import pathway transports a broad spectrum of cargos, including core histones, HIV Rev and Tat, cyclin B, and histone H1, which it shares with importin 7 (as reviewed in (102)). Other notable importins include Transportin (1), which interacts with the M9 domain of hnRNPA1, and transports ribosomal proteins and mRNA binding proteins. Transportin SR1 and SR2 interact with the arginine-serine repeat domains of SR proteins, importing them into the nucleus. Importins 5 and 7 transport ribosomal proteins, core histones, and other basic proteins (103). The most versatile exportin is CRM1 (Exportin 1), which recognizes leucine-rich NESes on macromolecules in the nucleus, including HIV Rev protein, an adaptor for U snRNAs, the adaptor protein snurportin1 (104), and the 60S pre-ribosomal proteins (reviewed extensively in (105)). Other exportins include CAS, which mainly recycles importin α back into the cytosol, exportin 5, which is responsible for tRNAs, dsRNA-binding proteins, pre-miRNAs and 60S pre-ribosomal units (reviewed extensively in (105)). Some karyopherins are bi-directional, and these include importin 13, transporting histone fold heterodimers into the nucleus and eIF1a out into the cytoplasm (106), and exportin 4, which imports Sox2 and SRY, and exports eIF5A and Smad3 (reviewed in (105)). While the transportins listed above require Ran GTP/GPD gradients for directionality, there are also non-Ran dependent (non-karyopherin) transportins, particularly TAP/NXF1-p15/NXT1, which exports the majority of mRNA to the cytoplasm (reviewed in (107)).

It is estimated that more than 60,000 macromolecules translocate through each pore per minute (82), with the total net traffic of a single vertebrate nucleus around 1 million macromolecules per second, totaling 4×10^{10} Da (108). Each transportin transiently associates with a particular subset of FG-repeat Nups, traversing the pore in a stepping stone-like fashion (reviewed in (107, 109)). It has been estimated, given the fact that there are 5-50 repeats present on each Nup, and about 200 FG-repeat Nups per pore, that there are more than 1000 binding sites per pore (83).The FG-repeat Nups are natively uncoiled, and form a selective barrier through which

the karyopherins must cross. There are several theories of how this translocation occurs; the simplest models predict that the FG-repeat Nups act as a 'polymer brush', with diffusion driving translocations (110, 111). Other models describe a partial (112) or full (113) hydrogel matrix through which karyopherins 'melt' through by binding to FG-repeats, dissolving the crosslinks between the Nups and allowing karyopherins to cross. Recent studies measuring stiffness of the central plug Nups support the 'full hydrogel matrix' theory (114).

Native Nup phosphorylation

As previously mentioned, some Nups are post-translationally modified. These include the OGlyNac glycosylations, which may form additional binding sites for various proteins. During mitosis, some Nups become phosphorylated by the cyclin dependent kinases and others, and this causes their departure from the pores as demonstrated by cyclin dependent kinase 1 (CDK1) and members of the NIMA-related kinase family, triggering Nup98's exit the pore before mitosis (115). Other studies show that CKD1 causes deconstruction of the nuclear pores, and use of a broad spectrum phosphatase inhibitor okadaic acid prevented pores from forming (116). Another research group used this phosphatase inhibitor to induce nucleocytoplasmic trafficking inhibition for the classical NLS pathway, though not for the CRM1-mediated export pathway, implying a basal level of phosphorylation and turnover present in normal cells (117). Oxidation, heat and other stresses have been shown to activate some kinase pathways, particularly the mitogen activated protein kinase (MAPK) pathway and PI3 kinase pathways, which decreased interaction of Nups with the pores as well as cargos (118, 119). A phosphoproteomics study detected phosphorylation of Nup50 by ERK1/2, and this phosphorylation was shown to decrease that Nup's affinity for Importin β (120). There is clearly a level of kinase regulation for nucleocytoplasmic trafficking outside of mitosis, but this remains to be described.

Kinases overview

Phosphorylation of nuclear pore proteins facilitated by cellular kinases is a major theme of this thesis. There are over 520 kinases in a mammalian cell (121). These proteins are enzymes that phosphorylate other proteins, usually on a specific amino acid. Kinases are commonly grouped by their phospho-acceptor, as either as serine/threonines or tyrosine kinases. While the exact substrate sites are fairly generic, kinases are more specifically targeted to a particular docking domain on their substrate proteins. An example of this is the DEJL domain, a motif of basic residues followed by a hydrophobic patch used by kinases in the MAPK family. Kinases themselves are frequently activated by phosphorylation, and arranged in phosphorylation cascades (Fig. 1.6) triggered by a cellular event (for instance, receptor binding) to culminate in amplification of this signal. The result is a cellular process, for instance activation of transcription factors to promote cellular growth or apoptosis. Inactivation occurs by removal of phosphate(s) from their active site(s) by phosphatases. Scaffolding proteins, which bind kinases in the inactive state, offer another level of regulation. In quiescent cells, most of the MAPK components are found in the cytoplasm. Most kinases belong to a particular 'cascade' defined by a set of three core kinases. For the purpose of this thesis, the MAPKs will be highlighted. These cascades have 3 core kinases; MAPK-activated protein kinases (MAPKAPs) are activated by MAPKs, which are activated by MAPK-kinases (MAPKKs), which are activated by MAPKK-kinases (MAPKKKs) (Fig. 1.6). Most of these kinases have multiple (closely related) isoforms that vary by localization, regulation, activation or other factors (122), and indeed, many of the kinases themselves contain similar domains (Fig. 1.7).

There are several separate 'modules'/pathways or cascades belonging to the MAPK family. Briefly, the ERK module causes cellular growth and proliferation and is activated by mitogens, to result in mitosis. Inflammatory cytokines, environmental stress and pathogens activate the p38 (so-called for the proteins' size) pathway. The c-Jun N-terminal kinase (JNK) pathways are activated by cellular stress and cytokines, and can yield either cellular apoptosis or proliferation.

Kinase pathways overview
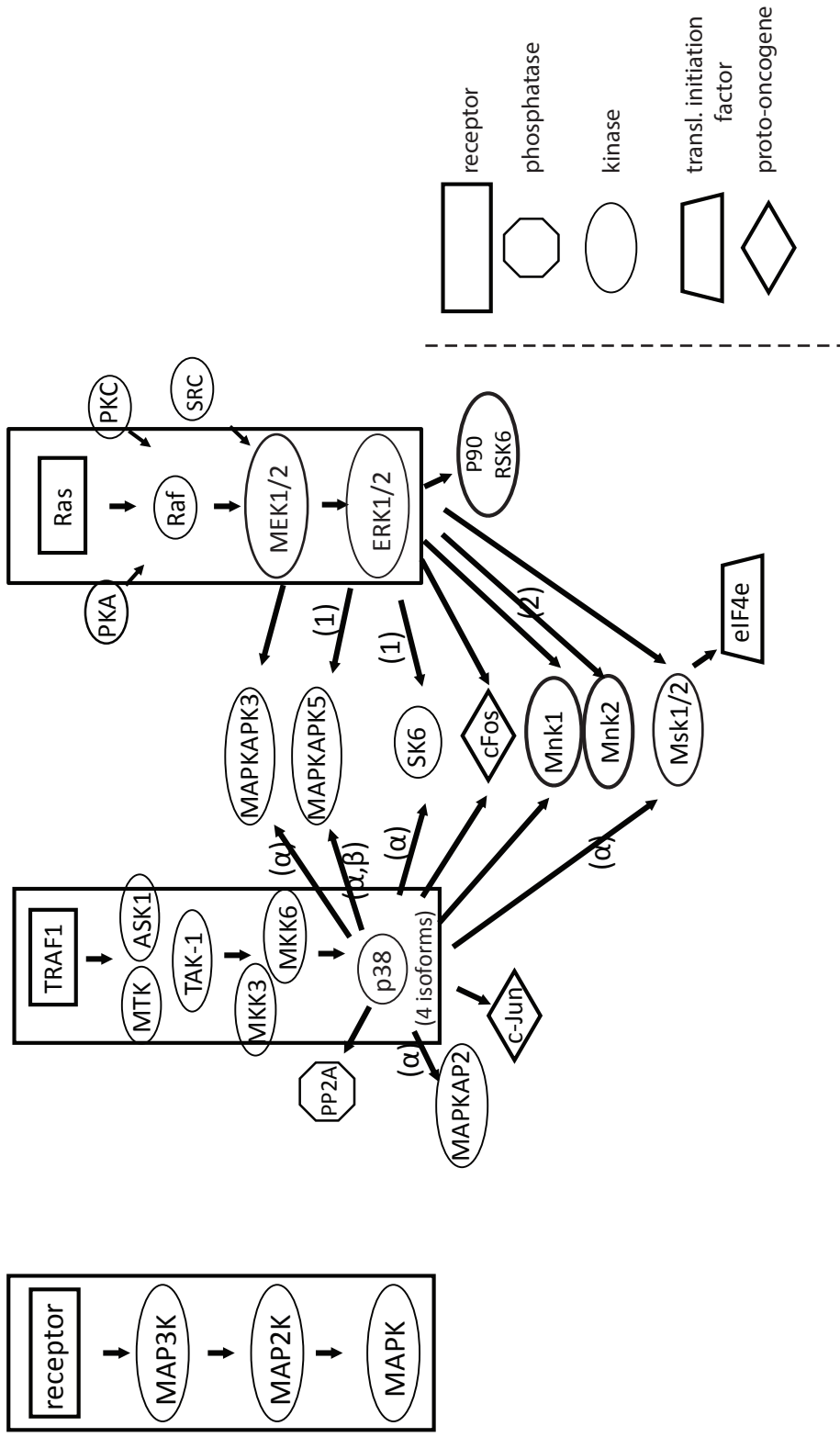
Figure 1.6 General organization of MAPK kinase modules. (Parentheses indicate specific isoforms of activating kinases.)

Kinase domains
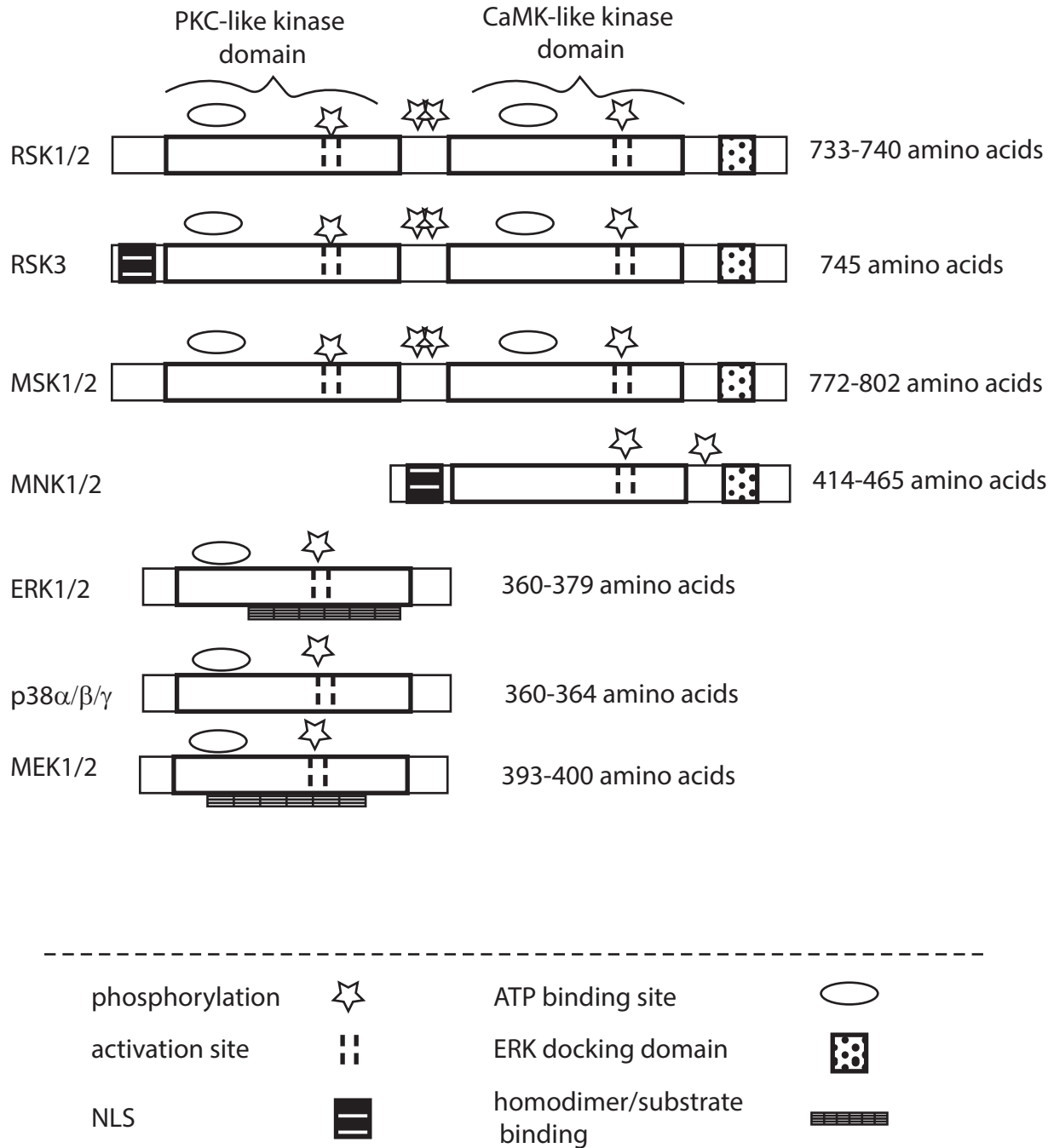
Figure 1.7 Kinase domains. Many kinases belong to protein superfamilies that contain similar domains. The above illustration outlines some of these domains and motifs found on kinases relevant to this thesis. References [123] and genecards.org

Finally, the ERK5 pathway is not as well described nor as extensive, but it promotes cellular proliferation and survival. There are also three atypical pathways, the Nemo-like kinase (NLK) pathway, the ERK3/4 pathway, and ERK7(ERK8) pathway.

ERK MAPK pathway

The ERK1/2 pathway is mediated by Raf; the pathway is activated by platelet-derived growth factor (PDGF), epidermal growth factor (EGF), nerve growth factor (NGF), and in response to insulin, ligand for heterotrimeric G-protein coupled receptors (GPCR), microtubule disorganization, cytokines, and osmotic stress (123). Multiple kinases like protein kinase A (PKA), Akt (protein kinase B), PAK, Src, are specifically able to stimulate this pathway by phosphorylating Raf proteins (A-Raf, Raf-B, and Raf-1), the MAPKKK responsible for activation of MEK1/2. Atypcial among normally multi-activatable kinases, these are the only proteins to activate MEK1/2, which are the only kinase isoforms responsible for activating ERK1/2 (reviewed in (124)). This level of specificity is at least partially attributable to specific binding sites, D docking domains, which bind these proteins to their cognate substrates (125). By this interaction, mitogen activated protein kinase kinase (MEK) 1/2 usually holds ERK1/2 in inactivated form at cellular membranes; once MEK1/2 is activated, it phosphorylates ERK1/2 on highly conserved tyrosine and threonine residues, spaced by a glutamic acid (TEY). There may also be a nuclear mechanism for ERK1/2 activation not fully attributable to MEK activation, which requires D-domain binding (126). ERK1/2 dissociates from MEK, then translocates to the nucleus via where it activates various transcription factors, including NF-AT, myocyte enhancer complex (MEF2), c-fos, c-myc and STAT3. It also activates the MAPKAPKS MNKs, MSKs, and RSKs. In normal cells, ERK1/2 activation is required for cells to progress from G1 to the S-phase in mitosis. ERK1/2 has been reported to contain a potential novel nuclear translocation sequence in the kinase domain which then interacts with transportin7 and traffics into the nucleus (127), as well as being reported to translocate into the nucleus without engaging any

karyopherins (128, 129).

ERK1 (44 kDA, called MAPK3 and p44 in early studies) and ERK2 (42 kDA, called MAPK1 and p42 in early studies), share 85% homology, predominantly in substrate binding regions (130). While they are expressed in many cell types, ERK2 is the slightly more common species, particularly in immune cells. There are additional splice variants, for instance ERK1b, which are not well studied. To interact with MAPKAPKs, ERK1/2 recognize DEF (Docking site for ERK, FXFP) domains on substrates, characterized by the sequence Phe-xxx-Phe-Pro, though a Tyr can replace one of the Phe. These sites are within 6-20 amino acids upstream of the phospho-acceptor serine or threonine. ERK1/2 is inactivated upon dephosphorylation of the TEY domain by dual specificity phophatases (DUSPs) 1, and 5-7 found in the nucleus. Protein phosphatase 2a (PP2A) has been shown to remove phosphates from ERK1/2 and MEK1/2 activation loops (131) in the cytoplasm, and other MAPK phosphatases also inactivate ERK1/2 in the cytosol. Because of ERK1/2's direct relevance in many cellular pathways, drug inhibitors have been determined. These act by binding to the kinase phospho-transfer domain of MEK1 and 1/2 (PD98059 and UO126, respectively (132, 133)) identification of a novel inhibitor of mitogen-activated protein kinase kinase), and thus prevent activation ERK1/2 and the remainder of the pathway. Once inactivated, ERK1/2 has been shown to bind to MEK1/2, which then carries it out of the nucleus by the CRM1 pathway. A notable kinase substrate for ERK1/2 includes p90 RSK1/2/3 (RSK1/2/3), which requires co-activation by phosphoinositide-dependent protein kinase 1 (PDK1). ERK1/2 has been shown to bind to RSK1/2/3, which upregulates stimulation by PDK1 sevenfold; this causes RSK1-3 to activate a broad range of targets to effect gene transcription, cell proliferation, growth and survival by phosphorylating substrates on amino acid sequences R/K-X-R-X-X-pS/T (134) (including c-Fos and eIF2 kinase; reviewed extensively in (123)). It has been shown that RSK3, a kinase downstream of ERK1/2, can bind to ERK2 in a prolonged fashion.

p38 and JNK MAPK pathways

The p38 pathway is activated by environmental stresses (119, 135)) and inflammatory cytokines, including hypoxia, isochemia, oxidative stress, UV irradiation, GPCRs, Rac, Cdc42, tumor necrosis factor alpha (TNFα) and interlukin 1 (IL-1), which cause activation of sundry MAPKKK p38 pathway proteins by recruiting activating factors TRAF adaptor proteins (123). MAPKKKs proteins, MEKKK-1, -2, -3, MLK2/3, ASK1, TAK1, and TAO1/2, stimulate MEK3, MEK6 and MEK4. MEK6 can activate all 4 isoforms of p38, while MEK3 has only been shown to phosphorylate α, β, and γ (136). Activation for p38 occurs on a threonine-glycine-tyrosine (TGY) activation loop. Prior to activation, MK2, MK3, and MK5 act as scaffolding proteins, holding inactivated p38 at the membranes in the cytoplasm. Once activated, p38 can translocate to the nucleus via to activate ATF1/2/6, Elk-1, GADD153, ETS1, MSK1/2, MEF2 and p53. In the cytoplasm, p38 activates MNK1/2, MK2/3, MAPKAPK2 MAPKAPK3, PRAK, Bax, and Tau. Isoforms p38α and β are expressed in a wide range of cell and tissue types, but p38γ and δ have more specific expression (genecards.org).

The isoforms of p38 share some sequence identity; p38α (MAPK14, also called stress activated protein kinase 2a (SAPK2a)), p38β (SAPK2b, MAPK11), p38 γ (MAPK12, SAPK3, ERK6), p38 δ (MAPK13, SAPK4). Interestingly, p38α seems to be the primary form of p38 responsible for its role in inflammation (137). Occasionally, the p38 isoforms have opposite effects. For instance, p38 α stimulates c-Jun (JUN) phosphorylation and is inhibited by p38γ. In the nucleus, p38 is inactivated by DUSPs, and MAPKAPK2 has been shown to remove p38 from the nucleus. During the cell cycle, p38α has been shown to prevent cell cycle progression from G1 to S-phase and G2-M in several ways, including downregulating the activity of CDKs (138); while there are a few instances where p38 isoforms promote cell proliferation, this pathway mainly has apoptotic effects. SB203580 and BIRB0796 are chemical inhibitors of the p38 pathway, and

these act as competitive inhibitors of ATP binding (either by direct competition as with SB203580 (139), or as indirect ATP binding inhibitor (140).

The JNK pathway is also called the stress activated protein kinase (SAPK) pathway. There are three JNK isoforms (α, β and γ) which share 85% homology (reviewed in (123)). The MAPKKKs in this pathway include MEKK1-4, MLK1-3, Tpl-2, DLK, Ask1/2, TAK1, and Tao1/2, which activate MKK4 (SEK1) and MKK7. The activation loops on JNKs are a conserved threonine-proline-tyrosine (TPY) motif, and once phosphorylated, JNKs have many cytoplasmic and nuclear substrates, including transcription factor c-Jun, which promotes cell proliferation.

MAPK pathway overlaps

Substantial crosstalk occurs between the MAPK pathways, illustrated by the somewhat labyrinthine figure models (Fig. 1.6). Regulation is one effect - for instance, p38 activates PP2a, which inactivates the ERK1/2 pathway (141). As evidenced above, many of the downstream kinases are shared between these pathways, likely due to conserved substrate docking and activation sites P-X-[S/T]-P, where the serine or threonine is the phospho-acceptor site; an example of this is MNK1/2 (activator of eIF4E), which is activated by both p38 and ERK1/2 (142), and MSK1/2 (activator of nuclear targets), also a co-substrate for these two pathways (143). The effects of these common downstream targets are usually tempered by localization and downstream substrate availability.

Native kinase regulation by nucleocytoplasmic trafficking

Outside of the cardiovirus-directed Nup phosphorylation events mentioned in previous sections of this chapter, a few recent studies have implicated kinases in the regulation of nucleocytoplasmic trafficking (144). ERK1/2 have been shown to bind to Nup214 (128) and Nup153 (129). Nup153 was demonstrated to be a substrate for ERK1/2 *in vitro* (145). Another substrate relevant to this thesis is Nup50. It was identified by a phosphoproteomics screen

and confirmed with *in vitro* studies as a substrate of ERK-directed phosphorylation, which decreased that Nup's ability to bind to karyopherin B1 (120). Interestingly, Nup30 may also be phosphorylated by ERK1/2 and p38 (146). There are additional studies in which nucleocytoplasmic trafficking is impacted by phosphorylation. Oxidative stress stimulates the MEK-ERK and PI3-Akt pathways, Nup153 became phosphorylated and further glycosylated, and the import of classical NLS was inhibited, though specific kinases were not determined (135). Okadaic acid is phosphatase inhibitor of both PP2a and protein phosphatase 1 (PP1), and when it is incubated with cells, Nup153 becomes hyperphosphorylated ((135) and the appendix of this thesis).

Model of L function

The model we present here (Figure 1.8) involves a L and 2A interaction after cleavage from the cardiovirus polyprotein, and trafficking of 2A:L to the nuclear pore by use of 2A's putative NLS. Once at the pores, L becomes phosphorylated, first on Thr47 by Casein kinase 2, then on Y41 by spleen tyrosine kinase, which strengthens L's affinity for other binding partners CRM1 and Ran. The binding of these supplants 2A, which travels alone to the nucleolus. L:CRM1:Ran then interacts with MAPK kinases ERK1/2 and RSK2/3 (and possibly others) to phosphorylate appropriate substrates within Nups 62, 153, 214 and 98 to prevent their interaction with karyopherins and completely inhibit trafficking through the pores.

Thesis Overview

The work in this thesis (1) establishes the extent of L-directed nucleocytoplasmic trafficking inhibition, (2) additional potential binding partners responsible for L's activities at the nuclear pores, and (3) clearly defines the kinases responsible for this inhibition. The second chapter

Figure 1.8 Working model for L-directed nucleocytoplasmic trafficking inhibition. L and 2A associate and travel to the nucleus. There, L becomes phosphorylated, binds CRM1, Ran and ERK2, and this complex phosphorylates nuclear pore proteins to inhibit nucleocytoplasmic trafficking.

resolves specific cellular pathways inhibited by cardioviruses, that L does not stimulate cytosolic kinases, that Nup98 (and not Nup50) becomes phosphorylated, and that the Nups themselves must be in the context of the native pore complex to become phosphorylated, suggesting that localization of Leader at the pores is required for trafficking inhibition. The third chapter establishes that Leader can bind to exportins CRM1 and CAS, forms a trimeric complex with Ran and CRM, and that knocking down CRM1 decreases L-directed Nup phosphorylation and viral replication. The fourth chapter focuses on siRNA studies and *in vitro* reconstitution assays to establish that kinases ERK1/2 and RSK2/3 (and to a lesser extent p38 α/β) can phosphorylate Nups in the presence of L. Collectively, these results present a model wherein L:CRM1:Ran:kinase complexes are tethered to the nuclear pore, phosphorylating Nups to inhibit nucleocytoplasmic trafficking. The data presented are important for not only for the picornavirus field, but also implicate MAPKs as potential regulators of nucleocytoplasmic trafficking.

Chapter 2: Three Cardiovirus Leader Proteins Equivalently Inhibit Four Different Nucleocytoplasmic Trafficking Pathways

Figures 2.1E and 2.3 were performed by Holly Basta (Palmenberg Lab)

Abstract

Cardiovirus infections inhibit nucleocytoplasmic trafficking by Leader protein-induced phosphorylation of Phe/Gly-containing nucleoporins (Nups). Recombinant Leader from Encephalomyocarditis virus, Theiler's murine encephalomyelitis virus and Saffold virus target the same subset of Nups, including Nup62 and Nup98, but not Nup50. Reporter cell lines with fluorescent mCherry markers for M9, RS and classical SV40 import pathways, as well as the CRM1-mediated export pathway, all responded to transfection with the full panel of Leader proteins, showing consequent cessation of path-specific active import/export. For this to happen, the Nups had to be presented in the context of intact nuclear pores and exposed to cytoplasmic extracts. The Leader phosphorylation cascade was not effective against recombinant Nup proteins. The findings support a model of Leader-dependent Nup phosphorylation with the purpose of disrupting Nup-transportin interactions.

Introduction

Cardioviruses, as members of the *Picornaviridae* family, are positive-sense, single-stranded

RNA viruses. Their preferred hosts are rodents, although some will readily infect other mammals. Of the three recognized species in this genus, two are represented by encephalomyocarditis virus (EMCV) and Theiler's murine encephalomyelitis virus (TMEV). Saffold virus (SafV), within the same Cardiovirus B species as TMEV, is one of the few members of this genus to infect humans (147). While cardioviruses have similar polyprotein organizations, each encodes a variable-length Leader (L) protein, none of which have homologs or analogs in other viruses or cells. Leader proteins are unique determinants of cardiovirus anti-host activities. Although not kinases themselves, the Leaders induce intense hyper-phosphorylation of certain Phe/Gly-containing nuclear pore proteins (Nups), including Nup62, Nup153 and Nup214 shortly after infection (71, 73). Phosphorylation of Nups within nuclear pore complexes (NPC) down-regulates active nuclear import by hindering importin association with the Nups (117, 120). This novel mechanism can be recapitulated by transfection of L-encoding cDNAs into cells or by the addition of recombinant L protein into cell extracts containing nuclei as targets (63, 73). The *in vitro* assays directly mimic the trafficking inhibition observed by cardiovirus infection-directed Nup phosphorylation.

The EMCV L (L_E) is 67 amino acids (aa) long. The NMR solution structure for the closely related Mengo L (L_M) shows an unusual N-proximal zinc-finger domain. The rest of the protein configures as random coil (78). Functionally, the L_M coiled region has a C-proximal acid-rich domain and a central hinge segment which forms the primary induced-fit binding contacts with RanGTPase, a requisite partner in the anti-host activity (53, 64, 74). L_E is shuttled to the nucleus after its polyprotein synthesis presumably by interactions with the viral 2A protein with which it can also interact (48). In the presence of guanine nucleotide exchange factor, RCC1, just inside the nuclear rim, L_E then exchanges 2A for Ran (48). The L_E interaction with this key trafficking regulator is very tight, with a measured K_D of about 3 nM (77). Before, or shortly after this nuclear exchange, L_E becomes phosphorylated at Thr_{47} and Tyr_{41}, in steps which are obligate

for the consequent L_E-dependent Nup phosphorylation activities (63). The NMR orientation of L_M, when bound to Ran, shows the pairing forces Ran into an allosteric conformation which mimics the RanGTP-bound active state of this transport regulator. As such, Ran (with L_M) becomes competent to bind exportins and their cargos for putative shuttling to the cytoplasm (78). It has been proposed that this complex (L_M:Ran:exportin), formed in the nucleus, subsequently recruits activated kinase cargos, such as p38 and/or ERK1/2 (75), and the full unit, unable to dissociate because of the bound Leader, becomes trapped in the nuclear pore, where the kinases catalyze the cell-debilitating hyper-phosphorylation of Nup62, Nup153 and Nup214 (78).

The L proteins of SafV (L_S) and TMEV (L_T) are similar in many respects. Cardiovirus B species Leaders are 4 (L_S) to 9 (L_T) aa longer than L_E or L_M, with the added length mostly evident as short contiguous insertions C-terminal to the Ran-contact hinge domain. Each also has an additional small relative deletion next to the N-terminal initiating Met. Like L_M/L_E, the TMEV and SafV proteins become dually phosphorylated in cells or in recombinant form, but at different sites (i.e. Ser_{57} and Thr_{58}, respectively) and by different kinases (AMPK, not CK2) than the better studied EMCV systems (64). When recombinant L_T or L_S, are introduced into cells, even in the absence of infection, they can indeed induce Nup62 phosphorylation, the common assay for hyperphosphorylation (63).

There are many elements of the L-directed Nup phosphorylation model that are not well understood. It is unknown, for example, if there are other Nup proteins which are targets (or non-targets) of the activated kinase complexes. The matrix protein of vesicular stomatitis virus (VSV) causes nucleocytoplasmic trafficking inhibition (148) by complexing with Nup98 and the exportin Rae1 (149). Similar to a phenotype described for TMEV infections, where Nup98 is also reported to be phosphorylated (63, 150), VSV inhibition of Nup98-dependent trafficking

stops the export of cellular mRNAs and prevents the transcription of interferon and chemokine

products (70, 73, 151, 152). The full collection of Nup62, Nup98, Nup153 and Nup214 are also

among the demonstrated substrates for human rhinovirus (RV) protease 2A. These cousins of

the cardioviruses inactivate NPC import/export by multiple Nup cleavage reactions rather than

by phosphorylation cascades (65, 68). The sequence differences in specific 2A[pro] which are

characteristic of the multiple RV genotypes allow individual viruses to preferentially cleave

selected cohorts of Nup substrate panels with different avidities and rates (68). Consequently,

not all import/export pathways are equivalently disabled by every RV, allowing each 2A[pro]

sequence to manifest as a strain-specific Nup degradation pattern (69).

With the cardioviruses, it isn't known whether L_E-directed Nup hyper-phosphorylation is aimed

more generically at all transport pathways, or like the RV, is more selectively directed at only

those import/export units which use particular subsets of Nups. Cardiovirus systems to test

these parameters have typically linked traceable reporters (e.g. GFP) to peptide fragments (e.g.

SV40) with non-specific nuclear import localization signals (NLS), or tried to follow common

cellular mRNAs as the metric for nuclear egress (74). These previous experiments are less

sensitive than the newer, path-specific assays recently described for the RV (69). Application of

those new systems now provides clarification on the scope of L_X disruption of trafficking

pathways for the L_E, L_S and L_T proteins, and as described here, show all 3 of these viruses act

ubiquitously against 4 tested pathways, including a path dependent upon a nuclear export signal

(NES) for protein egress. Moreover, observation of L_X-dependent Nup phosphorylation becomes

accelerated in cell-free systems by the presence of okadaic acid (OA), an inhibitor which

prevents counterproductive phosphatase activities on both the susceptible Nups and on the

required cellular kinases.

Results

Nup98 and Nup50.

Transfection of cells with L_X-encoding cDNAs, followed by Western analyses is the standard assay for L_X-dependent Nup phosphorylation (74). Some prior experiments also evaluated Westerns or $\gamma^{32}P$ incorporation after incubation of recombinant L_X proteins with fractionated cell nuclei and cytosol (53). The size (67-72 aa) and charge (pI ~3) of L_X proteins presents technical issues unless these segments are linked to fusion tags, such as GST or GFP (75). For L_E, the observed Nup phosphorylation after cDNA transfection was comparably strong (63) whether the tag was N-terminal (e.g. GFP-L_E), or C-terminal (e.g. L_E-GST), as illustrated in Fig 2.1A. The common detection antibody (mAb414) recognizes multiple Phe/Gly-containing Nups, albeit with differing affinities. Typically, Nup62 modifications manifest on gels as a "smear" towards higher mobility when multiple phosphates are added sequentially. The change is distinctive whether L_E is assayed after transfection of cDNA (e.g. Fig 2.1A), or as recombinant protein in cell-free extracts (e.g. Fig 2.1B). The same is true for Nup153 and Nup214 (73). Nup50 and Nup98, however, are only intermittently detectable with this mAb (e.g. Fig 2.1B). For these, evaluation of the L_X-dependent changes required different reagents. Cytosol/nuclei mixtures similar to Fig 2.1B, were labeled with $\gamma^{32}P$-ATP, and then extracted with mAbs specific to Nup50 or Nup62. While Nup50 was observable by Western analysis (Fig 2.1B), the presence of GST-L_E, did not direct detectable label incorporation (Fig 2.1C), nor did it shift in molecular weight. Nup62 on the other hand, was demonstrably labeled with ^{32}P by the inclusion of GST-L (Fig 2.1D). Equivalent Nup98 reagents are not effective in similar immunoprecipitation experiments. For this evaluation, HeLa cells were transfected with cDNAs encoding L_E-GST, L_S-GST, L_T-GST, and also with corresponding cognates encoding Cys-to-Ala L_X-inactivating mutations (63). In every case when there was active L_X protein, the Nup98 mAb detected the upward "smear" of L_X-dependent phosphorylation. The activities ranked as $L_E > L_S > L_T$ for these particular conditions.
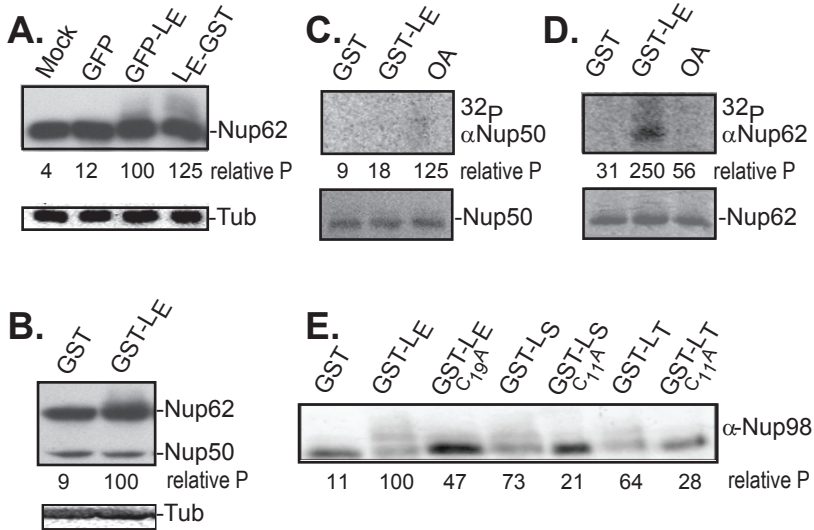
Figure 2.1 Nup phosphorylation assays for Nup98 and Nup50. (A) HeLa cells were transfected with cDNAs encoding the indicated proteins. After 16 hrs, harvested lysates were probed in Western assays using mAb414 (Nup62) or α-tubulin (Tub). (B) Recombinant L_E-GST or GST-L_E proteins (5 µg) were incubated with HeLa cytosol supplemented with isolated nuclei. After 45 min, the samples were fractionated, then probed by Western analyses as in A. (C) HeLa nuclei, cytosol and recombinant GST or GST-L_E were incubated with γ-32P-ATP in the presence or absence of okadaic acid (OA). After incubation at 37°C for 45 minutes, proteins reactive with α-Nup50 were extracted and fractionated. Upper panel is an autoradiogram. Lower panel is a silver stain of the same materials. (D) Same as C, except immunoprecipitation was with α-Nup62. (E) Similar to A, unlabeled transfected lysates were fractionated, then probed in Western assays with α-Nup98. In panels A, B, E, the "relative P" is pixel count (TotalLab software) in the phosphorylated product, normalized to GFP-L_E or GST-L_E controls. For C, D, these values are the relative pixels in the labeled bands, normalized to the silver stain signals.

Therefore, Nup98 but not Nup50, is a target of the L_E-dependent phosphorylation cascades (Fig. 2.1E).

Import/export Pathway Imaging

During EMCV infections, L_X cDNA transfections, or cell-free reactions with recombinant proteins, NPC active import/export is abrogated. Small proteins (<40 kD) and metabolites then diffuse across the NPC to equilibrium (73). Visualization of this process requires addition of fluorescent reporters linked to NLS sequences to record relative changes in nuclear/cytoplasmic cellular distribution. Recombinant GST-GFP$_{NLS}$, for example, was previously tracked in digitonin-treated HeLa cells to document GST-L_E concentration and rate effects (73). HT$_{NLS}$ (Halotag), transfected as cDNA into cells, showed similar relocalization (70, 71, 73). In all these previous experiments however, the tested reporter-NLS was from SV40, which traffics via the importin α/β pathways and is responsive only to particular segments of the Nup cohort (Table 2.1) specific to that karyopherin passage through the NPC (153-155).

The impact of L_X on other characterized transport pathways was assessed with HeLa cell lines transduced with mCherry reporter genes (~30 kD) linked to additional NLS/NES segments (~15-45 aa; (69)). After infection with vEC$_9$ (3 hr), the cells and controls were fixed, stained with DAPI and imaged (Fig 2.2). Averaged pixel scans centered over the width of individual nuclei showed that the mCherry signals, compared to steady-state DAPI, diminished measurably after infection of cells, if the reporter was linked to the SV40 NLS, the M9 NLS (156), or the RS domain NLS from an SR protein, splicing factor 2 (157). Previous characterization of these cells with rhinovirus reagents confirmed the cell-wide stability of the total mCherry signal (69). The reporter signal redistributes out of nuclei during infection, but is not degraded. The fourth tested cell line expressed mCherry linked to the leucine-rich NES from PKI (158). This segment is sensitive to CRM1-mediated active nuclear egress. Here, the initial nuclear exclusion of the reporter was reversed after infection, allowing a stronger mCherry signal to accumulate in the
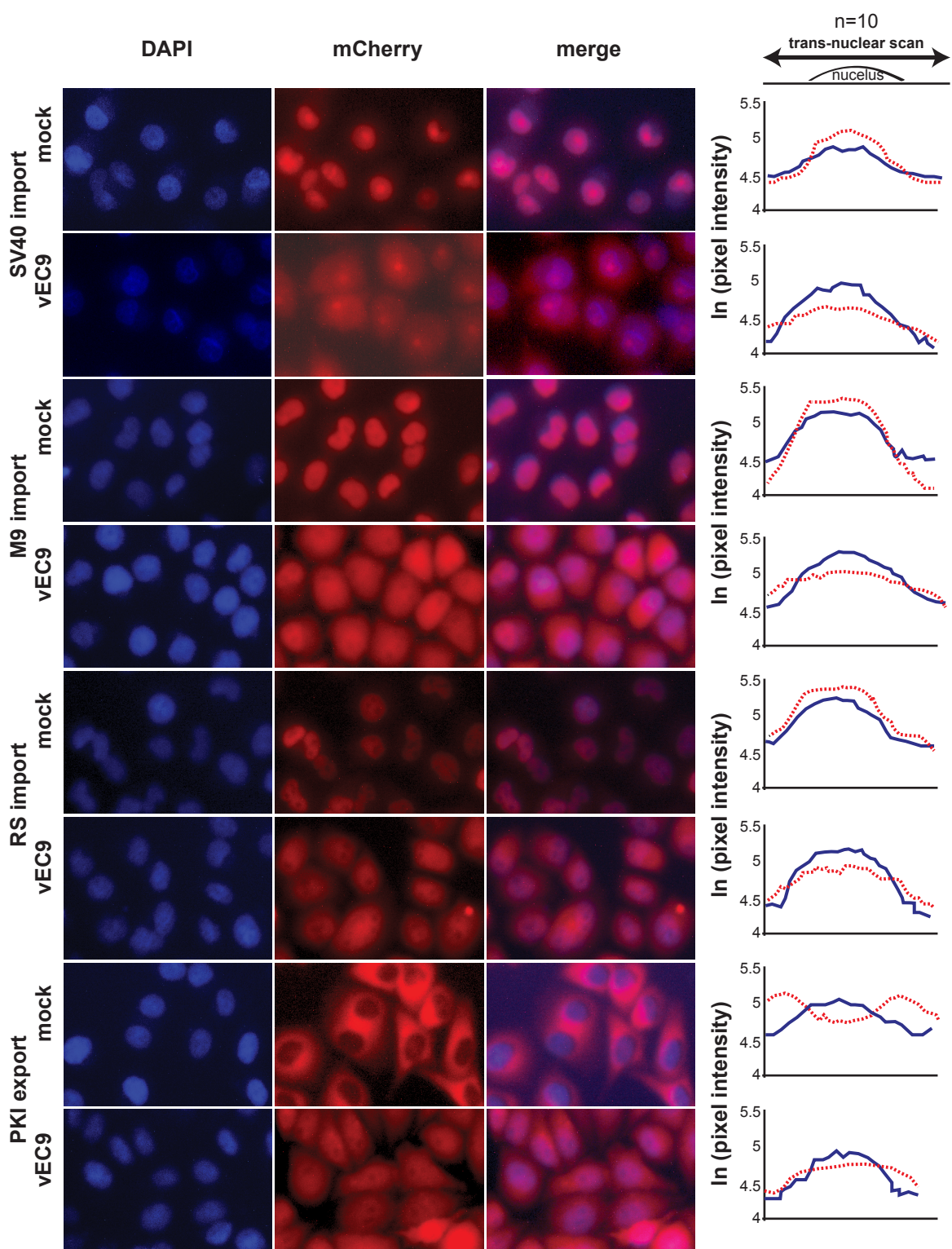
Figure 2.2 Trafficking disruption by EMCV. Transduced HeLa cells expressing mCherry fusion proteins linked to NLS (SV40, M9 or RS) or NES (PKI) import/export sequences, were infected with vEC9 (MOI=15). At 3 hrs, the cells were fixed, stained with DAPI and imaged. For each condition, randomly selected individual cells (n=10) were scanned for pixel intensity (linear stretch of 80 pixels), centered on the DAPI signal. The values were averaged and plotted as the natural log of each signal for DAPI (blue solid line), and mCherry (dashed red line). The average standard deviation was 0.210 ln(x) (range: 0.124 to 0.274).

nuclei relative to control cells. For each of these 4 lines, infection with vEC_9 impacted the respective mCherry-labeled NPC transport pathway. Virus disruption of active transport into or out of the nuclei resulted in reporter redistribution by diffusion relative to the steady-state DAPI signals.

The L_E protein of intact vEC_9 is the effector for the experimental set depicted in Fig 2.2. Cell visualization assays with the same mCherry cell lines were repeated after transfection with cDNAs encoding L_E-GST, L_T-GST or L_S-GST. Again, averaged pixel scans centering on the nuclei illustrated the impact of L_X on mCherry relocalization (Fig 2.3), this time in live, unfixed cells. Within these graphs, the solid lines now represent the mCherry profiles observed in control cells (i.e. equivalent to Fig 2.2, mock). Relative to this, expression of all three L_X proteins mediated measurable reporter diffusion out of (NLS lines), or into (NES line) nuclei. Unlike the rhinovirus $2A^{pro}$ which can discriminate these respective import/export systems according to virus genotype (69), the 3 cardiovirus L_X proteins seemed equivalently adept at disrupting all 4 tested transport pathways (Fig 2.3).

Context for Nup Phosphorylation

L_X-dependent Nup phosphorylation assays typically present the substrates in the context of intact NPC, either by testing within whole cells (transfection, infection), or by reconstituting isolated cytoplasm and nuclei in the presence of recombinant L_X (73, 75). The current hypothesis predicts that Ran-bound L_X, complexed with an exportin and activated kinase cargo, becomes trapped within an NPC, leading to Nup hyperphosphorylation (78). Recombinant GST-Nup62 (68) and His-Nup98 (personal communications, K.E. Watters) have been demonstrated as native-like substrates for RV $2A^{pro}$. But when either protein was added to dounce-homogenized HeLa cell whole-cell extracts, or to subcellular fractionated HeLa cytosol, GST-L_E failed to induce detectable phosphorylation (Fig 2.4A,B). The whole-cell lysates and HeLa cytosol each contain endogenous Nups, either as precursors to nascent NPC assembly
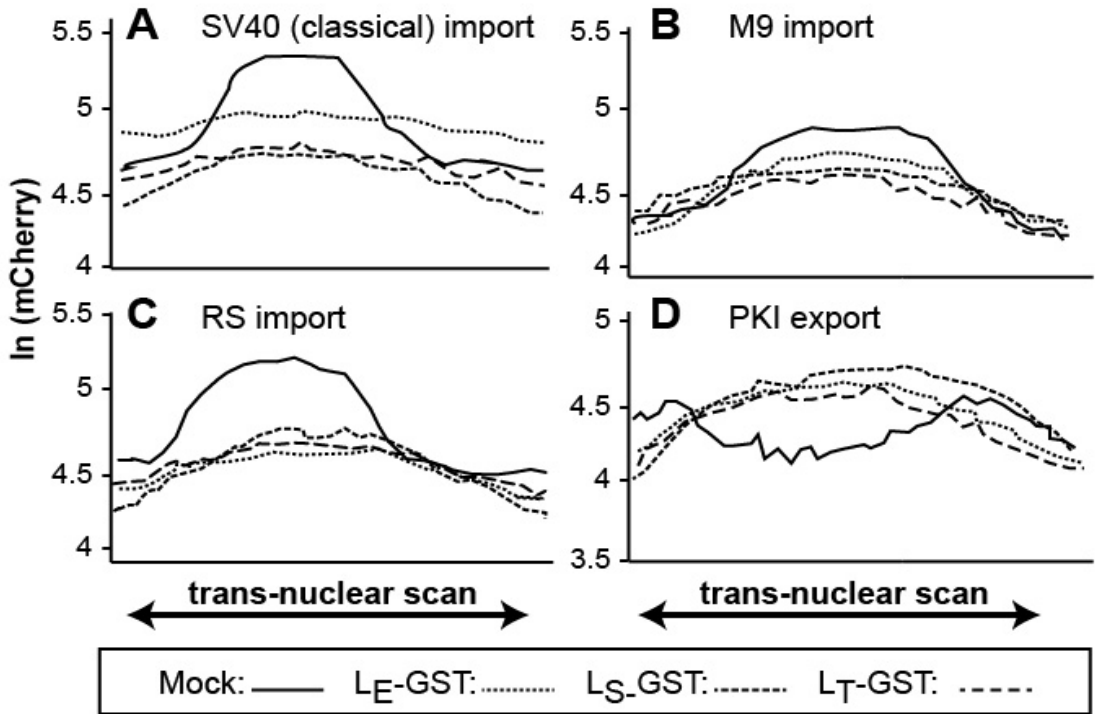
Figure 2.3 Trafficking disruption by cardiovirus cDNAs. Similar to Fig 2.2, transduced HeLa cells expressing mCherry fusion proteins linked to the SV40 NLS (A), M9 NLS (B), RS NLS (C) or PKI NES (D) were transfected with cDNAs for L_E-GST, L_S-GST or L_T-GST. After 16 hrs, individual live cells (n=8) were imaged for mCherry pixel intensity (linear stretch of 80 pixels) centered on the nucleus. Mock cells (solid lines) were transfected with cDNA for GST alone. The average standard deviation was 0.1274 ln(x) (range: 0.64 to 0.244).
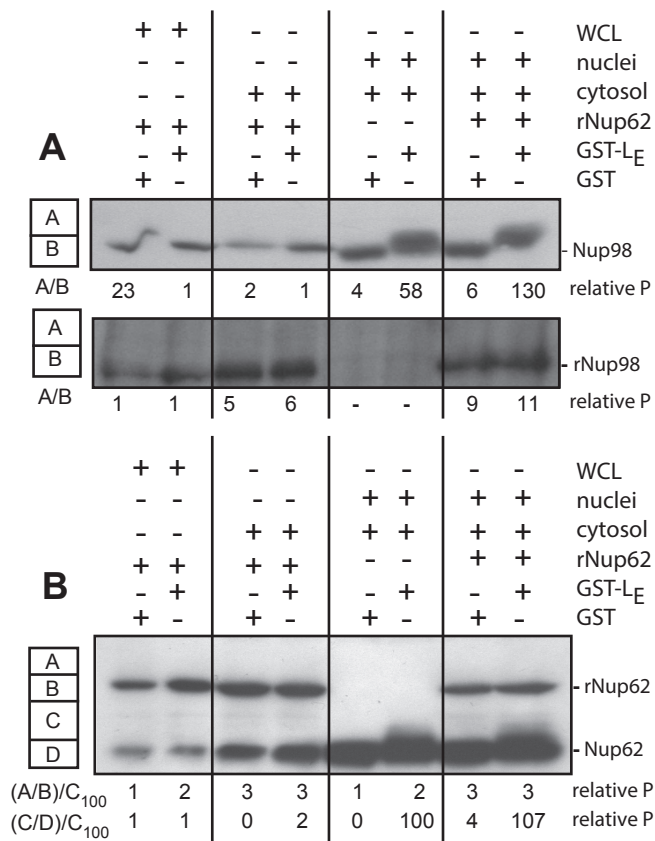
Figure 2.4 Nup format for L-directed phosphorylation. Cell-free systems containing HeLa whole-cell lysates (WCL), cytosol, or cytosol plus isolated nuclei were reacted with recombinant GST or GST-L_E, in the presence or absence of recombinant His-Nup98 (A) or recombinant GST-Nup62 (B). After 45 min of incubation, the samples were fractionated, probed by Western analyses using α-Nup98 and α-His (A), or α-Nup62 (B). Pixel counts in the A, B, C, D boxes for each lane show the areas recorded and normalized to the control samples, as relative measures of observed phosphorylation.

(cytosol), or from the cell disruption (whole cell lysates). For Nup62 the native and recombinant forms are easy to distinguish by size (Fig 2.4B). For Nup98, the proteins co-migrate, but rNup98 phosphorylation would still be evident by measuring the A/B area ratios on the Western blot as detected with the His-tag mAb (Fig 2.4A). Although all these samples also contain Ran, CRM1, and kinases, in the absence of intact nuclei, neither the recombinant nor the endogenous Nups became phosphorylated in an L_E-dependent manner. It required the addition of intact nuclei back to these mixtures to see evidence of Nup phosphorylation. Even then, however, recombinant proteins were still not viable substrates. The Nup phosphorylation mechanism was capable of discriminating context and modified only the native Nups, presumably those presented by the nuclei NPC.

Kinase Activation

Inhibitor experiments have implicated mitogen-activated protein kinases (MAPK), particularly ERK1/2 and p38, as the probable pathways involved in Nup phosphorylation during EMCV infections or L_E-dependent cDNA transfections ((75), Chapter 4). In intact cells, activation of both enzymes can be observed in the presence of L_E, independent of the simultaneous activation of their upstream signaling cascades, including MEK1/2, MKK3, MKK6 and cRaf. The pathway activation points must then be at or near the effector enzymes themselves (75), potentially involving phosphatases rather than kinases as the regulatory mediators. This idea was tested with the reconstituted cytosol and nuclei mixes, supplemented with GST-L_E (Fig 2.5). As described above, this experimental combination gives effective Nup hyperphosphorylation. Surprisingly though, only very weak signals were detected with mAbs specific to the phosphorylated effector kinases (Fig 2.5AB, GST-L_E lanes). Reasoning that the activated kinases could be cycling, the protein phosphatase 1/2a inhibitor, okadaic acid (OA) was added at a concentration that inhibits such enzymes (159). The OA increased the phosphorylated ERK1/2 and p38 signals by at least 10-20 fold, presumably by preventing dephosphorylation
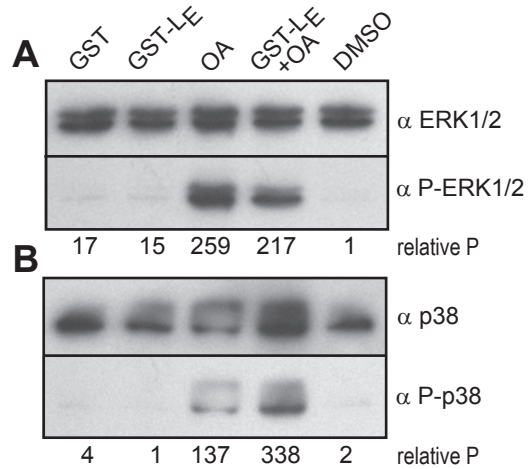
Figure 2.5 Kinase activation in cytosol. HeLa cytosol was reacted with recombinant GST or GST-L$_E$ in the presence or absence of okadaic acid (OA) and/or DMSO. After 45 min of incubation, the samples were fractionated then probed by Western analyses using (A) α-ERK1/2, α-P-ERK1/2, or (B), α-p38, α-P-p38. Pixel normalization for each lane was relative to the respective, unactivated (unphosphorylated) forms of the kinases.

within the MAPK pathways and allowing the intermediates to accumulate (160). In the absence of GST-L_E, OA had only a modest effect on Nup62 phosphorylation in these reactions, as measured by autoradiography (Fig 2.1D, OA lane). It is known that some Nups, including p150 in *Drosophila* cells, can become phosphorylated by CDK1 in the presence of OA (116), as are other non-specific Nups in mammalian cells (117). Nup50 contains a phosphatase-sensitive phosphorylation site (120). Indeed, in the cell-free reconstitution assays this observation was confirmed by low-level incorporation of $\gamma^{32}P$ into Nup50-specific material (Fig 2.1C) in the presence of OA.

Discussion

ERK1/2 and p38 have been implicated as effector kinases in L_E-dependent Nup hyper-phosphorylation ((75), Chapter 4). In phosphor-proteomics studies (120) Nup50 has been suggested as a potential substrate for ERK1/2, and it was therefore of interest to assay this protein's putative alterations in the presence of L_E. Although in the presence of the phosphatase inhibitor OA (without GST-L_E), Nup50 did become labeled with $\gamma^{32}P$, L_E did not direct this event (Fig 2.1). Under similar circumstances, in addition to the previously described phosphorylation of Nup62, Nup153 and Nup214, the phosphorylation of Nup98 was readily observed and dependent upon the presence of active L_E, L_T and/or L_S sequences. The Nup phosphorylation within this cohort required the substrates to be presented in the context of intact nuclei, because when tested with parallel recombinant versions of Nup62 or Nup98 that do not become incorporated into nuclear pores, the L_E-dependent mechanism only altered the native proteins (Fig 2.5). Though some substrate-altering aberration of the recombinant Nups cannot be entirely ruled out, proximity (possibly through trapping the L_X:Ran complexes within the NPC) is the most likely explanation for this observed mechanistic preference. If captured within the NPC, limited catalytic amounts of the L_X complexes might then direct massive hyperphosphorylation of the preferred substrates.

When rhinoviruses infect cells, the virus-encoded 2A^{pro} cleave many of the same subset of NPC Nups affected by L$_X$-dependent hyperphosphorylation (65, 68). As it is with the cardioviruses, the effect is down regulation of active nuclear import/export and redistribution of diffusible proteins throughout the cell. A special characteristic of the rhinovirus system, though, is that not all import/export pathways are affected equivalently. The genotype-specific sequences of individual 2A^{pro} have different Nup cleavage preferences (68), and therefore, the order, rate and location of each NPC cleavage can be used by these viruses to regulate the specific activities of nucleocytoplasmic cargo exchange. This has been demonstrated for the SV40, M9 and RS NLS-dependent import pathways and the CRM1-dependent export pathway (69). The classical NLS (SV40) pathway uses karyopherins importin α/β to transport a broad range of cargos (161, 162). After the cargo:karyopherin complex is formed, it traverses the NPC via transient interactions with preferred Phe/Gly sites on multiple Nups (see Table 2.1), including Nup62, Nup98, Nup153, Nup214 and Nup358 (163). The M9 nuclear localization signal is from the mRNA binding protein hnRNPA1. It is recognized by transportin1 (karyopherin B2 in yeast, reviewed in (92), which is also responsible for import of HIV-1 Rev into the nucleus. The RS sequence from splicing factor 2 is recognized by transportin 3, a member of the karyopherin β family, and mediates the transport of SR proteins containing Arg-Ser-rich domains (RS) involved in the regulation of pre-mRNA splicing (164, 165). The PKI nuclear export pathway uses CRM1 (XPO1), a transportin which interacts with cargos or adaptors bearing leucine-rich motifs (101) such as the HIV-1 Rev protein, the protein kinase A inhibitor (PKI), 5S rRNAs, and U snRNAs (158, 166).

It has been proposed that rhinoviruses, by subtly balancing the trafficking unique to these pathways, can tailor the cell's cytokine responses to needs of each genotype (69). The cardiovirus L$_X$ activities, however, when tested with these same pathways (Fig 2.2, Fig 2.3) seemed to show an indiscriminant, brute force NPC attack mode. Although activated kinases

Table 2.1 Nups Associated with NPC Pathways

NLS/NES Motif sequence	Required Nups[1]		Karyopherin[1]
Classical import pathway. NLS is from the SV40 large T-antigen protein	Nup62 Nup98 Nup153	Nup214 Nup358	importin α/β
M9-mediated import pathway. NLS is from the M9 domain of mRNA binding protein hnRNPA1	Nup62 Nup98 Nup153		transportin 1
RS-mediated import pathway. NLS is from the RS domain of splicing factor 2, an SR (Arg/Ser-rich) protein.	Nup98 Nup153		transportin 3
Leucine-rich NES-mediated export pathway. NES is from the protein kinase A inhibitor (PKI)	Nup62 Nup98 Nup153	Nup214 Nup358	CRM1

[1] Nup and karyopherins assignments are reviewed in (107, 109)

frequently transit the NPC in their roles as transcription regulators (167), there are few reports of coincidental (or accidental?) Nup phosphorylation. In uninfected cells, some Nups do become partially phosphorylated during mitosis, contributing to the transient dissociation of the NPC, but the cardiovirus-fostered events are unique biological phenomena in the strength and extent of Nup targeting. Not only were all 4 tested import/export pathways compromised within 3 hr of vEC_9 infection, but all 3 L_X-GST proteins, L_E, L_T and L_S, were equivalently effective against all of the pathways. Apparently, phosphorylation is a much less discerning method of NPC disruption than rhinoviruses' incisive proteolytic cleavage. The monitored processes also included measurable disruption of karyopherin-mediated NPC cargo export (i.e. CRM1). Although not directly tested here, one might expect the $\beta3$ importin 5 pathway, responsible for the transport of various ribosomal proteins, to be additionally hindered by L_X, as it requires the same subsets of altered Nups, including Nup62, Nup98, Nup153, and Nup214 (103, 168). Still, despite the obvious broad-based NPC changes brought about by hyper-phosphorylation, it was somewhat surprising to find a level of L_E-dependent substrate selection within these pores. Nup50, which is not phosphorylated by L_E, is also not implicated in any of the above transport pathways. This is despite observations that Nup50 can indeed, during normal cell cycling, be phosphorylated by ERK1/2 (120), one of the enzymes in the L_E mechanism (75). The potent phosphatase 1 and phosphatase 2a inhibitor OA, increased the pools of activated kinases, including ERK1/2 in the cell extracts, and allowed Nup50 phosphorylation. Phosphatases generally serve custodial roles during certain normal cellular events. In particular, protein phosphatases 1 and 2a interfere with MAPK pathways and are responsible for reversing any cyclin dependent kinase conferred- Nup phosphorylations acquired during mitosis (116). Full reconstitution of NPC during cell cycling actually requires this type of phosphate curating, and these processes are therefore sensitive to OA (116).

Conclusions

Here, we present data that Nup hyper-phosphorylation pathways by L_E, L_T and L_S, all target Nup98, in addition to Nup62 (73). Nup50, on the other hand was not phosphorylated by recombinant L_E protein, and by inference, during infection. Furthermore, L_E-dependent Nup phosphorylation in cell-free assays requires the substrates to be presented in the context of full nuclear pores (i.e. intact nuclei), as supplemented with cytosol (74). When this happens, at least 3 independent cellular importin pathways (importin α/β, transportin-1, transportin-3), and an exportin pathway (CRM1) become compromised, as monitored with cell lines transduced to express path-specific mCherry NLS/NES reporters.

Materials and Methods

<u>HeLa Cell Lines.</u>

Suspension cultures were maintained in modified Eagle's medium (37°C, 10% calf serum, 2% FBS, under 5% CO_2). In addition to standard cells (ATCC CRL 1958), stable transduced cell lines carrying mCherry reporter genes linked to defined NLS/NES sequences have been described (69). Briefly, the SV40 large T antigen NLS, M9 NLS (156), the RS NLS from splicing factor 2 (157), or the leucine-rich NES from PKI (158) were engineered in-frame, C-terminal to an mCherry gene in the context of a retroviral vector plasmid encoding neomycin resistance (169). Murine leukemia virus (MLV) vectors were used in combination with these plasmids to create virus stocks harboring the respective genes. Infection of HeLa cells, genome integration and antibiotic selection gave cell lines with highly visible, constitutive expression of the mCherry derivatives. Before visualization, plated cells were rinsed with PBS (2x, 137 mM NaCl, 2.7 mM KCl, 10mM Na_2HPO_4, pH 7.4), treated overnight at 4°C with 4% paraformaldehyde, and then rinsed with PBS (3x) before the addition of DAPI (1ug/ml).

Cell Fractionation

HeLa cytosol was isolated after swelling suspension cells in hypotonic buffer (0.75 Mg(OAc)$_2$,

0.15 mM EDTA, 1 mM PMSF, 0.01 mg/ml leupeptin, 20 mM pepstatin A, 3 mM DTT), followed

by dounce homogenization and clarification (16,000×g, 20 min, 4°C). TB (1/10 volume, 10x at

20 mM hepes pH 7.3, 2 mM Mg(OAc)$_2$, 110 mM K(OAc), 1 mM EGTA) was added before

storage at -80°C. Whole cell lysates were prepared similarly, by the addition of WCLB (50mM

Tris pH7.4, 50 mM NaF, 5mM Na$_4$O$_7$P$_2$, 1 mM EDTA, 1mM EGTA, 250mM mannitol, 1% triton

x100; 1mM DTT, 1mM PMSF, 20 mM pepstatin A, and 1x protein phosphatase inhibitor cocktail

3, Sigma Aldrich) to cells, followed by sonication (2x, 30 sec, 4°C) and clarification (16,000xg,

10 min). The materials were aliquoted and snap-frozen before storage at -80°C. Nuclei were

isolated from suspension cells following treatment with digitonin and clarification to remove

cytosol (170). Briefly, the cells were collected, washed (2x, PBS), then incubated (10 min, 4°C)

in RSB (10 mM Tris-HCl, pH 7.4, 100 mM NaCl, 2.5 mM MgCl) with digitonin (40ug/ml, Sigma

Aldrich). The samples were clarified (2000xg, 8 min), and the pellets were rinsed with RSB, then

TB (plus 1 mM DTT, 3x). Quantitation was with a hemocytometer after staining with tryphan

blue.

Transfection and Infections

Eukaryotic expression plasmids for GST, GFP, GFP-L$_E$, L$_E$-GST, L$_T$-GST (BeAn), and L$_S$-GST

(SafV-2) were as described (64, 75). The GST-L$_X$ panel also had matched cognates encoding

corresponding, inactive L$_X$ sequences (C$_{19}$A, or C$_{11}$A). Cells were transfected (3x10^5 cells per

well, 1 ug cDNA) using lipofectamine (1 ul, Invitrogen) in Opti-MEM media (Invitrogen), and then

incubated (37°C under 5% CO$_2$). Infections with vEC9 (171) used an MOI=15, in PBS. At

harvest, the wells were rinsed (2x, PBS) before 2x SDS buffer was added. Cell materials were

collected and boiled (15 min) before fractionation by SDS-PAGE and protein detection in

Western assays.

Microscopy.

Cells (live or fixed with paraformaldehyde) were visualized with a Ti-E ECLIPSE inverted wide-field microscope (Nikon Corporation). The images were collected using a CoolSnapHQ camera (Photometrics). Excitation/emission filter sets detected 460 nm (DAPI) and 632 nm (mCherry). Nikon NIS Elements software (version 4.30.01) was used to tabulate individual pixel intensities across an 80 pixel-window, centered on the nucleus, per cell. DAPI and mCherry data for a minimum of 10 live cells, or 8 fixed cells per experimental condition were collected. The values were compiled in Excel and averaged across the 80 pixel windows. To compare conditions with fixed cells, the averaged DAPI levels were normalized. The natural log of each point in the intensity profile was plotted.

Recombinant Proteins

Recombinant engineering, bacterial expression and protein isolation for GST and GST-L_E have been described (74). The isolation of recombinant GST-Nup62 (human) is also described (68). Purified recombinant His-Nup98 (human) was a gift from Dr. Kelly Watters.

Westerns and Antibodies

Samples were boiled with SDS buffer before the proteins were resolved by SDS-PAGE, and transferred to polyvinylidene difluororide membranes (Immobilon-P, Millipore). The membranes were blocked (30 min) in TBST (20 mM Tris, pH 7.6, 150 mM NaCl, 0.5% Tween 20) with 10% dry milk as described (73). For Western assays, the membranes were incubated with a primary antibody (in TBST, 1% dry milk, overnight, 4°C), before rinsing (3x, TBST), and addition of a secondary antibody (1 hr, 20°C). After additional rinses (3x, TBST), the membranes were developed according to manufacturers' specifications for enhanced chemiluminescence (Pierce, GE Lifesciences). Antibodies included: α-Nup98 (goat mAb, IgG, Sigma, 1:10000), α−FG-repeat Nups (murine mAb414, IgG, Covance, 1:2000), α-Nup62 (murine Ab, IgG, BD Transduction

Laboratories, 1:2000), α-tubulin (murine Ab, IgG, Sigma, 1:10000), α-Nup50 (goat Ab, Abcam, 1:2000), α-GST (murine mAb, IgG, Novagen, 1:10000), α-His (6x His, murine Ab, Abcam, 1:2000), α-P-p38 (activated, phospho-Thr180/Tyr182; rabbit Ab, IgG, Cell Signaling Technology, 1:3000), α−p38 (unactivated, rabbit Ab, IgG, Cell Signaling Technology, 1:3000), α-P-ERK1/2 (activated, phospho-Thr202/Tyr204 ERK 1/2; rabbit Ab, IgG, Cell Signaling Technology, 1:2000), α-ERK1/2 (unactivated, ERK1/2, rabbit Ab, IgG, Upstate, Millipore, 1:5000), α-mouse (secondary Ab, IgG, Sigma Aldrich, 1:8000), α-rabbit (secondary Ab, IgG, Promega, 1:8000) α-goat (secondary Ab, IgG, Sigma, 1:8000).

Nup50 and Nup62 Immunoprecipitation

HeLa nuclei (10^6 cell equivalents) and fractionated cytosol ($3x10^5$ cell equivalents) were combined with γ-^{32}P-ATP (10 μCi). Recombinant GST or GST- L_E (2 μg), were added. Some samples were supplemented with okadaic acid (250 nM). Reactions were incubated at 37°C for 45 min before the addition of RIPA (300 μl/sample, 50 mM Tris, pH 7.4, 150 mM NaCl, 0.1 % SDS, 1% Triton x100, 0.5% Na deoxycholate, 1mM PMSF, 20 mM pepstatin A, and protein phosphatase inhibitor cocktail 3, Sigma Aldrich) and sonication. Protein G-conjugated beads (10 μl, G.E. Lifesciences) were added. Incubation was for 1 hr before the beads were removed by centrifugation. Fresh protein-G beads conjugated to α-Nup50 or α-Nup62 (saturated) were incubated with agitation (4°C, 3 hr) and then collected. After extensive washing (6x, PBS with 0.02% triton), samples were denatured with SDS buffer, boiled and fractionated by SDS-PAGE. Protein bands were detected by silver-staining and autoradiography, with densitometry performed using a Typhoon imager (GE Healthcare).

Chapter 3: Cardiovirus Leader proteins bind exportins: implications for virus replication and nucleocytoplasmic trafficking inhibition

Figure 3.2B was performed by Holly Basta (Palmenberg Lab)

Abstract

Cardiovirus Leader proteins (L_X) inhibit cellular nucleocytoplasmic trafficking by directing host kinases to phosphorylate Phe/Gly-containing nuclear pore proteins (Nups). Resolution of the Mengovirus L_M structure bound to RanGTPase, a trafficking regulator, led to suggestions that these complexes must interact further with specific exportins (karyopherins), which in turn mediate the kinase selection. Pull-down experiments, recombinant protein complex reconstitution, and shRNA knockdowns now confirm that CRM1 and CAS exportins can form direct, stable dimeric complexes with Encephalomyocarditis virus L_E, and also larger complexes with L_E:Ran. Similar activities could be demonstrated for recombinant L_S and L_T from Theiloviruses. When mutations were introduced to alter the L_E zinc finger domain, acidic domain, or dual phosphorylation sites, there was a reduced exportin selection. These regions are not directly involved in Ran interactions, so the Ran and CRM1 binding sites on L_E must be non-overlapping. The involvement of exportins in this mechanism is very important to both viral replication and the inhibition of trafficking by L_X.

Introduction

Vertebrate nuclei have double-layered membranes studded with an estimated 2800 channels called nuclear pore complexes (NPC). Each pore is comprised of about 30 nucleoporin proteins

(Nups) arranged with octagonal symmetry (107). Many of these Nups, especially those lining the central channel, are hydrophobic, displaying characteristic Phe/Gly-repeat units which serve as a physical barrier to casual diffusion of molecules >40 kDa. Larger macromolecules cannot, by themselves, navigate the disordered, hydrophobic Nup tangle that constitutes the central channel. Instead, directionally targeted cargos display short nuclear localization signals (NLS) or nuclear export signals (NES) that are recognized and bound by karyopherin receptors (importins or exportins) traveling in the required direction. The cargo/receptor selection process is regulated by a RanGTPase-moderated energy gradient, which determines the active, or inactive status of the various karyopherins (172).

There are multiple virus types which usurp these transport pathways to enhance their own replication or prevent activation of innate responses. Cardioviruses in the *Picornaviridae* family use the unique strategy of induced hyper-phosphorylation directed at multiple Phe/Gly (FG) Nups, to bring about a rapid, virtually complete inhibition of cellular import/export processes ((74), Chapter 2). The effect is toxic to cells, but allows these cytoplasmic viruses to replicate with apparent impunity. Encephalomyocarditis virus (EMCV), Mengovirus, Theiler's murine encephalyomyelitis virus (TMEV) and Saffold virus (SafV) are characteristic isolates which have been studied for these activities (64, 73).

Each cardiovirus encodes a small, highly-charged Leader protein (L_X, 67-76 amino acids) at the N-terminus its polyprotein, which when introduced into cells, is sufficient to recapitulate the entire Nup hyper-phosphorylation phenomenon (74). Solution structures of the Mengo protein (L_M) show a CHCC amino-proximal zinc finger domain as the dominant motif in an otherwise flexible conformation (78, 173). A central "hinge" region and C-proximal acidic region assume more defined induced-fit conformations only when L_M interacts with RanGTPase, a strong (3 nM) preferred binding target when tested with recombinant proteins, or as detected with native proteins within the infected cells' nuclear rims (74, 77, 78). The complex locks Ran into an

irreversible "active" structure, nearly identical (~1.6 Å RMSD) to nucleotide-bound RanGTP. In uninfected cells, this conformer of Ran would normally chaperone interactions between export karyopherins and their cargos, and then participate in shuttling these complexes through the NPC from nucleus to cytoplasm. But since neither Ran nor L_X is a kinase, it is clear that neither can be directly responsible for catalyzing infection-dependent Nup phosphorylation. Instead, it has been proposed that L_M:Ran complexes serve to nucleate subsequent (irreversible?) reactions with exportins, which in turn then carry the culpable activated kinase cargos directly to Nup targets (78). In recent support of this model, recombinant L_E-GST (EMCV), when reacted with HeLa cytosol was shown to pulldown immunologically detectable amounts of CRM1 (chromosomal maintenance 1 protein, XPO1) and CAS (cellular apoptosis susceptibility protein, XPO2) exportins (78). The responsible kinases, as implicated with parallel inhibition studies (Chapter 4), are known to include MAP pathway agents, ERK1 and p38 (75). Presumably, these enzymes, for which the activated forms have dominant nuclear localizations (123), are somehow preferentially selected for Nup phosphorylation activities, by the L_X:Ran:exportin complexes.

Other than the L_X:Ran interactions, though, few of these steps have been broadly explored experimentally. Moreover, complicating the overall picture is an additional mechanistic requirement for duel L_X phosphorylation. Ran interactions with L_M do not require these modifications, but exportin extraction by recombinant L_X (78), and ultimately Nup phosphorylation (63, 64), are sensitive to the motif phospho-status. Cardiovirus L_X proteins vary somewhat in the sequence and lengths of their hinge and acidic regions, and it is within this context that the required phosphorylation residues occur. We now report new results showing direct, reciprocal binding interactions between native and recombinant L_X proteins with cellular and recombinant variants of the exportins CRM1 and CAS. My findings refine the existing mechanistic model, and moreover suggest that these specific interactions may be mediated by

the L_X zinc finger, acidic domains and phosphorylation sites, which do not directly participate in Ran binding.

Results

Screen for L_E binding partners.

RanGTPase, as a binding partner for GST-L_E, was previously identified by reciprocal pull-down activities and confirmed with Western analyses using anticipated reactive antibodies (74, 78). Related experiments suggest the phosphorylation status of L_E was a key determinant for additional relevant interactions, particularly with exportins (78). As a broader screen for dominant cytosolic partners, HeLa lysates were pre-cleared with glutathione beads and then reacted with GST-L_E in the presence of additional ATP. These conditions allow efficient dual phosphorylation of L_E (63) while reducing background binding by non-specific proteins. After SDS-PAGE fractionation, 7 prominent band regions (Fig. 3.1) were excised, pooled, digested with trypsin and submitted for orbi-trap mass spectrometry. Table 3.1 summarizes the strongest sequence hits as defined by positive identification of at least 30 unique peptides each. The list includes exportin 1 (CRM1) and exportin 2 (CAS), the nuclear transport-associated karyopherins which had been modeled previously with probable L_E:Ran interactions (78). The sizes of these proteins, 123 kDa and 110 kDa, respectively, are consistent with the principal band 2 included in mass spec analysis, pool A. Therefore, L_E, as it is phosphorylated in this cytoplasmic context, does indeed react strongly with exportins. Interestingly, 6 of the 9 strongest hits (Cover %) found in both pools identified several other proteins with structurally analogous HEAT repeat motifs, similar to those characteristic of the exportins, perhaps indicating a topological class of preferred contact interactions with L_E.

L_E association with exportins.
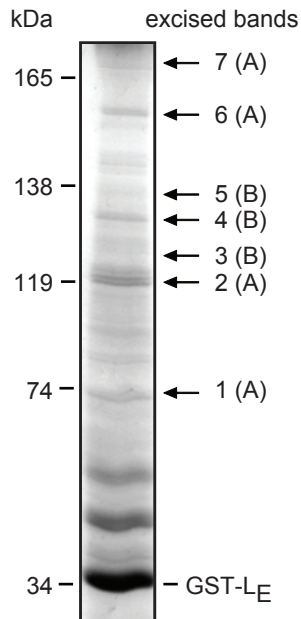
Figure 3.1. Cytosol selection by GST-L$_E$ for Mass Spec. HeLa cytosol proteins (prey) reactive with GST-L$_E$ (bait) were collected, gel fractionated and visualized with silver stain. Bands of interest (1-7) were excised, pooled (A or B), digested with trypsin, and analyzed by orbi-trap mass spectroscopy for protein identity. kDa indicates the MW of proteins in a parallel marker lane.

Table 3.1. Proteins identified by mass spectroscopy

Pool [A]	Protein Name	[B]Heat repeat	GenBank (ID)	[c]Size (kDa)	[D]Frags (#)	[E]Cover (%)
A	DNA-dependent protein kinase catalytic subunit	Yes	P78527	460	127	39
A	E3 ubiquitin-protein ligase UBR5	No	O95071	309	35	20
A	Translational activator GCN1	Yes	Q92616	234	85	41
A	CAD protein	No	P27708	242	52	34
B	Proteasome-associated protein ECM29 homolog	Yes	Q5VYK3	204	53	38
B	Ras GTPase-activating-like protein IQGAP1	No	P46940	189	30	26
B	Bifunctional aminoacyl-tRNA synthetase	No	P07814	171	33	31
B	Mitocondrial leucine-rich PPR motif-containing protein	No	P42704	158	48	48
B	Condensin complex subunit 1	Yes	Q15021	157	39	40
B	Isoleucyl-tRNA synthetase, cytoplasmic	No	P41252	144	30	31
B	DNA-directed RNA polymerase II subunit RPB2	No	P30876	134	32	40
B	DNA polymerase delta catalytic subunit	No	P28340	124	33	42
A	Exportin-1 (CRM1)	Yes	O14980	123	37	50
A	Exportin-2 (CAS)	Yes	P55060	110	43	57
B	Protein KIAA1967	No	Q8N163	103	33	50
A	Alpha-actinin-4	No	O43707	105	44	61
A	Heat shock cognate 71 kDa protein	No	P11142	71	31	55

[A]Figure 1 gel bands 1,2,6,7 were pool A, bands 3,4,5 were pool B
[B] protein has HEAT repeats (Huntington elongation factor 3, regulatory subunit A of protein phosphatase A, and TOR1), consisting of pairs of anti-parallel helices arranged in a consecutive parallel stack (Groves and Barford, 1999 Curr Opin Struct Biol, 9:383-389)
[C] As per genecard.org
[D] Number of peptide fragments by mass spec, identifying this protein
[E] Sum of peptide fragment coverage of full protein sequence

Mutational mapping (53), as well as determination of the solution structure of L_M bound to

RanGTPase (78) explored sequence contributions from the central hinge region (aa 35-40), the

zinc finger (aa 14-20), the acidic domain (aa 37-59) and phosphorylation sites (Tyr_{41}, Thr_{47}) as

important to the observation of L_X-dependent Nup phosphorylation. However, $Cys_{19}Ala$ (zinc

finger), 4D4A (acidic domain) and $Tyr_{41}Ala$/$Thr_{47}Ala$ phosphorylation changes did not

significantly affect L_E:Ran interactions with endogenous or recombinant proteins because those

contacts are mediated primarily by the L_X hinge region (53). With regard to exportins though, a

subset panel of GST-L_E proteins with same sequence changes (3D3A not 4D4A) were less

efficient than unmodified protein (wt) at associating with endogenous CRM1 and CAS from

HeLa cell lysates (Fig. 3.2A). Relative to the acidic domain deletion (ΔA) negative control, which

misfolds the remainder of the protein (53), all 4 tested substitutions in the other crucial Nup

phosphorylation areas reduced exportin extraction by 50-90%. Exportin extraction was not

unique to the L_E sequences. Equivalent experiments with L_S (Saf) and L_T (TMEV) recombinant

proteins showed these materials too, reacted (Fig. 3.2B). In a reciprocal challenge, antibodies to

CRM1, when attached to beads, similarly bound both intended target (native CRM1) and (wt)

GST-L_E spiked into the lysates (Fig. 3.2C). Again, the most efficient conditions for these mutual

pulldowns required the full, unmutated (wt) L_E sequence.

Direct interaction with CRM1.

HeLa lysates contain endogenous RanGTPase. Moreover, these systems will efficiently

phosphorylate any added cardiovirus Leader ($L_{X)}$ proteins with intact sequences. With

recombinant GST-L_E, the phosphorylation status can be controlled by sequential addition of the

relevant kinases. Syk activity at Tyr_{41} requires pre-phosphorylation with AmpK or CK2 at Thr_{47}

(63, 64). GST-L_E (singly phosphorylated on Thr_{47}) extracted purified recombinant CRM1

(rCRM1) from reactions that contained 300 or 500 mM salt, indicating tight association (Fig.

3.3A). Surprisingly, the presence or absence of recombinant Ran (rRan) did not seem to have

A GST-tagged L$_E$ | bait

input | GST | wt | ΔA | W$_{40}$A | 3D3A* | A41/A47* | C$_{19}$A

αCRM1

4 100 2 42 48 34 31 % intensity

αCAS

5 100 2 10 31 18 10 % intensity

B L$_X$-GST | bait

input | GST | L$_E$ | L$_S$ | L$_T$

αCRM1

100 95 86 % intensity

αCAS

100 130 120 % intensity

αGST

C GST-L$_E$ | prey

input | mock | GST | wt | ΔA | W$_{40}$A

- CRM1
- VH+VL   αCRM1 bait

- VH
- GST-L$_E$ αGST
- VL
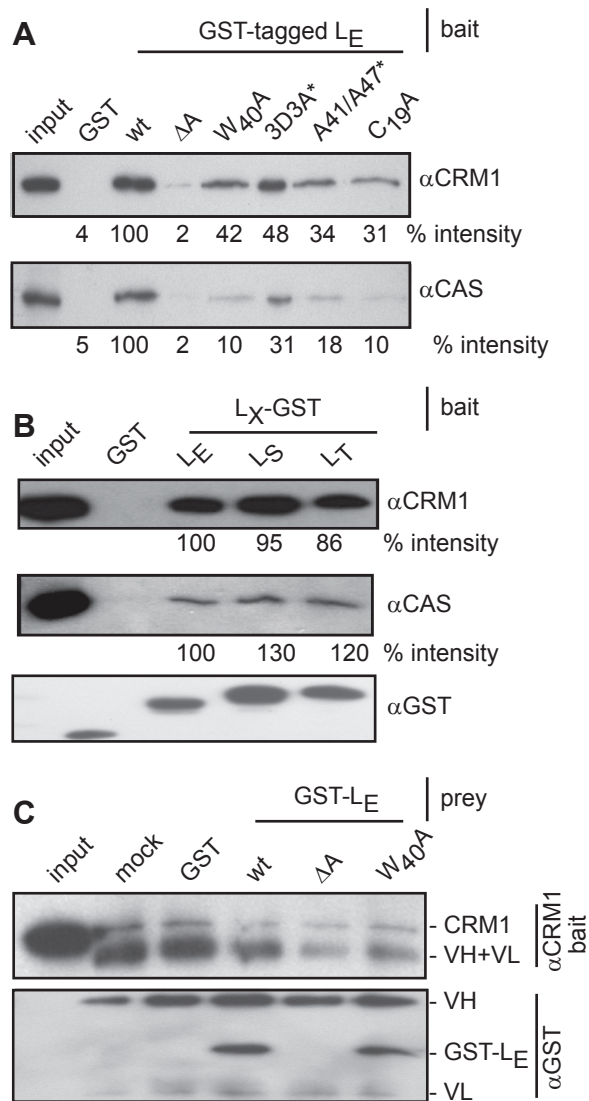
Figure 3.2. GST-tagged L pulldowns for exportins. Bait proteins, GST-L$_E$ and related mutant derivatives (A) as well as GST-L$_S$ and GST-L$_T$ (B), were incubated with HeLa cytosol. (*) Indicates L$_E$-GST derived proteins were used, instead. After glutathione sepharose bead extractions, Western analyses were used to determine the amount of bound CRM1 and CAS, relative to the wt samples (% intensity). (C) GST-L$_E$ and mutant derivatives (prey) were mixed with HeLa cytosol (+ ATP) then incubated with protein-G sepharose beads linked to αCRM1 (bait). After boiling and protein fractionation, the CRM1 and GST signals were detected by Western analyses. In these blots, the VH and VL coupling antibody proteins were also reactive with the secondary antibodies.

an effect on rCRM1 pulldown, and Ran itself was also extracted whenever present. These experiments were carried out at stoichiometry, so it isn't clear whether the GST-L_E was partitioning between its potential partners or facilitating an inclusive complex. In either case, as previously reported with native CRM1/CAS from cell lysates (78), the relative extraction efficiency was sensitive to the phosphorylation status of L_E (Fig. 3.3B). With or without rRan, 1 or preferably 2 pre-phosphorylation GST-L_E events, reproducibly (n=5) gave 50-70% stronger rCRM1 signals per unit of GST (L_E).

CRM1:L:Ran Complex formation.

When the Fig. 3.3A experiment was repeated with stepwise addition of the components, again, GST-L_E (1 added phosphate) extracted rCRM1 regardless of whether rRan (+RCC1) was added before ("a"), or after ("b") as the tertiary component. As a preliminary estimate of whether these 3 known proteins could collectively interact *in vitro*, dual phosphorylated GST-L_E, rRan and rCRM1 were mixed, incubated and then fractionated over a Superdex 200 column. The absorbance values (Fig. 3.4B) and parallel silver-stained gels (Fig. 3.4C) placed about 20% of the signals from all 3 proteins within early eluates, near the trailing edge of the void volume (fractions 35-40). There were additional strong peaks consistent with GST-L_E:rCRM1 complexes (fractions 67-75) and also monomers of rRan (fractions 85-90). It can't be excluded that some material at the front edge of the late-eluting peak also contains some Leader complexes (GST-L_E:rRan?), although these amounts were below the limits detectable by silver-stain. The central fractions show conclusively that rCRM1 (120 kDa) and phosphorylated GST-L_E (35 kDa) do readily interact in apparent 1:1 stoichiometry. Similar to the pulldown experiments (Fig. 3.3B), parallel chromatographs confirmed that the intensity of this peak and the observation of complexes near the void volume, were dependent on the phosphorylation status GST-L_E (not shown).

shRNA knockdown of CRM1.
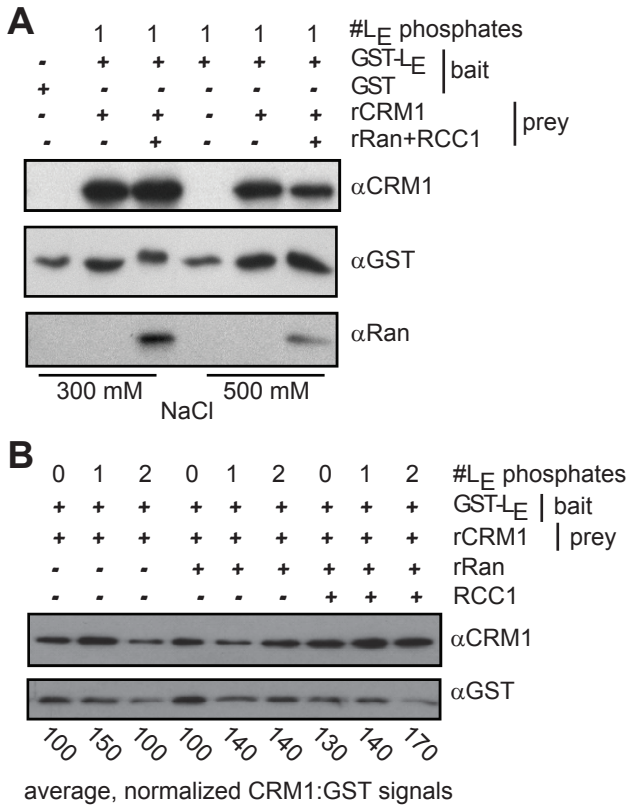
Figure 3.3. Recombinant CRM1 and Ran selection by GST-L$_E$ with varying salt or phosphorylation. (A) GST-L$_E$ reacted with CK2 (adds 1 phosphate) was incubated with stoichiometric amounts of rCRM1 and rRan (+RCC1) at 300 mM or 500 mM NaCl. After glutathione bead extraction, bound proteins were visualized by Western analyses. (B) Similar to A, with no added NaCl, GST-L$_E$ without no phosphates (0), 1 added phosphate (1, CK2) or 2 added phosphates (2, CK2 plus Syk) was mixed with combinations of rCRM1, rRan and RCC1. Glutathione bead-extracted proteins were visualized by Western analyses. The bands were quantified by densitometry. For each lane, the ratio of CRM1 to GST signal was normalized to the 0 phosphate, no rRan sample (100). This full experiment was carried out 5 times, and the averaged values per sample type are indicated.
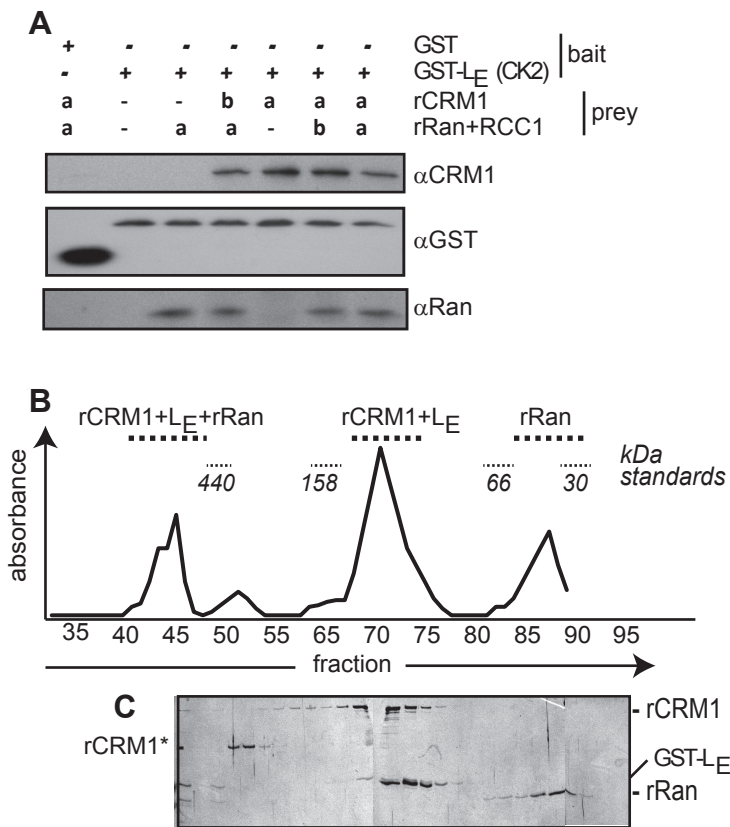
Figure 3.4. CRM1:L:Ran Complex formation. (A) GST-L_E pretreated with CK2 (adds 1 phosphate) was pre-incubated with stoichiometric amounts of rCRM1 and rRan (+RCC1) for lanes labeled with "a". Then, rCRM1 and rRan (+RCC1) were added to previously deficient samples ("b") before a second incubation period. Glutathione bead extraction and Western visualization was as in Fig. 3.3. (B) Duel phosphorylated GST-LE (CK2 plus Syk) was incubated with rCRM1 and rRan (+RCC1). The sample was fractionated on a size exclusion column pre-calibrated with MW markers. Fraction absorbance and SDS-PAGE (silver stain) identified eluted complexes. Bands labeled "rCRM1*" are minor bacterial contaminants from the rCRM1 purification procedure.

Ultimately, Nup phosphorylation itself is the test for mechanistic involvement in L_X-dependent activities. CRM1 is an essential protein with multiple cellular roles (174), especially during mitosis, and CRM1 functions are not entirely compensated by alternative exportins like CAS (reviewed in (175)). HeLa cells transduced with an shRNA against CRM1 can survive about a week after doxycycline induction. Under such experimental conditions, within the first 2 days, ~60% of the protein was turned over (Fig. 3.5A). By day 3, this value increased to ~80%. Induction alone did not cause Nup phosphorylation, but if the cells were also infected with vEC9, the diagnostic upward smear of Nup62 became readily apparent. If the infection were delayed, however, until 2, 3 or 4 days post-knockdown (PK) there was correspondingly lower levels of Nup62 phosphorylation and the virus replicated more poorly. This was evidenced both by the lower levels (normalized to tubulin per sample) of viral polymerase proteins 3D and 3CD (Fig. 3.5A) and by 5-fold reductions in progeny titer, as determined by plaque assay (Fig. 3.5C). Clearly, vEC9 was disadvantaged in cells with reduced levels of CRM1. This phenomenon is attributable to the L_X mechanism, because when shRNA-induced cells were transfected (4 days PK) with cDNAs for the L_E, L_T or L_S proteins, Nup62 phosphorylation was once more directly decreased (Fig. 3.5B).

CRM1 inhibition.

Leptomycin B (LMB) is a well-studied fungal antibiotic (176) which alkylates most iterations of eukaryotic CRM1 proteins. It binds covalently to Cys_{528}, effectively blocking the interaction with potential cargo nuclear export signals (NES) that would normally intercalate into a cleft between HEAT repeats H11 and H12 (177). Essentially, LMB is a diagnostic for CRM1 partners which use this canonical binding site. When added to the GST-L_E pull-down assays (Fig. 3.6A), the recombinant proteins (singly phosphorylated GST-L_E) behaved the same as they did in Fig. 3.3A, binding to CRM1 independently of Ran. None of the rRan and rCRM1 pulldowns were obviously altered by the presence of this drug. Infected cells, monitored for Nup62

A.

	mock				infected				days PK
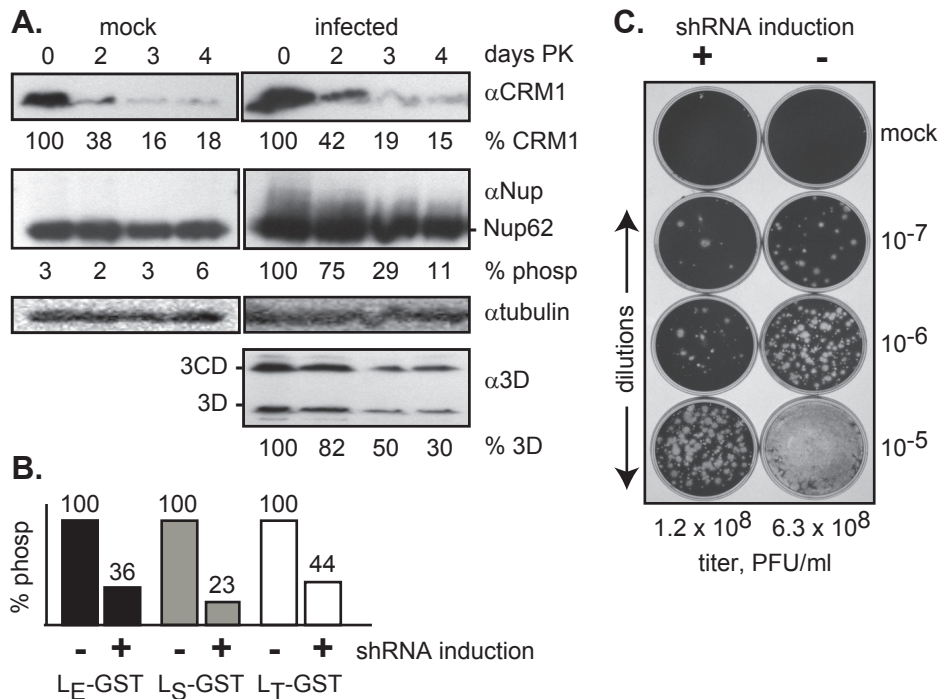
Figure 3.5. CRM1 shRNA knockdown. (A) Plated HeLa cells transduced with an shRNA against human CRM1 were treated with doxycycline. After 0-4 days post-knockdown (PK) the cells were infected with vEC9 (MOI of 10). Lysates harvested 4 hr later were fractionated for Western analyses. Band intensities for 4 separate experiments, normalized to day 0 values and to the tubulin loading controls, are indicated. (B) Similar cells with (+) and without (-) induction were transfected (4 days PK) with LX-GST cDNAs. Harvest was at 16 hr post-transfection. Nup62 phosphorylation was determined as in A (n=2). (C) Infected cell lysates from A, after 0 days (-) and 4 days (+) PK were titered on normal HeLa cells. Plaque formation was evaluated after 28 hr. Observed titers (PFU/ml) are averaged from (n=3) replicate plates (SD, 0.02-0.28).
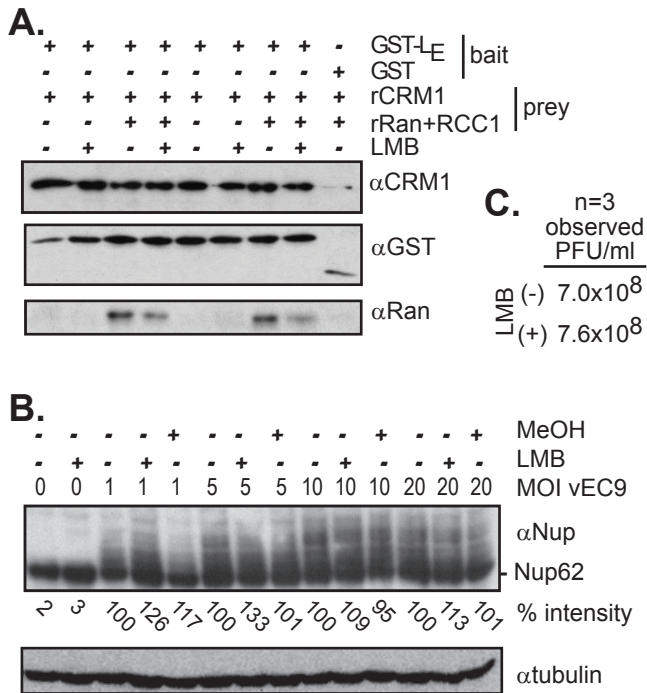
Figure 3.6. Impact of CRM1 inhibition by Leptomycin B on L. (A) LMB (4 nM) was pre-incubated with rCRM1 before the addition of bait proteins (singly phosphorylated GST-L_E or GST) and (putative) auxiliary prey proteins (rRan with RCC1). The complexes were extracted with glutathione-sepharose beads, fractionated on gels, and detected by Western analyses. (B) Plated HeLa cells were pre-incubated with LMB or its carrier (MeOH) before infection with vEC9 at the indicated MOI. The cells were harvested at 4 hr PI. Nup62 phosphorylation levels (% intensity) were determined by Western analyses and densitometry relative to samples with no inhibitor or virus, and as normalized to each lane's tubulin levels. (C) Plates of confluent HeLa cells were infected with vEC9 (MOI of 10) after pretreatment (or not) with LMB. After 6 hrs, recovered progeny virus was titered by plaque assay. Observed PFU/ml averaged from 3 independent experimental iterations are indicated (SD, 0.44-0.49).

phosphorylation over a range of vEC9 MOI, gave similar results (Fig. 3.6B); the presence of the drug was essentially ineffective. Such cells gave equivalent progeny titers regardless of whether LMB was added (Fig. 3.6C). The GST-L_E recognition of CRM1 must be independent of this usual binding site.

Discussion

In cells or recombinant assays, cardiovirus Leader proteins react tightly with RanGTPase, forcing this nuclear trafficking regulator into a conformation indistinguishable from the "active" GTP-bound format required for subsequent exportin binding (78). Formation of this complex is absolutely required as a preliminary step of virus-induced Nup hyper-phosphorylation, the ultimate cause of nucleocytoplasmic trafficking inhibition by these viruses (73). Resolution of the L_M:Ran structure confirmed the central hinge region of L_M (e.g. Trp_{40}), tucked under the C-tail of Ran, forms the key interaction domain. The L_M zinc finger (e.g. C_{19}), phosphorylation sites (Y_{41}, T_{47}), and the majority of C-proximal acidic domain (e.g. Asp_{48}, Asp_{51}, Asp_{52}), do not contribute to these contacts, even though each of these regions has proven essential to L_X-dependent Nup phosphorylation (53, 74). The resolved structure further predicts a model whereby these non-Ran binding segments might instead mediate subsequent interactions with the karyopherin class of exportins (e.g. CRM1, CAS), which require exactly this GTP-like Ran conformation for nuclear egress (78). Validation of this idea, that L_X and exportins can directly interact, was the rationale for the experiments described here.

Native cardiovirus L_X proteins are refractive to Western analyses and antibody induction because of their small size and high charge. Nonetheless, recombinant GST-tagged L_X materials recapitulate most of the protein phenotypes in cells and extracts and are typically used to explore these mechanisms (48, 53, 73). With both native (HeLa cytosol) and recombinant (rCRM1) sources, reciprocal pulldown experiments indicated strong, salt-resistant direct interactions between 3 different cardiovirus (GST-)L_X sequences and CRM1/CAS (Fig. 3.2, Fig.

3.3). Mass spec analyses showed these particular exportins, as well as other structurally analogous proteins with characteristic HEAT-repeat folds, were among the dominant GST-L_E binding partners extracted from HeLa cytosol (Table 3.1). Ran would not have been expected as an partner here, because its efficient interaction with L_E requires the catalytic presence of nuclear bound guanine exchange factor, RCC1, to facilitate essential conformational morphs (77).

Once identified, as the majority example exportin, CRM1 was then examined further, both as native and recombinant protein and singly or in combination with rRan, for GST-L_E binding. Neither cellular protein was found to block the other's extraction, nor was extraction of either or both, apparently sensitive to the sequence of addition (Fig. 3.3, Fig. 3.4, Fig. 3.6). Such results were not entirely surprising, because the structure model predicts that the L_M zinc finger, acidic domain and phosphorylation sites, which do not make Ran contacts, are exactly the segments which should mediate putative exportin contacts (78). In other words, the binding domains are non-overlapping. In support of this idea, mutations in GST-L_E affecting all 3 of the predicted contact regions significantly diminished the extraction of native and recombinant CRM1 (Fig 3.2A). The reduced affinity was particularly apparent when the L_E phosphorylation sites (Tyr_{41}, Thr_{47}) were mutated, or when recombinant GST-L_E was restricted in its phosphorylation status. Dual phosphorylated GST-L_E, reacted with rCRM1, fractionated by gel filtration at the size expected for a stoichiometric complex. An additional finding in favor of the current model is that L_E interaction with CRM1 apparently did not involve the NES cargo recognition site (HEAT repeats H11 and H12) inhibited by LMB. Within fully assembled CRM1:L_E:Ran complexes, the Nup phosphorylation kinases (activated ERK and p38) would presumably need to bind here as preferred export cargos (78).

Clearly, exportins, particularly CRM1 and CAS are strong viable partners for L_X. An inducible CRM1 knockout cell line was created to link these requirements for CRM1 to EMCV replication.

As was shown previously for the Ran mechanistic requirement (74), Nup62 phosphorylation and viral fecundity, as measured by 3D/3CD synthesis and by progeny titers, were strongly dependent upon the pool of native CRM1. This CRM1 dependency was also true when induced cells were transfected with cDNAs from any 3 cardiovirus L_X proteins, indicating a common requirement for CRM1, if not other analogous exportins, in the collective Nup phosphorylation pathways.

The current mechanism for L_X-dependent Nup hyper-phosphorylation predicts that within the nuclear rim, L_X:Ran complexes select exportins carrying activated kinases such as ERK1 and p38, and it is this multiplex which tethers within the nuclear pores and phosphorylates the Nups ((78) and Chapter 4). Interestingly, we could not define with the current reactions a required sequence of addition for rRan and rCRM1 to a mutual GST-L_E complex. Both proteins appeared to interact with L_E independently, especially if L_E was properly phosphorylated. Near the void volume of the fractionation column, though, about 20% of the added mass eluted with signals from all 3 proteins. Whether these are the expected trimers, or other high-mass complexes is not clear at present. Three additional unexpected findings from this experiment, the significant peak of free Ran, the dominance of GST-L_E:rCRM1, and the lack of rRan:rCRM1 complexes, suggest that we don't yet understand all of the parameters for interplay among these proteins. In cells, especially within the context of nuclear pores, the cooperative, active formats of L_E, Ran and CRM1 (or CAS) are sure to be influenced by the local environment, especially the GNP nucleotide gradient and perhaps other cellular (catalytic?) proteins.

In cell-free reactions, a catalytic amount of RCC1 significantly accelerates binding saturation (77), locking L_E and Ran into (virtually) in-dissociable complexes which mimic the topology of RanGTP even in the absence of any nucleotide (78). The same RanGTP format is required for Ran:CRM1 (or CAS) interactions (178). From our experiments, it is now clear that GST-L_E, preferably with at least 1 phosphate attached, can interact strongly and independently with both

rRan and rCRM1 (or CAS). Void-volume complexes were observed with all three proteins, but we don't yet know how to drive these assemblages to saturation. Possibly, the RCC1-dependent Ran morphing, an aid for good GST-L_E interactions, works contrary to simultaneous rRan:rCRM1 binding, by stripping all endogenous nucleotides from the added Ran. This situation would explain the observed pool of free Ran, unable to dislodge GST-L_E which is already tied up in rCRM1 complexes. It would also explain the lack of an observable of rRan:rCRM1 peak, independent of the presence of GST-L_E, as this should have been a strong native interaction, and indeed a driving force in normal nuclear trafficking. If true, then within the context of real nuclear pores, the innate nucleotide gradient could play a significant role in ternary complex assembly efficiency.

Materials and Methods

<u>Recombinant proteins.</u>

Plasmids encoding GST- L_E, GST-$L_E\Delta A$, GST-$L_E W_{40}A$, and related derivatives are described (53, 77, 173), as are analogous L_X-GST proteins from Saffold 2 and Theiler's virus (BeAn), L_S-GST, L_T-GST, L_E-GST and L_E-GST $Thr_{41}Ala/Tyr_{47}Ala$ (64, 72). L_E-GST 3D3A was made similarly by introducing point mutations to alter the 3 codons for Asp_{48}, Asp_{51} and Asp_{52} to Ala. For recombinant proteins, these cDNAs were transformed into BL21 *E. coli.* The cells were incubated in media (0.5% glucose, 20uM $ZnCl_2$, 50 mg/mL ampicillin, 30°C, 3 hr) before induction with IPTG (1 mM) and harvest (6 hr). Cells were re-suspended in GST buffer (50 mM Tris pH 7.4, 125 mM NaCl, 20 uM $ZnCl_2$, 1mM PMSF, 0.2 mM DTT, 0.5 mg/ml lysozyme), then sonicated. Debris was removed by centrifugation (20,000 x g, 45 min). The proteins were collected with GSTrap HP columns (GE Healthcare Bio-sciences, Pittsburgh PA) into modified GST buffer (10 mM glutathione disulfide, 50 mM Tris, pH 8.0). Protein fractions were dialyzed into buffer QA (10mM Bis-Tris Propane, 50mM NaCl, 2 mM DTT, pH 7.4), then applied to a Macro-Prep High Q anion exchange column (BioRad, Hercules, CA). The fractions were eluted

(buffer QA, 1M NaCl) before dialysis (25 mM hepes, 150 mM KCl, 2 mM DTT, pH 7.3), and

assay for concentration and purity. A cDNA construct encoding amino-terminal, His-tagged

murine CRM1 (rCRM1) was a kind gift from Dr. Dirk Görlich. Bacterial induction and protein

isolation was as described (178) Recombinant His-tagged human RanGTPase (rRan) and

GST-RCC1 (human) were also prepared as described (53, 77). All recombinant proteins were

snap frozen in liquid nitrogen and then stored at -80°C as single-experiment aliquots. Casein

kinase 2 (CK2, phosphorylated, recombinant, New England Biolabs) and spleen tyrosine kinase

(Syk, activated, recombinant, SignalChem) were used singly or doubly phosphorylate

recombinant GST-L_E at concentrations of 5 U/μg and 0.5 ng/μg, respectively as described (63).

Cell lysates.

HeLa cells (ATCC CRL-1958) were grown in suspension (modified Eagle's medium, 10% calf

serum, 5% CO2, 37°C). Lysates were prepared after collecting the cells with centrifugation (500

x g), washing the pellets (PBS), and resuspension (2x volume) in hypotonic buffer (0.75mM

MgAc, 0.15 mM EGTA, 1mM PMSF, 0.01 mg/ml luepeptin, 20 μM pepstatinA, 3mM DTT). After

a brief incubation (10 min, 0°C) the samples were homogenized (dounce) or sonicated (2 x 30

sec, 0°C) before clarification (10 min, 16,000 g). The soluble fraction was supplemented with

1/10th volume 10 x TB (200 mM HEPES pH 7.3, 10mM EGTA, 20 mM MgAc, 110 mM KAc),

before aliquots were snap frozen and stored at -80°C. Before use in pull-down experiments, the

lysates were pre-reacted with glutathione sepharose beads and then re-clarified (as below).

Protein extraction.

GST tagged L_E and mutant derivatives (bait, generally 2 μg) was incubated (37°C, 45 min) with

HeLa lysate (prey, 40 μl) before dilution (RIPA buffer, 50 mM Tris, 150 mM NaCl, 0.1% SDS,

0.5% Na deoxycholate, 1% IGEPAL, pH 7.6), addition of glutathione sepharose beads

(generally 2 μl per sample, GE Healthcare Bio-sciences) and agitation (3 hr, 4°C). When the

pulldown prey was a recombinant protein, bait and prey were mixed stoichiometrically, diluted (to 100μl, with TB, 200 mM HEPES pH 7.3, 1mM EGTA, 2mM MgAc, 110 mM KAc, 2 mM DTT), before bead addition as above. Both types of samples were then further diluted (2x) with binding buffer (50mM HEPES, pH 7.4, 150 mM NaCl, 0.5% IGEPAL), and mixed end-over-end (1 hr, 22°C). For immunoprecipation (IP), protein-G sepharose beads were conjugated to antibodies (bait, e.g. α-CRM1, 0.6 μl per 10μl beads, overnight, 4°C) before being rinsed, (1 x PBS, 0.02% Triton X-100), added to samples (prey, cytosol or recombinant protein, 10μl/sample) and incubated (with rocking, 3 hr, 4°C). After pulldown or IP, the beads were rinsed (6x, 500μl PBS, triton X-100, then 2x 120 mM Tris, pH 6.8, 10% glycerol w/v 2% SDS w/v, 200 mM DTT, 0.2% bromophenol blue) before the samples were denatured in a boiling water bath (10 min).

Mass spectroscopy.

Protein bands extracted by GST-L_E pulldown, were fractionated by SDS-PAGE and visualized by Coomassie staining before excision and digestion with trypsin according to protocols recommended UW-Madison Biotechnology Center. Briefly, gel samples were treated with ACN (200 μL, mM NH_4HCO_3, 50% acetonitrile, 45 min), and then dehydrated (100% ACN, 5 min) under vacuum. The samples were resuspended (40 μl, 40 mM NH_4CHO_3, 10% ACN) in the presence of trypsin gold (Promega, 20 μg/ml, plus 0.025% Protease Max surfactant, 1 hr, 27°C). Subsequently, ACN was added (200 μl, 40mM NH_4CHO_3, 10% ACN) followed by incubation (overnight, 25°C) and re-extraction (2x, 60 min, 50 μl 50% ACN, 5% triflouroacetic acid). Resultant peptides from select bands (see Table 3.1) were pooled, dehydrated (2 hr under vacuum) before purification and concentration via Ziptips (Millipore). The pool A and pool B samples were submitted for orbi-trap mass spectroscopy at the UW-Madison Biotechnology Center.

Western analyses.

Prepared samples were resolved by SDS-PAGE. The proteins were electro-transferred to polyvinylidene difluoride membranes (Immobilon-P, Millipore). The membranes were blocked (1 hr, 10% NFD milk in TBST: 20 mM Tris pH 7.6, 150 mM NaCl, 0.5% Tween20) then incubated with a primary antibody (1% NFD milk in TBST, overnight, 4°C) before washing (3 x TBST) and reaction with an appropriate secondary antibody (1 hr, 20°C). Antibodies included: αNup (murine mAb414, IgG, Covance, 1:2000), αtubulin (murine Ab, IgG, Sigma, 1:10,000), αGST (murine mAb, IgG, Novagen, 1:10,000), αCRM1 (rabbit Ab, IgG, Abcam, 1:2000), αCAS (goat Ab, IgG, Santa Cruz Biotechnology; 1:1000), αRan (goat Ab, IgG, Santa Cruz Biotechnology; 1:1000), αmouse (secondary Ab, IgG, Sigma Aldrich, 1:8000), αrabbit (secondary Ab, IgG, Promega, 1:8000), αgoat (secondary Ab, IgG, Sigma, 1:8,000). For band visualization, the membranes were rinsed (3x, TBST), incubated (1 min) with enhanced chemiluminescence substrate (GE healthcare) and then exposed to film. Densitometry analyses were as previously described (63).

Gel filtration

A HiLoad Superdex 200 16/600 chromatography column (GE Lifesciences) was calibrated with a commercial kit (Sigma-Aldrich MWGF1000-1kt) according to manufacturer's instructions. Recombinant protein combinations were incubated (37°C, 45 min), filtered (0.2 micron membrane) and volume adjusted (to 1 ml) before injection into the equilibrated column (50 mM HEPES, pH 7.4, 150 mM NaCl). After fractionation (0.2 ml/min, 4°C) the collected samples (1 ml) were assayed by SDS-PAGE, with silver stain, or Western techniques.

Cell procedures

HeLa cells plated to confluence, were infected with vEC9 (52) at an MOI of 1-20. At 3-6 hours post-infection (37°C, 5% CO_2) the cells were rinsed (2x, PBS) and collected into SDS buffer for protein analyses, or alternatively, subject to freeze-thaw (3x), lysate clarification and assays for plaque-forming units (52). Transfection assays used GST-L_E cDNA (2.6 μg per 10^6 cells in Lipofectamine 2000 (Life Technologies, Grand Island, NY). After incubation (18 hr, 37°C, 5% CO_2) the cells were rinsed (2x, PBS) and harvested in SDS buffer. Leptomycin B (LMB, Sigma Aldrich, St. Louis, MO), was added as required (to 4 nM), by pretreating cells or buffers for 1 hr. This concentration was then maintained throughout the experiment. A CRM1 knockout HeLa cell line was generated with the TRIPZ inducible lentiviral shRNA system (GE Dharmacon, shRNA V2THS-172053) according to manufacturer instructions with the help of Laraine Zimdars and Nate Sherer. The line was maintained under selection with puromycin. Plated cells were induced with doxycycline (0.25 nM, Sigma Aldrich). The media was refreshed daily (1-4 days) as required by the experiment.

Chapter 4: ECMV L directs ERK2 to inhibit nucleocytoplasmic trafficking

Abstract

Unlike enteroviruses which proteolytically remove Nups from the nuclear pores to inhibit nucleocytoplasmic trafficking, cardioviruses like Encephalomyocarditis virus (EMCV) direct cellular kinases to phosphorylate this same cohort of Nups solely through the activities of the viral Leader protein (L) (reviewed in (13)). Previous studies have narrowed the range of responsible kinases to the MAPK p38 and ERK pathways, but did not decisively identify which kinases were those directed by Leader (75). Here we present data that siRNAs against ERK2, p38α/β and RSK2/3 can decrease L-directed Nup phosphorylation. Furthermore, GST-L can associate with these kinases from HeLa cytosol. Using isolated HeLa nuclei, we reconstituted a Nup phosphorylation event through inclusion of L and recombinant ERK2, RSK3, and p38α, but not other kinases nor L alone. Because L is likely commandeering a endogenous regulatory pathway, these findings have implications for kinase regulation of nucleocytoplasmic trafficking in addition to cardiovirus infections.

Background

Many RNA viruses inhibit nucleocytoplasmic trafficking to prevent interferon responses and enhance available pools of necessary cellular factors, including ribosomes and essential nuclear factors like PTB and La auto antigen (13), for virus replication and translation. Venezuelan equine encephalitis virus and Vesicular stomatitis virus shut down nucleocytoplasmic trafficking by binding to cellular factors and blocking the nuclear pores (179, 180). Enteroviruses, including poliovirus and rhinovirus, selectively proteolyze nuclear pore proteins (Nups) necessary for nucleocytoplasmic translocation, out of the pores to effectively prevent this trafficking (65, 66,

69, 181, 182). As has been previously documented for Encephalomyocarditis virus (EMCV), cardioviruses direct cellular kinases to phosphorylate the same subset of Nups targeted by enteroviruses (64, 72, 75). These Nups remain at the pores, though active transport is shut down, yielding a general efflux of nuclear factors smaller than 40 kDA out into the cytoplasm, and preventing cellular interferon response (70, 71, 152, 183).

There are 2800 nuclear pores studding each vertebrate nuclei, each consisting of a 125 MDa structure. These structures are comprised of multiple copies of about 30 different proteins arranged in 8-fold symmetry, anchored in place by Nups with hydrophobic regions that insert into the nuclear envelope (82). Each nuclear pore has three distinct regions: the cytoplasmic fibrils, the nuclear plug, and the nuclear basket. The cytoplasmic tendrils include Nups 214 and 358 (also called RanBP2), extending into cytoplasm and serving as a docking region for cargos and transportins (also called karyopherins, and importins or exportins pending specific function). The nuclear plug sits in the nuclear envelope to act as a selective barrier comprised of Nups (including Nup62) containing phenylalanine-glycine (FG) -repeats, most of which are natively unfolded. The nuclear basket region includes Nups 153 and 98 and extends into the nucleus, serving as transportin binding and cargo docking domains akin to the cytoplasmic Nups.

Cargos larger than 40kDa require active transport, facilitated by the importins and exportins, and maintained by a RanGTP/GDP gradient (reviewed in (83)). There are about 20 identified human transportins, and these each take a distinct path through the pores by transiently binding to a particular subset of FG-repeat Nups. It has been shown that phosphorylation within the FG-repeats of Nups prevents transportin binding and can hinder nucleocytoplasmic trafficking (120). Cardioviruses take advantage of phosphorylation-based trafficking inhibition strictly through the activities of the anti-host protein Leader (L) (70, 73).

At 67-76 amino acids and PIs of about 3, the Leader (L) proteins of cardioviruses are small, highly charged, and linked to a number of activities. It is the sole viral protein necessary to

hinder nucleocytoplasmic transport ((70, 71, 74), Chapter 2). TMEV L has been shown responsible for shutting down interferon production and linked to prevention of stress granule prevention (80, 152, 183). Cells infected with an L-deficient EMCV produce very small plaques (52). L has been shown to localize to the nuclear pore via immunofluorescence using anti-L antibodies 5 hours post-infection of cells with vEC9 (74). Presumably by binding to viral protein 2A following polyprotein processing, L and 2A are targeted to the nuclear pores by the activity of 2A's nuclear localization motif. L also binds to RanGTPase in a nucleotide-free format with an affinity of 3 nm K_D (77) through the interaction of its hinge region (53). L becomes phosphorylated sequentially, first on Threonine 47 by Casein kinase 2, and then on Tyrosine 41 by Spleen tyrosine kinase (63). These phosphorylation events are necessary for L's actuation of Nup phosphorylation (63), but not for binding of Ran (53). Instead, phosphorylation has been shown to increase L's affinity for the exportin proteins CRM1 and CAS. Additionally, CRM1, L and Ran can form a high molecular weight complex (Chapter 3). CRM1 knockdown decreases L-directed Nup phosphorylation to less than 20% as well as decreasing virus replication (Chapter 3). The model proposes that this complex, localized to the pores by CRM1, picks up a cellular kinase partner (which then phosphorylates nucleoporins). Because Ran is nucleotide-free, the complex cannot be dissociated by normal GTP-to-GDP hydrolysis fostered by RanGAP. Kinases act enzymatically, and this complex would be highly effective at phosphorylating FG-containing Nups and shutting down nucleocytoplasmic trafficking.

There are over 518 predicted human kinases (121). While the exact L-directed Nup-phosphorylating kinase is unknown, studies have been performed using drug inhibitors to further narrow this range to those in the Mitogen-acting-protein-kinase (MAPK) family, with the most effective drugs including those targeting the p38 and ERK1/2 pathway (75). The p38 pathway is mainly activated by cellular stress to promote apoptosis, and also offers some negative regulation of other kinases by stimulating PP2a, a phosphatase responsible for inactivating

pathways promoting cell growth. The ERK1/2 pathway is activated by growth factors and others, and generally promotes cell proliferation. There are several downstream kinases shared between these two pathways (reviewed in (123)). For these 'shared' substrates, activities vary upon localization and compartmentalization, but include stimulation of various downstream kinases and nuclear transcription factors. The use of chemical inhibitors can have off-target effects (184), and inhibiting these kinases also prevents activation of kinases downstream, including MNK1/2, MSK1/2, RSK1/2/3, and many others.

In a normal cell cycle, Nups occasionally become phosphorylated. This is usually performed before mitosis by cyclin dependent kinases, causing the Nups to exit the interior of the pores and subsequent disassembly of the pores (185). Other studies, including proteomic studies to determine targets for ERK1/2 (120), involving cellular stress (119, 135), and studies using PP1 and PP2a phosphatase inhibitor Okadaic acid (OA), have demonstrated that these Nups can become phosphorylated (116). In these instances, transportins can no longer bind to these Nups, presumably precluding their translocation (120). Clearly, there must be a link between nucleocytoplasmic trafficking and kinase regulation, but details of these events remain undetermined. The results presented in this paper clarify specific cellular kinases used by L to phosphorylate Nups and thusly prevent cargo translocation. As such, these kinases may present common regulators of trafficking pathways that have been pirated for viral use.

Here we present data that ablation of ERK1/2, P38α/β, and RSK2/3 by use of siRNAs specifically decreased L-directed Nup phosphorylation in EMCV-infected cells, while other kinase siRNAs have no impact or enhanced Nup phosphorylation. A GST-tagged L can pull these kinases out of HeLa lysates, indicating an interaction. Additionally, we have reconstituted an L-dependent Nup phosphorylation event in isolated, sucrose-purified HeLa nuclei with recombinant forms of these kinases. These data suggest that these are the kinases used by

EMCV L during infections, and likely indicate kinases that may regulate nucleocytoplasmic trafficking pathways.

Materials and Methods

<u>siRNA knockdowns</u>

Suspension cultures of HeLa cells (ATCC CRL 1958) were maintained in modified Eagle's medium (37°C, 10% calf serum, 2% FBS, under 5% CO2). Cells were plated at 0.4 x 10^5 and allowed to attach overnight at 37°C. Pooled siGENOME Human SMARTpool siRNAs or siGENOME non-targeting siRNA #2 (Table 4.1; Dharmacon Inc, Thermo Fisher Scientific Biosciences) were transfected into cells at 25 nM in Dharmafect1 transfection reagent and Opti-MEM media (Life Technologies) as per manufacturer recommendations, and incubated for 48 hours to target kinases of interest. Cells were then infected with vEC9 (171) at an MOI of 15 for 4 hours at 37°C. Cells were harvested in 2x SDS buffer, boiled (15 minutes) before resolving on SDS-PAGE. Kinase knockdown was determined by immunoblot analysis, as was Nup62 phosphorylation, and all Nup phosphorylation values were normalized to tubulin levels using densitometry (63, 72).

<u>Kinase pulldowns</u>

Methods for recombinant engineering, bacterial expression and protein isolation of GST and GST-L$_E$, and L$_x$-GST have been described (64, 74). HeLa suspension cells were swollen in hypotonic buffer (0.75 Mg(OAc)$_2$, 0.15 mM EDTA, 1 mM PMSF, 0.01 mg/ml leupeptin, 20 mM pepstatin A, 3 mM DTT), followed by dounce homogenization and clarification (16,000×G, 20 min, 4°C) to isolate cytosol. Before storage at -80°C, TB (1/10 volume, 10x at 20 mM Hepes pH 7.3, 2 mM Mg(OAc)$_2$, 110 mM K(OAc), 1 mM EGTA) was added. Pulldowns proceeded as previously documented (Chapter 3); cytosol was precleared with 1/10 volume GST-Beads, end-over-end mixing for 1 hour at 4°C, and the beads were removed by centrifugation at 500xG.

Table 4.1 siRNAs used. siGENOME Human siRNAs, SMARTpool (Dharmacon, Inc/ThermoScientific, Lafayette, CO)

Protein target	Gene (NCBI accession number)
ERK1	MAPK3 (5595)
ERK2	MAPK1 (5594)
MEK1	MAP2K1 (5604)
MEK2	MAP2K2 (5605)
MSK1	RPS6KA5 (9252)
MSK2	RPS6KA4 (8986)
P38α	MAPK14 (1432)
P38β	MAPK11 (5600)
MNK1	MKNK1 (8569)
MNK2	MKNK2 (2872)
Non-targeting siRNA #2	

Recombinant L (2µg) was added to cytosol with ATP, incubated at 37°C for 45 minutes, mixing every 8 minutes, and GST buffer (50mM Hepes, 150 mM NaCl) was added with 10 µl of GST beads before incubating with agitation for one hour at room temperature. Beads were rinsed 6x with GST buffer and boiled 5 minutes with 2xSDS Buffer before resolving with SDS-PAGE. Gels were transferred to polyvinylidene difluoride membranes (Immobilon-P, Millipore), and proteins were blocked for 30 minutes at room temperature in 10% dry milk in TBST (20 mM Tris, pH 7.6, 150 mM NaCl, 0.5% Tween 20). Primary antibodies were incubated overnight at 4°C with 1% dry milk in TBST, rinsed 3x with TBST, and then the membranes were incubated for 1 hour with secondary antibody at room temperature. Following 3x rinsing with TBST, proteins were visualized with enhanced chemiluminescence (Pierce, GE Lifesciences) according to manufacturers' directions. Antibodies included: α−FG-repeat Nups (murine mAb414, IgG, Covance, 1:2000), α-Nup62 (murine Ab, IgG, BD Transduction Laboratories, 1:2000), α-tubulin (murine Ab, IgG, Sigma, 1:10,000), α–GST (murine mAb, IgG, Novagen, 1:10,000), α−p38α (rabbit Ab, IgG, Cell Signaling Technology, 1:3000), α−p38β (rabbit Ab, IgG, Cell Signaling Technology, 1:3000), α–ERK1/2 (unactivated, ERK1/2, rabbit Ab, IgG, Upstate, Millipore, 1:5000), α−MSK1 (rabbit Ab, IgG, Cell Signaling Technology, 1:3000), α−MSK2 (rabbit Ab, IgG, Cell Signaling Technology, 1:3000), α−MNK1 (rabbit Ab, IgG, Cell Signaling Technology, 1:3000), α−MEK1 (rabbit Ab, IgG, Cell Signaling Technology, 1:3000), α−MEK2 (rabbit Ab, IgG, Cell Signaling Technology, 1:3000), α−RSK1 (p90 RSK1 , rabbit Ab, IgG, Cell Signaling Technology, 1:3000), α−RSK2 (p90 RSK2, rabbit Ab, IgG, Cell Signaling Technology, 1:3000), α−RSK3 (p90 RSK3, rabbit Ab, IgG, Cell Signaling Technology, 1:3000), α−MNK2 (rabbit Ab, IgG, Abcam, 1:500), α-mouse (secondary Ab, IgG, Sigma Aldrich, 1:8000), α-rabbit (secondary Ab, IgG, Promega, 1:8000).

Recombinant kinases and isolated nuclei assays

Commercially available active kinases included ERK2 (New England Biolabs), RSK3 (Signal Biochem), CK2 (Signal Biochem). MEK4 and p38 constructs were kind gifts of Melanie Cobb, and purified as described (Khokhlatchev et al, 1997). In brief, these constructs were co-transformed with plasmids for constitutively active forms of their respective upstream kinases (MEKK-C or MEK4) into $E.\ coli$ BL21 cells, grown in 1L cultures, pelleted and sonicated with Hepes-based buffer. Lysates were clarified by centrifugation (20,000xG, 45 min, 4°C), the supernatant filtered through a 0.45 μm filter, and applied to a His-Trap column. The column was rinsed thoroughly, and recombinant kinases were eluted with a buffer. The resultant protein was dialyzed into a storage buffer, quantitated, and checked for activity using phosphorylation specific antibodies (Cell Signaling).

For sucrose-purified isolated nuclei, HeLa suspension cells were incubated on ice for 30 minutes with subcel buffer (10 mM Tris pH 7.4, 2 mM $MgCl_2$, 2mM DTT, 1mM PMSF), dounce homogenized for 100 strokes, and spun down at 10,000xG for 10 minutes at 4°C. Nuclei were rinsed with 0.35 M sucrose buffer (0.35 M sucrose, 10 mM Tris pH 7.4, 2 mM $MgCl_2$, 2mM DTT, 1mM PMSF), then resuspended in that .35 M sucrose buffer and layered over a 0.88M sucrose buffer cushion (0.88 M Sucrose, 10 mM Tris pH 7.4, 2 mM $MgCl_2$). Following centrifugation at 10,000xG for 10 minutes, nuclei that had migrated through the cushion were rinsed, counted with a hemocytometer and stored at 4°C for no more than 24 hours.

These nuclei were combined with γ-^{32}P-ATP (10 μCi), recombinant GST/GST-L, kinases and buffer, or HeLa cytosol as a positive control for L-directed native kinases. After incubation at 37°C for 45 minutes, these nuclei were lysed by 2x30 sec sonication in 1xRIPA buffer (300 μl/sample of 50 mM Tris, pH 7.4, 150 mM NaCl, 0.1% SDS, 1% Triton x 100, 0.5% Na Deoxycholate, 1mM PMSF, 20 mM pepstatin A, 1x protein phosphatase inhibitor cocktail 3 (Sigma Aldrich)), then precleared with 10μg protein G sepharose beads (G.E. Lifesciences), agitated at 4°C for 1 hour. The beads were removed by centrifugation, and the supernatants

were incubated at 4°C for 2.5 hours with protein G sepharose beads pre-bound to mab414 antibodies (saturated, Covance), to isolate Nup62 and other FG-containing Nups. These were resolved by SDS-PAGE, fixed by silverstain, and exposed to a phosphor-screen. Radioactivity was detected with a Typhoon imager, and densitometry was determined via TotalLab software (Newcastle upon Tyne, England). To determine the appropriate amount of recombinant kinase to use in these preps, titrations were performed to find a signal that was similar to one see with endogenous kinases using isolated nuclei and GST-L (data not shown).

Results

siRNA knockdowns and infections

As noted above, a previous study (75) showed that the L-directed Nup-phosphorylating kinases belongs to a downstream MAP kinase in the p38 and ERK1/2 families, as inhibitors against preceding kinases for these had no effect. To target specific kinases with less toxicity, we used siRNAs against to various isoforms of these kinases and others downstream, ultimately knocking down 13 kinases both singly and in combination (Table 4.1 and Fig. 4.1c). After infecting these kinase-knockdown cells, we assayed knockdown efficiency and Nup62 phosphorylation by westerns, specifically looking at which kinase knockdowns had the greatest effect on L-directed Nup62 phosphorylation. Nup62 phosphorylation was the most impacted by the knockdown of ERK1 (40%), ERK2 (14%), ERK1/2 in combination (15%), and RSK2 (76%) and 3 (67%) singly, though Nup phosphorylation was not decreased when RSK1/2/3 kinases were knocked down in combination (Fig. 4.1b,c). The knockdown of p38α/β in combination decreased Nup62 phosphorylation to 54%, though this effect was not observed when the p38 α/β kinase isoforms were targeted individually. When ERK1/2 and p38 α/β were knocked down in unison, Nup62 phosphorylation was decreased to 65% less than levels seen with non-targeting siRNAs. The knockdown of MEK1/2 increased L-directed Nup62 phosphorylation (up to
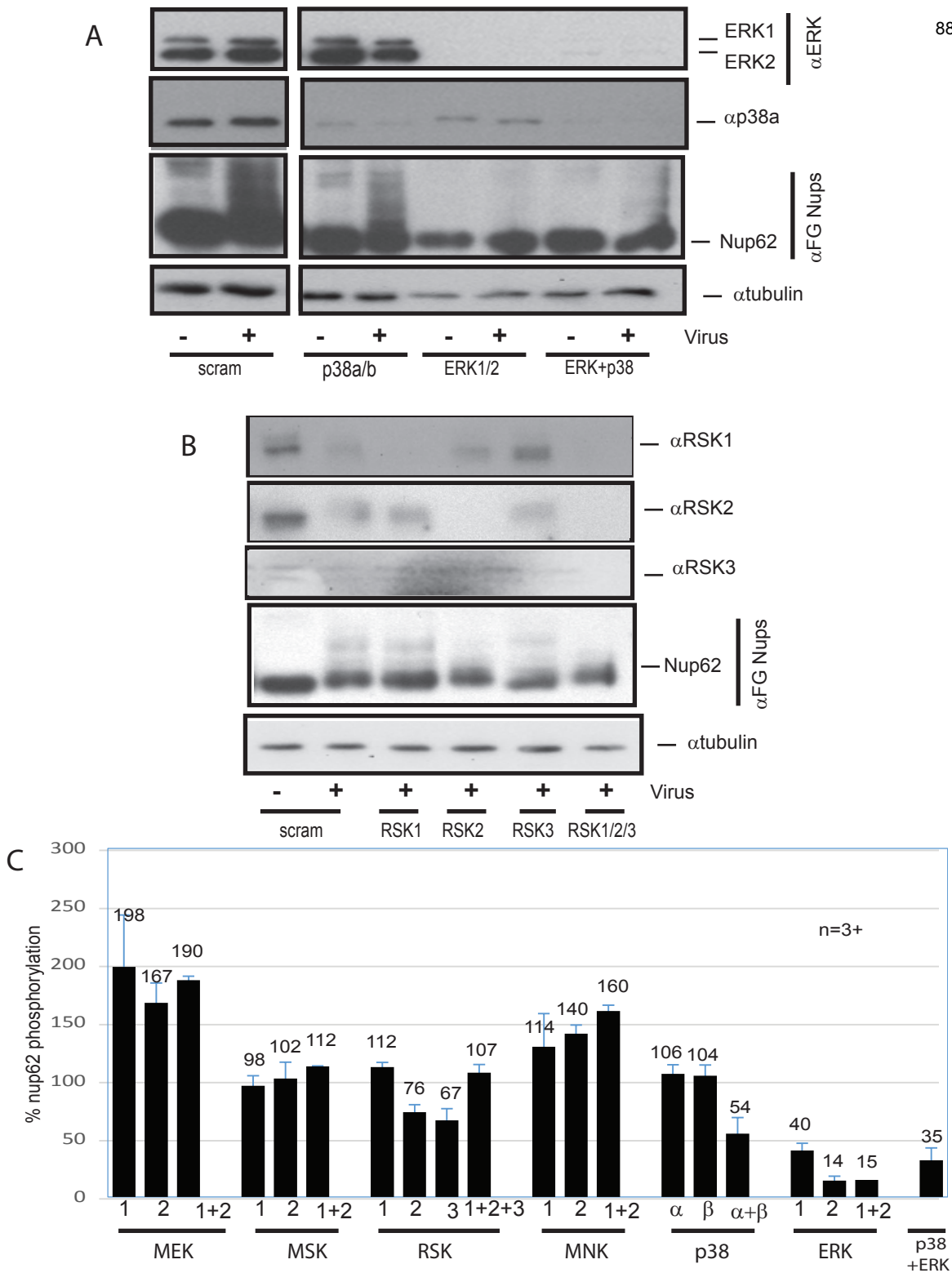
Figure 4.1 siRNAs were used to knockdown kinases, then cells were infected with EMCV at an MOI of 15 for 3.5 hours. Westerns were used to confirm kinase knockdown and determine Nup62 phosphorylation levels as depicted for ERK1/2 and p38α/β siRNAs (A) and RSK1/2/3 siRNAs (B). TotalLab Software was used to perform densiometry. Phosphorylation levels following knockdown of each kinase was graphed in (C) for an 'n' of 3+ samples.

190% with MEK1/2 knocked down in combination), and while slightly less, the knockdown of MNK1/2 increased Nup62 phosphorylation (160%) in combination. Particular kinases with the greatest impact on Nup phosphorylation were the focus of the next verification assays.

GST-L pulldowns

To determine if these kinases could be part of the L:CRM1:Ran complexes which we hypothesize form at nuclei during infections (Chapter 3, and (78)), we performed pulldowns with GST-tagged L proteins. These constructs retain full ability to direct Nup phosphorylation, as extensively documented (64, 72, 74), and provide highly effective tools for *in vitro* assays. L-GST from EMCV, SAFV, and TMEV were added to whole cell lysates (WCL), pulldowns were performed, and co-binding endogenous kinase partners were determined by western analysis. We find that GST-L from EMCV is capable of pulling down ERK1 and 2, as well as RSK1 and some p38 (Fig. 4.2). Despite inducing similar levels of Nup-phosphorylation, L_x-GST pulls down less kinase binding partners (for all tested cardiovirus Ls), and this may be attributed this to the c-terminal GST tag occluding the acidic domain. This domain has been predicted with *in silico* modeling to extend from the CRM1:L:Ran complex (78), and be the portion with which L interacts with kinases.

Reconstitution assays with isolated nuclei

To confirm which kinases were responsible for L-directed Nup62 phosphorylation, we developed an *in vitro* assay in which subcellular fractionation followed by sucrose cushion purification was used to isolate HeLa nuclei. Notably, these nuclei do not contain high amounts of kinases, but do contain some CRM1 and RanGTPase (Fig. 4.3). GST-L itself becomes phosphorylated when incubated with these isolated nuclei in buffer (Fig. 4.3). This is important to note, as L phosphorylation is required for L-directed Nup phosphorylation (63).
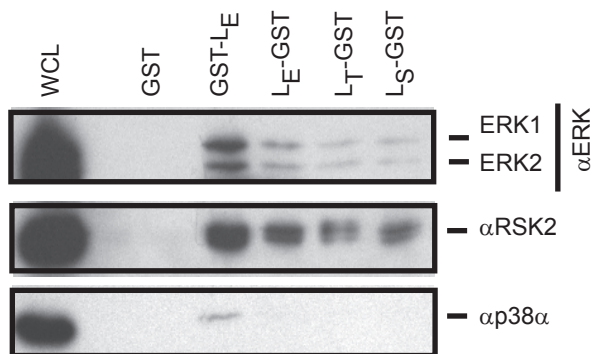
Figure 4.2: Cardiovirus pulldowns for endogenous kinases. GST-L_E or L_X-GST proteins were incubated with precleared HeLa whole cell lysates (WCL) and ATP for 45 minutes at 37°C. Glutathione beads were used to pull down GST-tagged L and associated native proteins. Bound cellular proteins were detected by western as indicated.
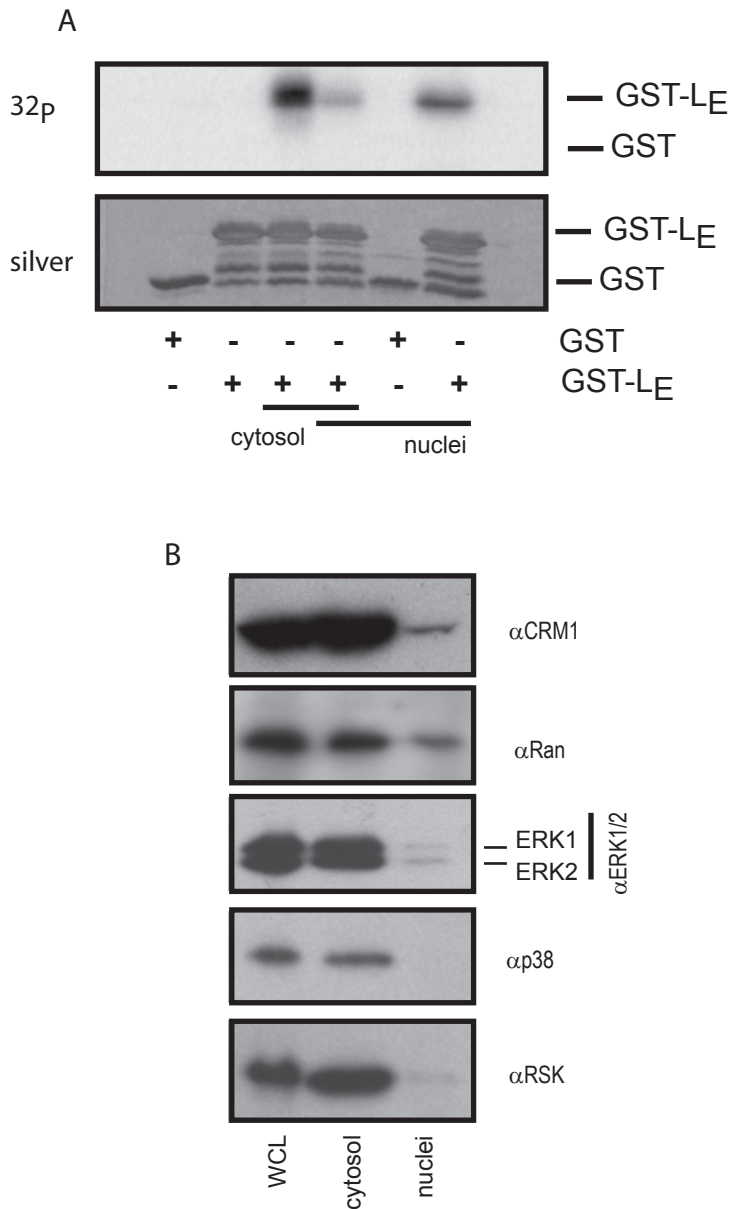
Figure 4.3 (A) GST or GST-L$_E$ phosphorylation state with HeLa cytosol or isolated, sucrose-purified nuclei. Recombinant proteins were incubated with nuclei or cytosol and γ-32P-ATP, for 45 minutes at 37°C. Pulldowns were performed with glutathione sepharose beads, and proteins were resolved by SDS-PAGE. The gel was silverstained and exposed to a phosphor-screen. (B) Cellular protein distribution: whole cell lysates (WCL), cytosol or fractionated, sucrose-purified nuclei as indicated were incubated at 37°C for 45 minutes, then boiled with 2xSDS buffer and resolved by SDS-PAGE. Westerns were performed with the indicated antibodies.

Isolated nuclei, GST or GST-L and active recombinant kinases or cytosol (as a positive control containing active native kinases) were incubated at 37°C for 45 minutes with γ-^{32}P-ATP. Following this incubation, samples were sonicated to break up to pores, Nup62 was immunoprecipitated from these samples, resolved by SDS-PAGE, and exposed to phosphor-screen to determine L-directed Nup62 phosphorylation. We find that singly, ERK2, RSK3 and p38α recapitulated Nup62 phosphorylation, but only with the inclusion of GST-L (Fig. 4.4). Other kinases were not able to detectably phosphorylate Nup62 at all, even with the inclusion of GST-L. Because RSK has been shown interact with TMEV L (186), we assayed whether other cardiovirus Ls could direct Nup phosphorylation under these assay conditions. While TMEV L was able to use endogenous kinases present in the cytosol positive control to phosphorylate Nup62, phosphorylation using recombinant RSK3 was undetectable. SafV was unable to direct Nup phosphorylation using recombinant or endogenous kinases in these assays.

Discussion

In these studies, we confirm that recombinant ERK1/2 and RSK3 phosphorylated Nup62 in the presence of cardiovirus L in a cell-free system (Fig. 4.4). A previous paper (75) showed that using chemical inhibitors, inhibition of p38 and ERK1/2 decreased L-directed Nup62 phosphorylation, which might suggest that either those kinases themselves, or a kinase stimulated by both of those pathways, or a co-target of the drugs used, like ERK5 (184), is responsible for this phosphorylation and subsequent nucleocytoplasmic trafficking inhibition. Our use of siRNAs for discrete kinase isoforms more finely tuned this kinase search, as isoforms vary by localization and sometimes function (reviewed in Chapter 1). These results depict that upon the knockdown of both ERK 1 and 2 isoforms, the phosphorylation of Nup62 is decreased in EMCV-infected cells (Fig. 4.1a,c), though not completely abolished. Knockdown of p38 α/β did not impact L-directed Nup62 phosphorylation to the same extent, despite early studies suggesting that the simultaneous knockdown of these kinases would further decrease
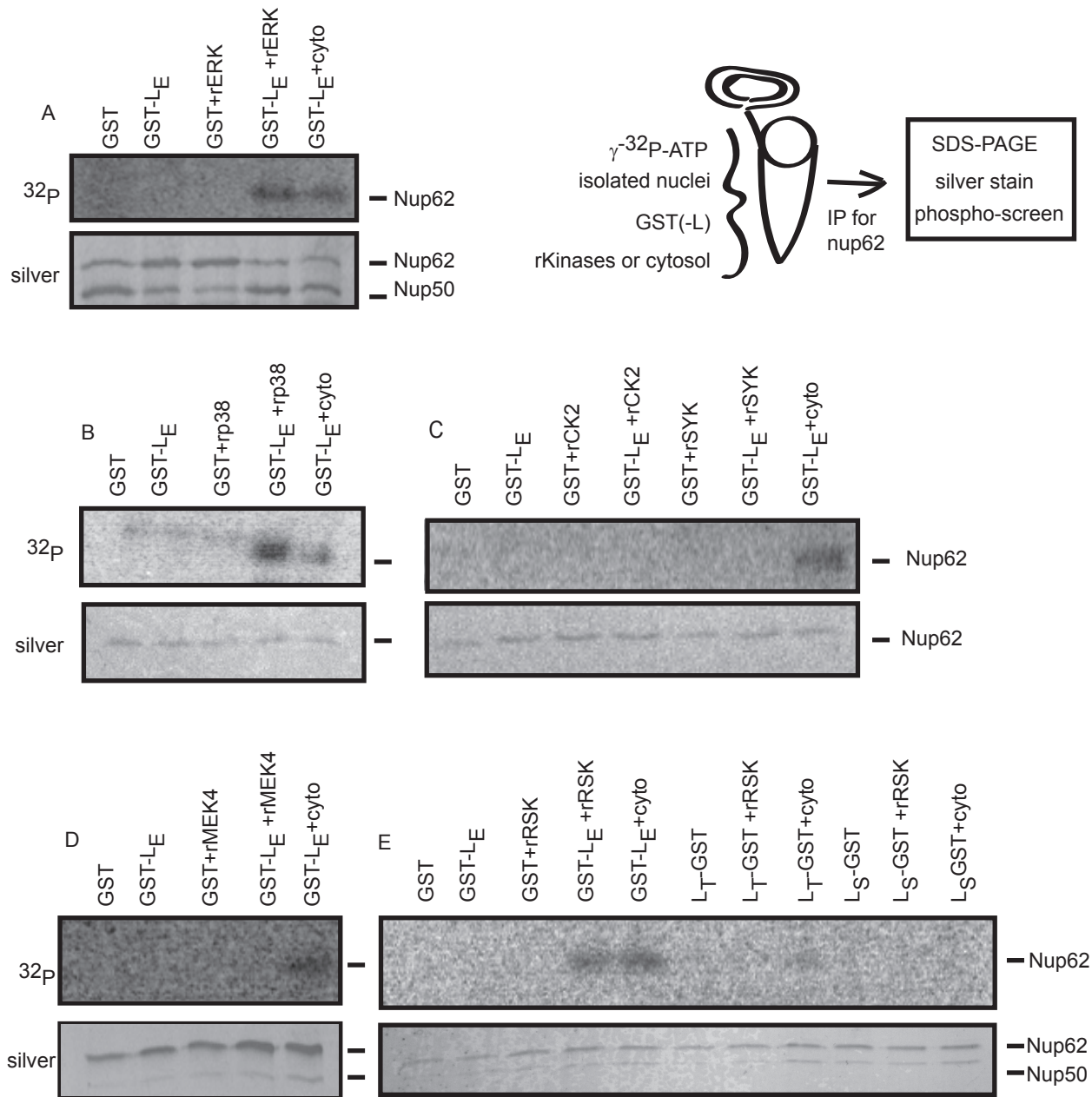
Figure 4.4 Recombint kinases and isolated nuclei assay: Nuclei were isolate by subcellular fractionation then further purified with a sucrose cushion. 10^5 nuclei were combined with GST or GST-L$_X$ as indicated with γ-^{32}P-ATP and the indicated recombinant kinase: rERK2 (A), rp38α (B), rMEK4 (C), rCK2 and rSYK (D), or rRSK3 (E), or HeLa cytosol for 45 minutes at 37^0C. Samples were sonicated with 1xRIPA, precleared with protein G sepharose beads, and supernatants were subjected to immunoprecipitation for FG-containing Nups (Nup62 and Nup50). These samples were boiled and resolved by SDS-PAGE, silverstained, and the gel was exposed to a phosphor-screen.

Nup62 phosphorylation (75). Many of the downstream kinases common to both of these pathways (MSK1/2, MNK1/2, etc.) did not show any impact on L-directed Nup-phosphorylation. Moreover, when other kinases were knocked down, this actually caused increased Nup62 phosphorylation during infections (Fig. 4.1c). For MEK1/2, we theorize that because these kinases are involved in the downregulation of ERK1/2, as a cytosolic scaffold for ERK1/2 sequestration (125), their knockdown actually allowed more ERK/2 to remain activated in this system. Additionally, previous studies have established that knocking down one portion of a kinase pathway increases activity of the remaining portions as a feedback loop. Due to functional redundancy, this particularly applies to isoforms, and may be why we see better decrease in Nup phosphorylation when multiple isoforms for p38 are targeted. While we cannot rule out that there may be additional kinases able to phosphorylate Nup62 in a cardiovirus infection, the 85% decrease in Nup62 phosphorylation with ERK2 siRNAs is a very solid demonstration that this is the responsible kinase.

To serve as a supplement to and confirmation of the primary siRNA results, we sought to recapitulate a Nup62 phosphorylation event using MAPK-free isolated nuclei, buffer, and recombinant GST-L and kinases, with γ-^{32}P gamma- ATP as an indicator (Fig. 4.4), and show that these kinases are necessary and sufficient to induce Nup phosphorylation. Importantly, isolated nuclei have been fractionated from unstimulated cells, which do not contain substantial amounts of activated MAPKs (Fig. 4.3), as the trafficking of activated MAPK kinases into the nucleus is a well-documented response to cellular stimuli predicating proliferation or apoptosis. In this system, GST, GST-L and the recombinant kinases do not cause Nup62 phosphorylation without both the presence of rkinase and L. GST-L and ERK2 in combination, or GST-L and RSK3 in combination, were able to phosphorylate Nup62. Other kinases, including MEK4, another MAPK, were not able to do phosphorylate Nup62 with or without GST-L (Fig. 4.4). These nuclei contain sufficient quantities of Ran and CRM1 for L interaction (Fig. 4.3b). The

phosphorylation of GST-L is necessary for Nup phosphorylation (63), likely to enhance binding of L to CRM1 and possibly to the kinases (Chapter 3) and we find that GST-L can be phosphorylated in these isolated nuclei reactions (Fig. 4.3a). Cytosol served as a positive control, with endogenous kinases (presumably ERK1/2) acting as they do in the context of intact cells (Fig. 4.4). Interestingly, we note that while TMEV L has been shown to interact with RSK3 (186), it does not stimulate nearly the same amount of Nup62 phosphorylation compared to equal amounts of EMCV L.

Endogenous kinases from whole cell lysates, including ERK1/2 and RSK3, can bind to GST-L (Fig. 4.2). Additional experiments were unable to confirm this result with recombinant kinases due to technical difficulties involving recombinant protein tags, though ERK2 does not seem to bind directly to L (data not shown). The binding of endogenous kinases to GST-L fits our model based on previous data ((78), Chapter 3), wherein GST-L sits between CRM1 and a nucleotide-free RanGTPase, with the L acidic domain extending out into the cargo-binding region of CRM1.

Little is known about nuclear pore complex regulation by post-translational modification. There are cell cycle dependent Nup phosphorylation events that cause exit of the Nups from pores, to eventuate nucleus deconstruction during mitosis (185, 187, 188). Others have shown that phosphorylation of nuclear pores can occur upon treatment of cells with a phosphatase inhibitor (116), and that some Nups can serve as a substrates for ERK1/2 (120); it is likely that cardioviruses are corrupting yet-undescribed native regulation pathways. While cardioviruses might just be taking advantage of activated kinases which traffic through the nuclear pores (discussed with appendix Fig. 3), the phosphorylation sites on the Nups themselves support a model in which Nup phosphorylation is a normal but not-yet-well described regulatory pathway.

Our data demonstrate that ERK2 is certainly a kinase used by L during infections to phosphorylate Nups. Isoforms ERK1 and ERK2 have the same substrate target domain and equivalently phosphorylate substrates *in vitro*, but ERK2 is the more prevalent form in different

cell types, and *in vivo* documented targets vary (reviewed in (189)). They have been shown to travel into the nucleus to activate various transcription factors. However, re-localization has been reported to traffic directly into the nucleus *sans* transportins (128, 129, 190) as well as through interactions with transportin 7 (127), or by possibly another method. To exit the nucleus, ERK1/2 is inactivated by MEK1/2, which draws it out of the nucleus and re-sequesters it onto membranes in the cytosolic space (191). The isoforms of ERK may also form homodimers (192, 193), and these may have higher activity than single kinases (reviewed in (189)).

It is worthwhile to note that MAPK kinases belong to the same family, and share homology and domains ((123) and Fig. 1.7) that may be co-opted for L's activities. Because our results with siRNAs against p38 do not decrease L-directed Nup phosphorylation to the same level as that of ERK, p38 is likely a secondary kinase partner of L. A recent report using TMEV L (50) suggests that the activation of the p38 pathway may instead have more involvement in L's anti-apoptotic roles than Nup phosphorylation. In that, p38 then goes on to activate p53, which alters downstream events to end up with release of pro-apoptotic proteins like Bax and resultant apoptosis (50). The idea of ERK as EMCV L's primary kinase partner may also explain the results seen for RSK2/3; ERK1/2 also binds to and activates the RSK kinases (194), along with 3'-phosphoinositide-dependent kinase 1, though they have different phosphorylation sites (195). This interaction between ERK1/2 and RSK1/2/3 may act synergistically as part of an L-containing complex that we hypothesize forms at nuclear pores ((78) and Chapter 3). As nucleocytoplasmic trafficking regulation by kinases becomes better understood, it will be interesting to note these kinases' interactions and activities in native functions.

The model suggested by prior studies ((78) and Chapter 3) is that cardiovirus L interacts with transportin CRM1 and RanGTPase in an indissociable unit, holding it at the nuclear pores to interact with kinases and cause Nup phosphorylation (Fig. 1.8). Our data presented here using both siRNA knockdown assays and *in vitro* reconstitution assays indicate that the primary

kinase used by L is ERK1/2, though other kinases like RSK2/3 may also be involved perhaps

due to their native affinities/associations.
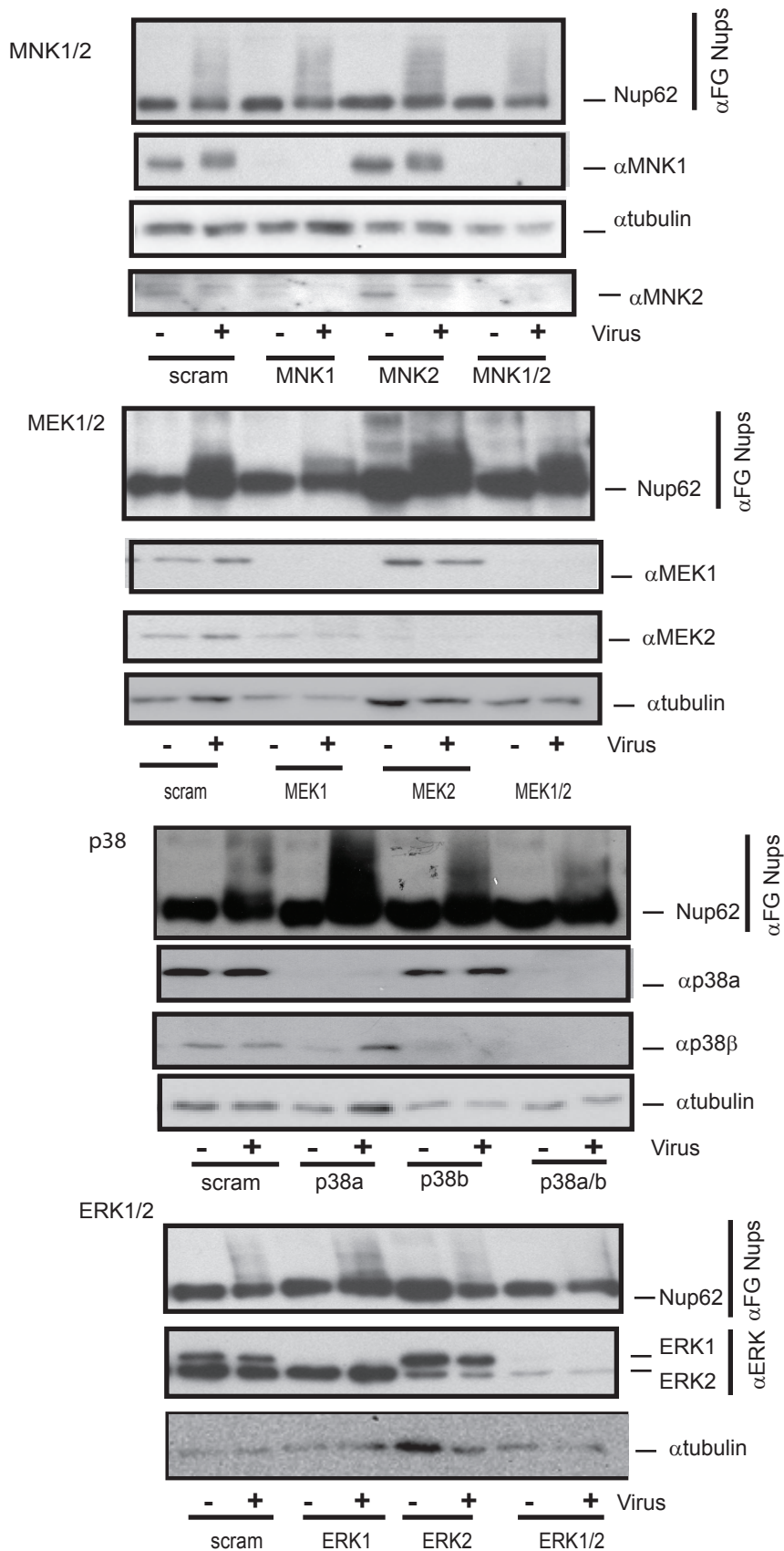
Chapter 5: Conclusions and Future Directions

Chapter Highlights

Chapter 1: Introduction

Chapter 2: Three Cardiovirus Leader Proteins Equivalently Inhibit Four Different Nucleocytoplasmic Trafficking Pathways

- All cardioviruses additionally phosphorylate Nup98, but not Nup50.
- Four nucleocytoplasmic trafficking pathways are inhibited by cardiovirus L proteins.
- Nups must be in a nuclear pore for cardiovirus L-directed phosphorylation
- L does not cause activation of kinases present in the cytosol alone

Chapter 3: Cardiovirus Leader proteins bind exportins: implications for virus replication and nucleocytoplasmic trafficking inhibition

- Cardiovirus L interacts with exportins CRM1 and CAS
- Phosphorylation of L_{Thr47} enhances CRM1:L affinity, and this binding can withstand high concentrations of salt
- Ran and CRM1 are not required for the binding of the other to L
- CRM1:L:Ran form trimeric complexes
- Knockdown of CRM1 decreases EMCV replication as well as L-directed Nup phosphorylation

Chapter 4: ECMV L directs ERK2 to inhibit nucleocytoplasmic trafficking

- L directs ERK1/2, RSK2/3 and to lesser extents p38α/β to phosphorylate nups, but not other kinases
- L becomes phosphorylated with only contents of nucleus in addition to kinases found in cytosol
- Quiescent nuclei contain CRM1 and RanGTPase, and can phosphorylate L
- Cardiovirus L can also pull ERK and RSK kinases out of cytosol, along with CRM1 and Ran

Summary and Future Directions

Nucleocytoplasmic transport is a vital cellular process: export of mRNAs regulate cellular activities, import of various machinery and signaling factors for cellular proliferation and defense. As such, inhibition of this transport is a frequent target for viral control of the cell, to prevent the host from mounting a response locally (reviewed in (196)). It also frees up cellular translation and replication factors for use by RNA viruses, which replicate in the cytoplasm (1). While other viruses block the nuclear pores using viral proteins in association with cellular factors (Vesicular stomatitis virus and Venezuelan equine encephalitis virus), and clip nups from the pores to prevent transport (enteroviruses), cardioviruses phosphorylate these same proteins by the sole activities of their Leader (L) protein, harnessing cellular kinases for this post-translational modification. Phosphorylation leaves nups at the pores, but prevents trafficking and provides a general efflux of cellular nuclear factors to enhance viral replication (70, 71, 74).

Data presented in Chapter 2 of this thesis demonstrated that all cardiovirus Ls shut down at least four nucleocytoplasmic trafficking pathways, preventing both import and export through the pores. While it has been known that TMEV phosphorylates Nup98 (152), EMCV L

phosphorylates Nups 62, 153 and 214, Chapter 2 also demonstrates that Nup98 is phosphorylated and Nup50 is not, suggesting some level of selection by the L-directed kinases. Experiments additionally indicate a localization requirement for nup phosphorylation. Nups (both recombinant and endogenous) not in the context of the pore do not become phosphorylated, and L itself does not activate kinases in the cytosol. This implies that L must be held at the nuclear pores, in agreement with prior microscopy showing L at the nuclear envelope (74).

L binds to RanGTPase, but there is not enough L made at the time that trafficking is shut down to fully saturate all Ran and prevent its activities. Additionally, Ran itself may not be adequate to target L to the nuclear pores for interaction with kinases. To further identify cellular binding partners who might target L to the pores, experiments presented in Chapter 3 included pulldowns of GST-L in HeLa cytosol, and subsequent identification of cellular binding partners by Orbi-trap Mass Spectrometry. Results acknowledged the nuclear exportins CRM1 and CAS as potential binding partners. Further experiments confirmed that GST-L does indeed interact with these exportins, and focused on CRM1 because it is a very broad range exportin (reviewed in (105)). L phosphorylation is not necessary for L:Ran binding (53), but enhances L's affinity for CRM1; doubly phosphorylated L binds 1.7 times more CRM1 than the unphosphorylated form. A CRM1:L:Ran complex can be eluted from a S200 gel filtration column, indicating that these three proteins are able to form a trimeric complex. Knocking down CRM1 by shRNAs decreases L-directed Nup phosphorylation to 11% and EMCV replication to 30% (Chapter 3). Because a Ran in this CRM1:L:Ran complex does not contain a nucleotide in the binding pocket, the complex is indissociable by typical Ran GTP-to-GDP hydrolysis (78).

Previous studies used drug inhibitors to narrow down the range of culpable L-directed kinases to those in the MAPK pathways (75). Chapter 4 identified exactly which of these pathway's kinases is being used by L to phosphorylate nups. For this, siRNAs were used to knockdown individual kinase isoforms singly and in combination. ERK2 and RSK2/3 knockdown decreased

L-directed Nup phosphorylation, as did knockdown of ERK1/2 plus p38α/β in combination. Further GST-L pulldowns indicate that these kinases associate with EMCV L (presumably fully phosphorylated, bound to endogenous CRM1 and Ran) in HeLa cytosol. To fully confirm these results, these recombinant kinases can be used to phosphorylate isolated nuclei (lacking activated kinases), though only upon the addition of L. Curiously, other cardiovirus Ls were tested for their ability to direct recombinant kinases for the phosphorylation of Nups, but none were as successful as EMCV L. This finding is consistent with previously published literature; EMCV shows the greatest activity in a study when compared to other cardioviruses in early cardiovirus- directed Nup phosphorylation studies done in transfected HeLa cells (64).

Experiments in Chapter 4 demonstrated that L is able to interact with kinases, though this may not be a direct association. CRM1 likely holds this complex at the pores, and the enzymatic function of kinases allows these highly active proteins then phosphorylate Nup substrates (i.e., the FG-repeats of Nups 214, 153, 98, and 62). It is likely that L is converting standard pathways wherein kinases are regulating nucleocytoplasmic trafficking. There are hints of these pathways in various literature, but these native regulatory pathways remain to be described in any detail. Chapter 4 identifies potential kinases for those impending studies.

Because science tends to yield more questions, there are a few possible directions for future work. Based on the reconstitution assays in Chapter 4, it would be really interesting to see if the recombinant kinases add comparable quantities of phosphates to the nups when compared to endogenous cytosolic kinases. This could easily be done using the isolated nuclei system outlined in Chapter 4 and 2D gel electrophoresis.

As alluded above, it is highly likely that L is using native kinase-based nucleocytoplasmic trafficking regulation pathways. Because phosphorylation events on nups are rarely detected as evidenced by their paucity in published studies, phosphatases likely play a role. Early collaborations with the Xing Lab (University of Wisconsin – Madison) indicate that L itself does

not interact directly with PP2a, but we see an activation of kinase pathways during infection

(75). This might partially be explained by the trapping of activated kinases in the pores; nuclear

kinases may be unactivatable (this occurs by sequestering inactivated kinases in cytosolic

membranes). As such, their downstream substrates would also remain active. However, there

are nuclear phosphatases (DUSPs) that typically downregulate nuclear kinases. The activation

state of these phosphatases remains to be established, as does any impact of Leader on native

DUSP cycles.

Further facets of L's activities to explore include its exact location at the pores. The data

presented in Chapter 3 and previous studies (77) suggest that Ran and L bind in the nucleus,

given the catalytic effect of RCC1 and known localization of that protein. However, the

cytoplasmic fibril Nups would provide a highly mobile tether for the CRM1:L:Ran:kinase

complex, and these are long/flexible enough to reach the entire pore, as well as neighboring

pores, for Nup phosphorylation. However, current technologies (lack of good antibodies and

sufficiently sensitive detection techniques) prohibit these experiments at present, despite

multiple attempts. Determining the exact localization would shed light on the possible order of

complex assembly and mechanism.

Chapter 4 makes a very convincing basis for kinase partners of L, but we cannot completely

preclude identification of all responsible kinases. MAPK kinases are strikingly similar in both

structure and redundant functions (Figs. 1.6 and 1.7), and it is likely that there are other kinases

that can phosphorylate Nups. Their trafficking through the pores also remains to be specifically

established - current literature defines at least 3 ways that ERKs translocate into and out of the

nucleus, with 2 separate ways described for p38 isoforms (reviewed in (123)). It will be

interesting to see what future kinase studies determine for the trafficking of MAPKs, their

interactions, and their substrate specificities. Again, the findings presented in that chapter hold

implications for virology as well as cancer research and nucleocytoplasmic trafficking/greater biology.

Taken as a whole, this thesis provides many of the details toward deciphering L's activities at the nuclear pores. In our current model (Chapter 1, Fig. 1.8), L associates with 2A and utilizes 2A's NLS to effectively traffic to the nuclear pore. At the pore, L becomes phosphorylated, and subsequently Ran and CRM1 associate, displacing 2A. The structure models show L acting as a sort of 'molecular glue', creating an indissociable CRM1:L:Ran complex, with the zinc finger of L extending into CRM1's cargo domain (78). Cellular kinases then associate, and are used to phosphorylate Nups and inhibit nucleocytoplasmic trafficking. Nucleocytoplasmic trafficking inhibition prevents cells from mounting an innate immune response, and from signaling neighboring cells. Moreover, an efflux of (nuclear) cellular factors necessary for viral replication can relocalize to the cytoplasm, allowing for a productive infection.

Appendix: Additional Experiments

Appendix Figure 1 was published in (63), *Journal of Virology. 88:2219-2226. (2014) Basta, H. A., V. R. Bacot(78)-Davis, J. J. Ciomperlik, and A. C. Palmenberg. 2014. Encephalomyocarditis virus Leader is phosphorylated by CK2 and Syk as a requirement for subsequent phosphorylation of cellular nucleoporins.*

Appendix Figure 2 was published in (78), *Proceedings of the National Academy of Sciences, 111:15792-15797. (2014) Bacot-Davis, V. R., J. J. Ciomperlik, C. C. Cornilescu, H. A. Basta, and A. C. Palmenberg. 2014. Solution structures of Mengovirus leader protein, its phosphorylated derivatives, and in complex with RanGTPase.* This experiment was designed by J.C. and H.B., performed by H.B, and analyzed by J.C.

Cardiovirus Leader (L) proteins were predicted to contain at least one (and possibly more) phosphorylation sites ((52, 57, 150)) and mutation to at least one of these sites at Thr47 was shown to disrupt L's nucleocytoplasmic trafficking activities (70). Experiments were undertaken to determine the exact location of those phosphorylation sites, possible kinases responsible for this event, and the impact of L phosphorylation on Nuclear pore protein (Nup) phosphorylation/ nucleocytoplasmic trafficking (63). Phospho-antibodies were used to determine that L contained a phospho-tyrosine site in addition to a phosphor-threonine site, and this was confirmed by

generation of phospho-deficient mutants at both sites, and testing of these with γ-32P-ATP and cytosol (Basta et al). Online post-translational modification prediction software (NetPhos2.0, Phosphomotif (197), and Phosida Gnad (198)) was used to identify potential kinases. One of these potential kinases included Casein kinase 2 (CK2), against which drug inhibitors can be used; these include TBCA [(E)-3-(2,3,4,5-tetrabromophenyl) acrylic acid] (Calbiochem, used at 10 µM) or TBB (4,5,6,7-tetrabromo-2-azabenzimidazole) (Calbiochem, used at 50 µM). As illustrated in Appendix Figure 1, incubation of L_E-GST with γ-^{32}P-ATP in either HeLa cytosol (Appendix Figure 1a) or recombinant CK2 (Appendix Figure 1b) in the presence of these inhibitors decreased L phosphorylation by 40-60%. Other experiments determined that L phosphorylation is sequential, and that Thr47 must be phosphorylated before phosphorylation of Tyr41 by Spleen tyrosine kinase. To confirm that L phosphorylation is important to direct Nup phosphorylation, plated HeLa cells were pretreated with both CK2 inhibitors for an hour, then infected at an MOI of 30. Westerns were used to determine Nup62 phosphorylation. With the inclusion of CK2 inhibitors, Nup62 phosphorylation decreased to 16% (with TBB, Appendix Figure 1c). CK2 is not one of the kinases responsible for Nup phosphorylation itself (Figure 4.4D), and from this data and data presented in Chapter 3, we concluded that L phosphorylation is required for Nup phosphorylation and subsequent nucleocytoplasmic trafficking inhibition.

Appendix Figure 2, a collaboration with Holly Basta, shows that phosphorylation-deficient mutants of L do not bind exportins CRM1 and CAS to the s ame level as wild type L. This figure was presented in conjunction with the solved crystal structure of L:Ran in (78). As demonstrated in this figure and Chapter 3, phosphorylation on L's Thr47 enhances binding of both CRM1 and CAS. Additionally, a CRM1:L:Ran structure was modeled for (78), indicating that the acidic domain of L likely sits between CRM1 and Ran, with the zinc finger region extending into the cargo binding site of CRM1.
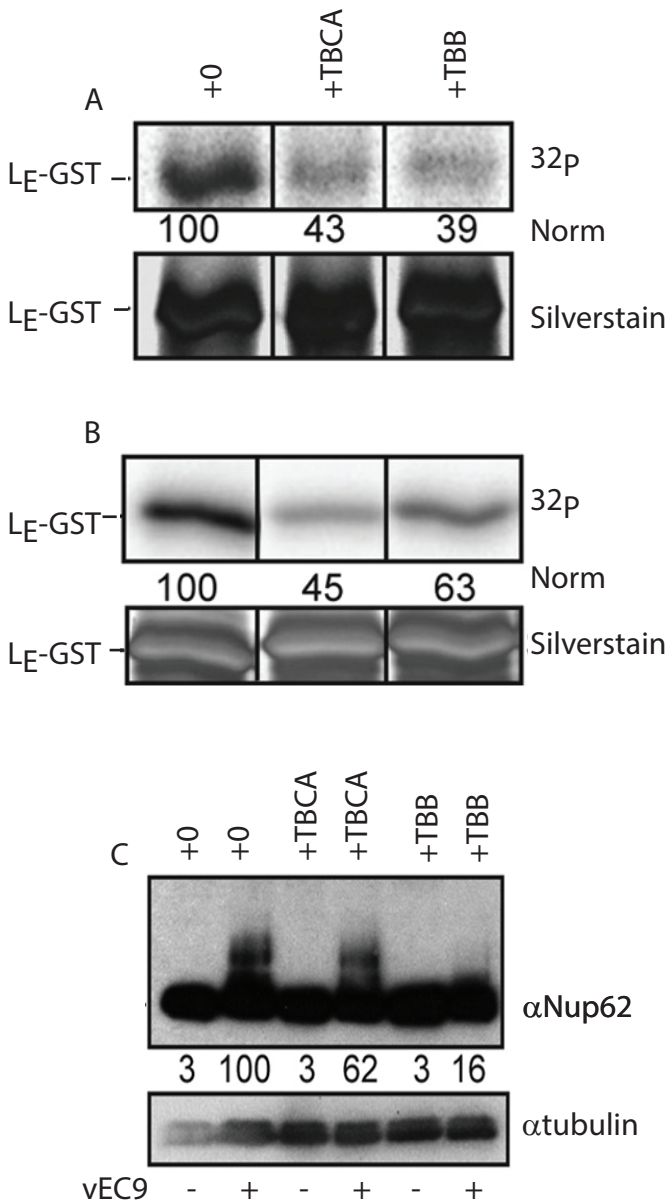
Appendix Figure 1 Leader phosphorylation inhibitors effects. Recombinant L_E-GST was incubated with HeLa cytosol (A) or recombinant Casein Kinase 2 (B) with or without Casein kinase 2 inibitors in the presence of γ-^{32}P-ATP (37^OC for 45 min) and pulled down with Glutathione sepharose beads. Proteins were resolved with SDS-PAGE and silverstained, then exposed to phosphor-screen to determine phosphorylation state of L. To determine how L phosphorylation affected Nup phosphorylation, plated HeLa cells were treated with TBCA or TBB as indiciated for 1 hr at 37^OC, then infected with vEC9 at an MOI of 30 as indicated. 4 hours post-infection, cells were harvested, and Nup phosphorylation state was determined by western. All quatitation was done with TotalLab (Sigma Aldrich). Casein kinase inhibitors TBCA and TBB were used at 10μM and 50 μM, respectively.
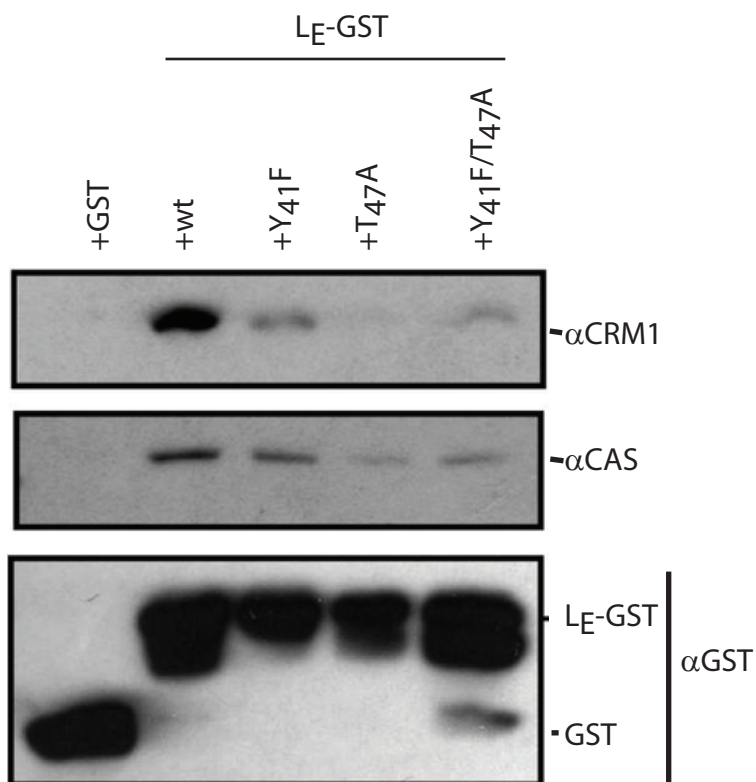
Appendix Figure 2 Exportin pulldown from HeLa cytosol. Recombinant GST, L_E-GST, L_E-GST phosphorylation deficient mutants were incubated with HeLa cytosol for 45 minutes at 37°C, then pulled down with glutathione sepharose beads. Westerns were performed for GST and exportins, to determine L binding partners. (Experiment designed by Jessica Ciomperlik and Holly Basta and performed by Holly Basta.)

Okadaic acid (OA), a phosphatase inhibitor for protein phosphatase 2a (PP2a) and protein phosphatase 1 (PP1) (159), was used as a control in Chapter 2 of this thesis to stimulate kinases by inactivating correlated phosphatases. The use of OA in another nucleocytoplasmic trafficking study indicated that it inhibits the classical nuclear import (importin α/β) and transportin pathways, though not the CRM1 export pathway, attributed to phosphorylation of the "nuclear transport machinery... most likely a component of the nuclear pore complex" (117). Evinced in Appendix Figure 3, incubation of OA with subcellular fractionated HeLa nuclei and L produces a minor phosphorylation of Nup62, at 29% of the Nup62 phosphorylation compared to that directed by GST-L (100%). The L-directed greater Nup phosphorylation event likely explains why more pathways, including CRM1, are inhibited in cardiovirus infections. However, the combination of GST-L and OA in nuclei/cytoplasm assays produces a synergistic phosphorylation of Nup62, increasing to 3.5 times that of GST-L alone. There are several possible interpretations of this data. Figure 2.5 demonstrated that L alone does not stimulate cytosolic kinases, but OA does. It may be that L utilizes whatever pool of activated kinases are present in the cell for Nup phosphorylation, and that inclusion of OA very effectively deepens that pool, producing more activated kinases upon which L can act. Alternately, it may be that the inclusion of OA prevents the turnover any phosphorylation events (either of the Nups, or of L itself, or both) before they can be detected by our standard assays. These interpretations are also not mutually exclusive. A further suggestion drawn from this figure (and supported by the kinase binding partners of L, Chapter 4) is that L is not somehow inhibiting PP2a or PP1 to activate MAPKs, or combining OA and L would either decrease or not affect Nup62 phosphorylation. Future experiments are necessary to confirm the activation state of phosphatases during infection.
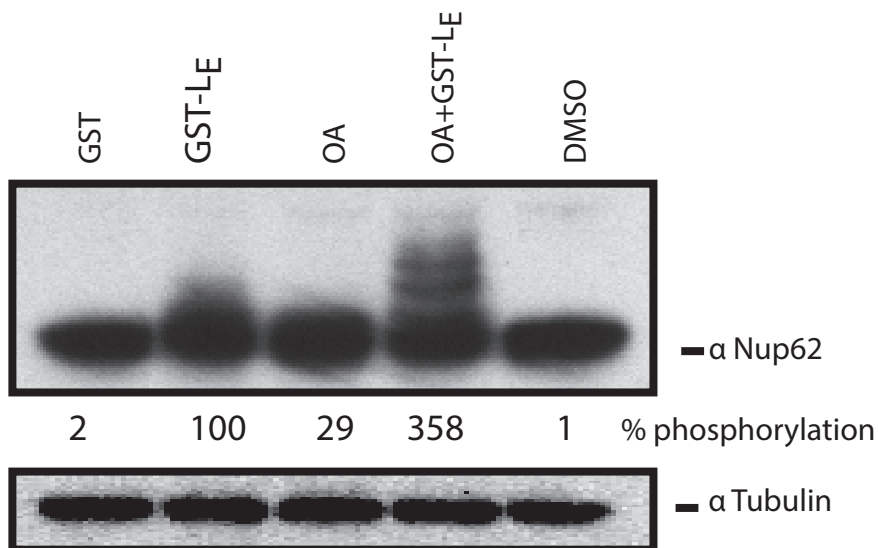
Appendix Figure 3 Effects of phosphatase inhibitor Okadaic acid and GST-L$_E$ on Nup phosphorylation. GST, GST-L$_E$, Okadaic Acid (OA, 250 nM), OA plus GST-L$_E$, or carrier DMSO were added as indicated to subcellular fractionated HeLa cytosol and 10^3 digitonin-isolated nuclei, incubated at 37°C for 45 minutes, and the phosphorylation of Nup62 was analyzed by wetern phospho-shift (C). Nup62 phosphorylation was quantitated by pixel count and normalized to tublin loading control using TotalLab software.

References

1. **Ehrenfeld E, Domingo E, Roos RP.** 2010. The Picornaviruses, 1 ed. ASM Press, Washington, DC. US.

2. **Rossmann MG, Arnold E, Erickson JW, Frankenberger EA, Griffith JP, Hecht H-J, Johnson JE, Kamer G, Luo M, Mosser AG, Rueckert RR, Sherry B, Vriend G.** 1985. The structure of a human common cold virus (Rhinovirus 14) and its functional relations to other picornaviruses. Nature **317:**145-153.

3. **Olson NH, Kolatkar PR, Oliveira A, Cheng RH, Greve JM, McClelland A, Baker TS, Rossman G.** 1993. Structure of human rhinovirus complexed with its receptor molecule. Proc.Natl.Acad.Sci.U.S.A. **90:**507-511.

4. **Luo M, Vriend G, Kamer G, Minor I, Arnold E, Rossmann MG, Boege U, Scraba DG, Duke GM, Palmenberg AC.** 1987. The atomic structure of Mengo virus at 3.0 A resolution. Science **235:**182-191.

5. **Shepard DA, Heinz BA, Rueckert RR.** 1993. WIN 52035-2 inhibits both attachment and eclipse of human rhinovirus 14. J.Virol. **67:**2245-2254.

6. **Racaniello VR.** 2001. *Picornaviridae*: The viruses and their replication, p. 685-722. *In* Knipe DM, Mowley PM (ed.), Fields Virology, 4th edition ed. Lippincott Williams and Wilkins, Philadelphia, PA.

7. **Zeichardt H, Wetz K, Willingmann P, Habermehl KO.** 1985. Entry of poliovirus type 1 and Mouse Elberfeld (ME) virus into HEp-2 cells: Receptor-mediated endocytosis and endosomal or lysosomal uncoating. J.Gen.Virol. **66:**483-492.

8. **DeTulleo L, Kirchhausen T.** 1998. The clathrin endocytic pathway in viral infection. EMBO **17:**4585-4593.

9. **Flore O, Fricks CE, Filman DJ, Hogle JM.** 1991. Conformational changes in polioviurs assembly and cell entry. Semin.Viol. **1:**429-438.

10. **Jang SK, Krausslich HG, Nicklin MJH, Duke GM, Palmenberg AC, Wimmer E.** 1988. A segment of the 5' nontranslated region of encephalomyocarditis virus RNA directs internal entry of ribosomes during *in vitro* translation. J.Virol. **62:**2636-2643.

11. **Pelletier J, Sonenberg N.** 1988. Internal initiation of translation of eukaryotic mRNA by a sequence derived from poliovirus RNA. Nature **334:**320-325.

12. **Spriggs KA, Bushell M, Mitchell SA, Willis AE.** 2005. Internal ribosome entry segment-mediated translation during apoptosis: the role of IRES-trans-acting factors. Nature **12:**585-591.

13. **Flather D, Semler B.** 2015. Picornaviruses and nuclear functions: targeting a cellular compartment distinct from the replication site of a postitive- strand RNA virus. Front. Microbio. **6:**594.

14. **Kaminski A, Belsham GJ, Jackson RJ.** 1994. Translation of encephalomyocarditis virus RNA: Parameters influencing the selection of the internal initiation site. EMBO Journal **13:**1673-1681.

15. **Ghadge GD, Ma L, Sato S, Kim J, Roos RP.** 1998. A protein critical for a Theiler's virus-induced immune system-mediated demyelinating disease has a cell type-specific antiapoptotic effect and a key role in virus persistence. J.Virol. **72:**8608-8612.

16. **Palmenberg AC.** 1990. Proteolytic processing of picornaviral polyprotein. Ann.Rev.Micro. **44:**603-623.

17. **Sommergruber W, Zorn M, Blaas D, Fessl F, Volkmann P, Maurer-Fogy I, Pallai PV, Merluzzi VJ, Matteo M, Skern T, Kuechler E.** 1989. Polypeptide 2A of human rhinovirus type 2: identification as a protease and characterization by mutational analysis. Virology **169:**68-77.

18. **Toyoda H, Nicklin MJH, Murray MG, Anderson CW, Dunn JJ, Studier FW, Wimmer E.** 1986. A second virus-encoded proteinase involved in proteolytic processing of poliovirus polyprotein. Cell **45:**761-770.

19. **Voss T, Meyer R, Sommergruber W.** 1995. Spectroscopic characterization of rhinoviral protease 2A: Zn is essential for the structural integrity. Protein Sci **4:**2526-2531.

20. **Martinez-Salas E, Ryan MD.** 2010. Translation and protein processing, p. 141-161. *In* Ehrenfeld E, Domingo E, Roos RP (ed.), The Picornaviruses. ASM Press, Washington D.C.

21. **Gamarnik AV, Andino R.** 1998. Switch from translation to RNA replication in a positive-stranded RNA virus. Genes Dev. **12:**2293-2304.

22. **Perera R, Daijogo S, Walter BL, Nguyen JHC, Semler BL.** 2007. Cellular protein modification by poliovirus:the two faces of poly(rC)-binding protein. J. Virol. **81:**8919-8932.

23. **Bienz K, Egger D, Rasser Y, Bossart W.** 1983. Intracellular distribution of poliovirus proteins and the induction of virus-specific cytoplasmic structures. Virology **131:**39-48.

24. **Bienz K, Egger D, Troxler M, Pasamontes L.** 1990. Structural organization of poliovirus RNA replication is mediated by viral proteins of the P2 genomic region. J.Virol. **64:**1156-1163.

25. **Aldabe R, Barco A, Carrasco L.** 1996. Membrane permeabilizations by poliovirus proteins 2B and 2BC. J.Biol.Chem. **271:**23134-23137.

26. **Doedens JR, Kirkegaard K.** 1995. Inhibition of cellular protein secretion by poliovirus proteins 2B and 3A. EMBO J. **14:**894-907.

27. **Paul AK, Cao X, Harris KS, Lama J, Wimmer E.** 1994. Studies with poliovirus polymerase 3D. J.Biol.Chem. **269:**29173-29181.

28. **Cui T, Sankar S, Porter AG.** 1993. Binding of encephalomyocarditis virus RNA polymerase to the 3'-noncoding region of the viral RNA is specific and requires the 3'-poly(A) tail. J.Biol.Chem. **268:**1-6.

29. **Flanegan JB, Tobin GJ, Oberste MS, Morasco BJ, Young DC, Collis PS.** 1990. Mechanisms of poliovirus negative-strand RNA synthesis and the self-catalyzed covalent linkage of VPg to RNA, p. 55-60. *In* Brinton MA, Heinz FX (ed.), New Aspects of Positive Strand Viruses. American Society for Microbiology, Washington D.C.

30. **Baltimore D, Girard M.** 1966. An intermediate in synthesis of poliovirus RNA. Proc.Natl.Acad.Sci.U.S.A. **56:**741-748.

31. **Rueckert RR.** 1996. *Picornaviridae:* The viruses and their replication., p. 609-654. *In* Fields BN, Knipe DM, Howley PM (ed.), Fields Virology, 3 ed. Raven Publishers, Philadelphia.

32. **Flanegan JB, Pettersson RF, Ambros V, Hewlett MJ, Baltimore D.** 1977. Covalent linkage of a protein to a defined nucleotide sequence at the 5' terminus of the virion and replicative intermediate RNAs of poliovirus. Proc.Natl.Acad.Sci.U.S.A. **74:**961-965.

33. **Adler CJ, Elzinga M, Wimmer E.** 1983. The genome-linked protein of picornaviruses. VII. Complete amino acid sequence of poliovirus VPg and carboxyterminal analysis of its precursor, P3-9. J.Gen.Virol. **64:**349-355.

34. **Paul AV, Rieder E, Kim DW, van Boom JH, Wimmer E.** 2000. Identification of an RNA hairpin in poliovirus RNA that serves as the primary template in the in vitro uridylylation of VPg. J.Virol. **74:**10359-10370.

35. **Reider E, Paul AV, Kim DW, van Boom JH, Wimmer E.** 2000. Genetic and biochemical studies of poliovirus cis-acting replication element cre in relation to VPg uridylylation. J.Virol. **74:**10371-10380.

36. **Philipps A, Dauber M, Groth M, Schirrmeier H, Platzer M, Krumbholz A, Wutzler P, Zell R.** 2012. Isolation and molecular characterization of a second serotype of the encephalomyocarditis virus. Vet Microbiol. **161:**49-57.

37. **Bodewes R, Ruiz-Gonzalez A, Schapendonk CME, van den Brand JMA, Oserhaus ADME, Smits SL.** 2014. Viral metagenomics analysis of feces of wild small carnivores Virology J. **11:**1-13.

38. **Carocci M, Bakkali-Kassimi L.** 2012. The encephalomyocarditic virus. Virulence **3:**351-367.

39. **Scraba DG, Palmenberg AC.** 1999. Cardioviruses (Picornaviridae), p. 1-10, The Encyclopedia of Viruses. Academic Press.

40. **Duke GM, Palmenberg AC.** 1989. Cloning and synthesis of infectious cardiovirus RNAs containing short, discrete poly(C) tracts. J.Virol. **63:**1822-1826.

41. **Michiels T, Dejong V, Rodrigus R, Shaw-Jackson C.** 1997. Protein 2A is not required for Theiler's virus replication. J.Virol. **71:**9549-9556.

42. **Huber SA.** 1994. VCAM-1 is a receptor for encephalomyocarditis virus on a murine vascular endothelial cells. J.Virol. **68:**3453-3458.

43. **Jin YM, Pardoe IV, Burness ATH, Michalak TI.** 1994. Identification of the cell surface 70 kD sialoglycoprotein(s) as a candidate receptor for encephalomyocarditis virus. J.Virol. **68:**7308-7319.

44. **Hahn H, Palmenberg AC.** 2001. Deletion mapping of the encephalomyocarditis virus 2A protein and the adjacent primary cleavage site. J.Virol. **75:**7215-7218.

45. **Groppo R, Brown BA, Palmenberg AC.** 2011. Mutational analysis of EMCV 2A protein identifies a nuclear localization signal and an eIF4E binding site. Virology **410:**257-267.

46. **Svitkin YV, Hahn H, Gingras AC, Palmenberg AC, Sonenberg N.** 1998. Rapamycin and wortmannin enhance replication of a defective encephalomyocarditis virus. J.Virol. **72:**5811-5819.

47. **Groppo R, Palmenberg A.** 2007. Cardiovirus 2A protein associates with 40S but not 80S ribosome subunits during infection. J. Virol. **81:**13067-13074.

48. **Petty RV, Basta HA, Bacot-Davis VR, Brown BA, Palmenberg AC.** 2014. Binding interactions between the encephalomyocarditis virus leader and protein 2A. J.Virol. **88:**13503-13509.

49. **Carocci M, Cordonnier N, Huet H, Romey A, Relmy A, Gorna K, Blaise-Boisseau S, Zientara S, Kassimi LB.** 2011. Encephalomyocarditis virus 2A protein is required for viral pathogenesis and inhibition of apoptosis. J.Virol. **85:**10741-10754.

50. **Son KN, Liang Z, Lipton HL.** 2013. Mutation of the Theiler's virus leader protein zinc-finger domain impairs apoptotic activity in murine macrophages. Virus Res. **177:**222-225.

51. **Chen H-H, Kong W-P, Roos RP.** 1995. The leader peptide of Theiler's murine encephalomyelitis virus is a zinc-binding protein. J.Virol. **69:**8076-8078.

52. **Dvorak CMT, Hall DJ, Hill M, Riddle M, Pranter A, Dillman J, Deibel M, Palmenberg AC.** 2001. Leader protein of encephalomyocarditis virus binds zinc, is phosphorylated during viral infection and affects the efficiency of genome translation. Virology **290:**261-271.

53. **Bacot-Davis VR, Palmenberg AC.** 2013. Encephalomyocarditis virus Leader protein hinge domain is responsible for interactions with Ran GTPase. Virology **443:**177-185.

54. **Brahic M, Stroop WG, Baringer JR.** 1981. Theiler's virus persists in glial cells during demyelinating disease. Cell **26:**123-128.
55. **Lipton HL.** 1976. Theiler's virus-induced demyelination: prevention by immunosuppression. Science **192:**62-64.
56. **van Pesch V, van Eyll O, Michiels T.** 2001. The leader protein of Theiler's virus inhibits immediate-early alpha/beta interferon production J.Virol. **75:**7811-7817.
57. **Zoll J, Melchers WJ, Galama JM, van Kuppeveld FJ.** 2002. The mengovirus leader protein suppresses alpha/beta interferon production by inhibition of the iron/ferritin-mediated activation of NF-kappa B. J.Virol **76:**9664-9672.
58. **Zoll J, Galama JMD, van Kuppeveld FJM, Melchers WJG.** 1996. Mengovirus leader is involved in the inhibition of host cell protein synthesis. J.Virol. **70:**4948-4958.
59. **Hoffman MA, Palmenberg AC.** 1996. Revertant analysis of J-K mutations in the encephalomyocarditis virus internal ribosomal entry site detects an altered leader protein. J.Virol. **70:**6425-6430.
60. **Delhaye S, van Pesch V, Michiels T.** 2004. The leader protein of Theiler's virus interferes with nucleocytoplasmic trafficking of cellular proteins. J.Virol. **78:**4357-4362.
61. **Paul S, Michiels T.** 2006. Cardiovirus leader proteins are functionally interchangeable and have evolved to adapt to virus replication fitness. J. Gen. Virol **87:**1237-1246.
62. **Hato SV, Ricour C, Schulte BM, Lanke KH, de Bruijni M, Zoll J, Melchers WJ, Michiels T, van Kuppeveld FJ.** 2007. The mengovirus leader protein blocks interferon-alpha/beta gene transcription and inhibits activation of interferon regulatory factor 3. Cell Microbiol **9:**2921-2930.
63. **Basta HA, Bacot-Davis VR, Ciomperlik JJ, Palmenberg AC.** 2014. Encephalomyocarditis virus Leader is phosphorylated by CK2 and syk as a requirement for subsequent phosphorylation of cellular nucleoporins. J.Virol. **88:**2219-2226.
64. **Basta HA, Palmenberg AC.** 2014. AMP-activated protein kinase phosphorylates EMCV, TMEV, and SafV Leader proteins at different sites. Virology **262:**236-240.
65. **Gustin KE, Sarnow P.** 2002. Inhibition of nuclear import and alteration of nuclear pore complex composition by rhinovirus. J. Virol. **76:**8787-8796.
66. **Gustin KE, Sarnow P.** 2001. Effects of poliovirus infection on nucleo-cytoplasmic trafficking and nuclear pore complex composition. EMBO J. **20:**240-249.
67. **Gustin KE.** 2003. Inhibition of nucleo-cytoplasmic trafficking by RNA viruses: targeting the nuclear pore complex. Virus Res. **95:**35-44.
68. **Watters K, Palmenberg A.** 2011. Differential processing of nuclear pore complex proteins by rhinovirus 2A proteases from different species and serotypes. J.Virol. **85:**10874-10883.
69. **Watters K, Inankur B, Warrick J, Sherer NM, Yin J, Palmenberg A.** 2015. Differential disruption of nucleocytoplasmic trafficking by rhinovirus 2A proteases. Mol.Biol. of Cell **submitted**.
70. **Lidsky PL, Hato S, Bardina MV, Aminev AG, Palmenberg AC, Sheval EV, Polyakov VY, van Kuppeveld FJ, Agol V.** 2006. Nucleo-cytoplasmic traffic disorder induced by cardioviruses. J.Virol. **80:**2705-2717.
71. **Bardina MV, Lidsky P, Sheval EV, Fominykh KV, van Kuppeveld FJ, Polyakov VY, Agol V.** 2009. Mengovirus-induced rearrangements of the nuclear pore complex: Hijacking cellular phosphorylation machinery. J.Virol. **83:**3150-3161.
72. **Ciomperlik JJ, Basta HA, Palmenberg AC.** Three cardiovascular leader proteins equivalently inhibit four different nucleocytoplasmic trafficking pathways.
73. **Porter FW, Palmenberg AC.** 2009. Leader-induced phosphorylation of nucleoporins correlates with nuclear trafficking inhibition of cardioviruses. J.Virol **83:**1941-1951.

74. **Porter FW, Bochkov YA, Albee AJ, Wiese C, Palmenberg AC.** 2006. A picornavirus protein interacts with Ran-GTPase and disrupts nucleocytoplasmic transport. Proc Natl Acad Sci USA **103:**12417-12422

75. **Porter FW, Brown B, Palmenberg A.** 2010. Nucleoporin phosphorylation triggered by the encephalomyocarditis virus leader protein is mediated by mitogen-activated protein kinases. J.Virol. **84:**12538-12548.

76. **Sorgeloos F, Vertommen D, Rider M, Michiels T.** 2011. Theiler's virus L* protein is targetd to the mitochondrial outer membrane. J. Virol. **85:**3690-3694.

77. **Petty RV, Palmenberg AC.** 2013. Guanine-nucleotide exchange factor RCC1 facilitates a tight binding between EMCV Leader and cellular Ran GTPase. J. Virol. **87:**6517-6520.

78. **Bacot-Davis VR, Ciomperlik JJ, Cornilescu CC, Basta HA, Palmenberg AC.** 2014. Solution structures of Mengovirus leader protein, its phosphorylated derivatives, and in complex with RanGTPase. Proc Natl Acad Sci USA **111:**15792-15797.

79. **Romanova L, Lidsky P, Kolesnikova M, Fominykh KV, Gmyl AP, Sheval EV, Hato SV, van Kuppeveld FJ, Agol V.** 2009. Antiapoptotic activity of the cardiovirus leader protein, a viral "security" protein. J.Virol. **83:**7273-7284.

80. **Borghese F, Michiels T.** 2011. The leader protein of cardioviruses inhibits stress granule assembly. J. Virol. **85:**9614-9622.

81. **van Eyll O, Michiels T.** 2000. Influence of the Theiler's virus L* protein on macrophage infection, viral persistence, and neurovirulence. J.Virol. **74:**9071-9077.

82. **Gorlich D, Mattaj IW.** 1996. Nucleocytoplasmic transport Science **271:**1513-1518.

83. **Wente SR, Rout MP.** 2010. The nuclear pore complex and nuclear transport. Cold Spring Harb Perspect Biol **2:**1-19.

84. **Devos D, Dokudovskaya S, Williams R, Alber F, Eswar J, Chait BT, Rout MP, Sali A.** 2006. Simple fold composition and modular architecture of the nuclear pore complex. PNAS **103:**2172-2177.

85. **Devos D, Dokudovskaya S, Alber F, Williams R, Chait BT, Sali A, Rout MP.** 2004. Components of coated vesicles and nuclear pore complexes share a common molecular architecture. PLoS Biol **2:**e380. Epub 2004 Nov 2002.

86. **Miller MW, Caracciolo MR, Berlin WK, Hanover JA.** 1999. Phosphorylation and glycosylation of nucleoporins. Arch. Biochem. Biophys. **367:**51-60.

87. **Feldherr CM, Akin D.** 1997. The location of the transport gate in the nuclear pore complex. J. Cell Sci. **110:**3065-3070.

88. **Keminer O, Peters R.** 1999. Permeability of single nuclear pores. Biophysical J. **77:**217-228.

89. **Pante N, Kann M.** 2002. Nuclear pore complex is able to transport macromolecules with diameters of ~39 nm. Mol Biol Cell. **13:**425-434.

90. **Mehlin H, Daneholt B, Skoglund U.** 1992. Translocation of a specific premessenger ribonucleoprotein particle through the nuclear pore studied with electron microscope tomography Cell **69:**605-613.

91. **Andrade MA, Bork P.** 1995. HEAT repeats in the Huntington's disease protein. Nat Genet **11:**115-116.

92. **Cook A, Bono F, Jinek M, Conti E.** 2007. Structural biology of nucleocytoplasmic transport. Annu Rev Biochem. **76:**647-671.

93. **Pemberton LF, Paschal BM.** 2005. Mechanisms of receptor-mediated nuclear import and nuclear export. Traffic **6:**187-198.

94. **Azuma Y, Renault L, Garcia-Ranea JA, Valencia A, Nishimoto T, Wittinghofer A.** 1999. Model of the Ran-RCC1 interaction using biochemical and docking experiments. J. Mol. Biol. **289:**1119-1130.

95. **Bischoff FR, Gorlich D.** 1997. RanBP1 is crucial for the release of RanGTP from imporin beta-related nuclear transport factors. FEBS Lett. **419:**249-254.

96. **Floer M, Blobel G, Rexach M.** 1997. Disassembly of RanGTP-karyopherin beta complex, an intermediate in nuclear protein import. J Biol Chem. **272:**19538-19546.

97. **Lounsbury KM, Richards SA, Carey KL, Macara IG.** 1996. Mutations within the Ran/TC4 GTPase. Effects on regulatory factor interactions and subcellular localization. J. Biol. Chem. **271:**32834-32841.

98. **Rexach M, Blobel G.** 1995. Protein import into nuclei: association and dissociation reactions involving transport substrate,transport factors and nucleoporins. Cell **83**.

99. **Gorlich D, Pante N, Kutay U, Aebi U, Bischoff FR.** 1996. Identification of different roles for RanGDP and RanGTP in nuclear protein import. EMBO J **15:**5584-5594.

100. **Kutay U, Bischoff FR, Kostka S, Kraft R, Gorlich D.** 1997. Export of importin α from the nucleus is mediated by a specific nuclear transport factor. Cell **90:**1061-1071.

101. **Fornerod M, Ohno M, Yoshida M, Mattaj IW.** 1997. CRM1 is an export receptor for leucine rich nuclear export signals. Cell **90:**1051-1060.

102. **Fried H, Kutay U.** 2003. Nucleocytoplasmic transport: taking an inventory. Cellular and Molecular Life Sciences **60:**1659-1688.

103. **Jakel S, Gorlich D.** 1998. Importin β, transportin, RanBP5 and RanBP7 mediate nuclear import of ribosomal proteins in mammalian cells. EMBO **17:**4491-4502.

104. **Monecke T, Guttler T, Neumann P, Dickmanns A, Gorlich D, Ficner R.** 2009. Crystal Structure of the nuclear Export Receptor CRM1 in Complex with Snurportin 1 and RanGTP. Science **324:**1087-1091.

105. **Guttler T, Gorlich D.** 2011. Ran-dependent nuclear export mediators: a structural perspective. EMBO J. **30:**3457-3474.

106. **Mingot JM, Kostka S, Kraft R, Hartmann E, Gorlich D.** 2001. Importin 13: a novel mediator of nuclear import and export EMBO **20:**3685-3694.

107. **Terry LJ, Wente SR.** 2009. Flexible gates: dynamic topologies and functions for FG nucleoporins in nucleocytoplasmic transport. Eukaryotic Cell **8:**1814-1827.

108. **Ribbeck K, Gorlich D.** 2001. Kinetic analysis of translocation through nuclear pore complexes. EMBO **20:**1320-1330.

109. **Ryan KJ, Wente SR.** 2000. The nuclear pore complex: a protein machine bridging the nucleus and cytoplasm. Curr Opin Cell Biol **12:**361-371.

110. **Rout MP, Aitchison JD, Magnasco MO, Chait BT.** 2003. Virtual gating and nuclear transport: the hole picture. Trends. Cell Bio. **13:**622-628.

111. **Lim RYH, Huang NP, Koser J, Deng J, Lau KHA, Schwarz-Herion K, Fahrenkrog B, Aebi U.** 2006. Flexible phenylalanine-gylcine nucleoporins as entropic barriers to nucleocytoplasmic trasnport. PNAS **103:**9512-9517.

112. **Patel SS, Belmont BJ, Sante JM, Rexach MF.** 2007. Natively unfolded nucleoporins gate protein diffusion across the nuclear pore complex. Cell **129**.

113. **Frey S, Gorlich D.** 2007. A saturated FG-repeat hydrogel can reproduce the permeability properties of nuclear pore complexes Cell **130:**512-523.

114. **Bestembayeva A, Kramer A, Labokha AA, Osmanovic D, Liashkovich I, Orlova EV, Ford IJ, Charas G, Fassati A, Hoogenboom BW.** 2015. Nanoscale stiffness topography reveals structure and mechanics of the transport barrier in intact nuclear pore complexes. Nat. Nanotechnol. **10:**60-64.

115. **Laurell E, Beck K, Krupina KA, Theerthagiri G, Bodenmiller B, Horvath P, Aebersold R, Antonin W, Kutay U.** 2011. Phosphorylation of Nup98 by mutiple kinases is crucial for NPC disassembly during mitotic entry. Cell Bio **144:**539-550.

116. **Onischenko EA, Gubanova NV, Kiseleva EV, Hallberg E.** 2005. CDK1 and okadaic acid-sensitive phosphatases control assembly of nuclear pore complexes in drosophila embryos. Mol. Biol. Cell **16:**5152-5162.

117. **Kehlenbach RH, Gerace L.** 2000. Phosphorylation of the nuclear transport machinery down-regulates nuclear protein import in vitro. J. Biol. Chem. **275:**17848-17856.

118. **Kodiha M, Crampton N, Shrivastava S, Umar R, Stochaj U.** 2010. Traffic control at the nuclear pore. Nucleus **1:**237-244.

119. **Crampton N, Kodiha M, Shrivastava S, Umar R, Stochaj U.** 2009. Oxidative stress inhibits nuclear protein export by multiple mechanisms that target FG nucleoporins and Crm 1. Mol Biol Cell **20:**5106-5116.

120. **Kosako H, Yamaguchi N, Aranami C, Ushiyama M, Kose S, Imamoto N, Taniguchi H, Nishida E, Hattori S.** 2009. Phosphoproteomics reveals new ERK MAP kinase targets and links ERK to nucleoporin-mediated nuclear transport. Nat Struct Mol Biol. **16:**1026-1035.

121. **Manning G, Whyte DB, Martinez R, Hunter T, Sudarsanam S.** 2002. The protein kinase complement of the human genome Science **298:**1912-1934.

122. **Roux PP, Blenis J.** 2004. ERK and p38 MAPK-activated protein kinases: a family of protein kinases with diverse biological functions. Microbiol Mol Biol Rev **68:**320-344.

123. **Cargnello M, Roux PP.** 2011. Activation and function of the MAPKs and their substrates, the MAPK-activated protein kinases. Microbio. Mol. Bio. Reviews **75:**50-83.

124. **Pearson G, Robinson F, Beers Gibson T, Xu BE, Karandikar M, Berman K, Cobb MH.** 2001. Mitogen-activated protein (MAP) kinase pathways: regulation and physiological functions. Endocr Rev. **22:**153-183.

125. **Grewal S, Molina DM, Bardwell L.** 2006. Mitogen-activated protein kinase (MAPK)-docking sites in MAPK kinases function as tether that are crucial for MAPK regulation in vivo Cell Signal **18:**123-134.

126. **Caunt CJ, McArdle CA.** 2010. Stimulus-induced uncoupling of extracellular signal-regulated kinase phosphorylation from nuclear localization is dependent on docking domain interactions. J Cell Sci. **123:**4310-4320.

127. **Yoon S, Seger R.** 2006. The extracellular signal-regulated kinase: multiple substrates regulate diverse cellular functions. Growth Factors **24:**21-44.

128. **Matsubayashi Y, Fukuda M, Nishida E.** 2001. Evidence for existence of a nuclear pore complex-mediated, cytosol-independent pathway of nuclear translocation of ERK MAP kinase in permeabilized cells. J. Bio. Chem. **276:**41755-41760.

129. **Whitehurst A, Wilsbacher JL, You Y, Luby-Phelps K, Moore MS, Cobb MH.** 2002. ERK2 enters the nucleus by a carrier-independent mechanism. PNAS **99:**7496-7501.

130. **Boulton TG, Nye SH, Robbins DJ, Ip NY, Radziejewska E, Morgenbesser SD, DePinho RA, Panayotatos N, Cobb MH, Yancopoulos GD.** 1991. ERKs: a family of protein-serine/threonine kinases that are activated and tyrosine phosphorylated in response to insulin and NGF. Cell **65:**663-675.

131. **Sontag E, Fedorov S, Kamibayashi C, Robbins D, Cobb M, Mumby M.** 1993. The interaction of SV40 small tumor antigen with protein phosphatase 2A stimulates the map kinase pathway and induces cell proliferation. Cell **75:**887-897.

132. **Alessi DR, Cuenda A, Cohen P, Dudley DT, Saltiel AR.** 1995. PD 098059 is a specific inhibitor of the activation of mitogen-activated protein kinase kinase in vitro and in vivo. J. Bio. Chem. **270:**27489-27494.

133. **Favata MF, Horiuchi KY, Manos EJ, Daulerio AJ, Stradley DA, Feeser WS, Van Dyk DE, Pitts WJ, Earl RA, Hobbs F, Copeland RA, Magolda RL, Scherle PA.** 1998. Identification of a novel inhibitor of mitogen-activated protein kinase kinase. J. Biol. Chem, **273:**18623-18632.

134. **Leighton IA, Dalby KN, Caudwell FB, Cohen PTW, Cohen P.** 1995. Comparison of the specificities of p70 S6 kinase and MAPKAP kinase-1 identifies a relatively specific substrate for p70 S6 kinase: the N-terminal kinase domain of MAPKAP kinase-1 is essential for peptide phosphorylation. FEBS **375:**289-293.

135. **Kodiha M, Tran D, Morogan A, Qian C, Stochaj U.** 2009. Dissecting the signaling events that impact classical nuclear import and target nuclear transport factors. PLoSOne **4:**e8420. doi: 8410.1371/journal.pone.0008420.

136. **Enslen H, Brancho DM, Davis RJ.** 2000. Molecular determinants that mediate selective activation of p38 MAP kinase isoforms. EMBO **19:**1301-1311.

137. **Kim C, Sano Y, Todorova K, Carlson BA, Arpa L, Celada A, Lawrence T, Otsu K, Brissette JL, Arthur JSC, Park JO.** 2008. The kinase p38α serves cell type-specific inflammatory functions in skin injury and coordinates pro- and anti-inflammatory gene expression Nature Immunology **9:**1019-1027.

138. **Thornton TM, Rincon M.** 2009. Non-classical p38 map kinase functions: cell cycle checkpoints and survival Int. J. Biol. Si. **5:**44-52.

139. **Lee JC, Laydon JT, McDonnell PC, Gallagher TF, Kumar S, Green D, McNulty D, Blumenthal MJ, Heys JR, Landvatter SW, Strickler JE, McLaughlin MM, Siemens IR, Fisher SM, Livi GP, White JR, Adams JL, Young PR.** 1994. A protein kinase involved in the regulation of inflammatory cytokine biosynthesis. Nature Immunology **372:**739-746.

140. **Regan J, Breitfelder S, Cirillo P, Gilmore T, Graham AG, Hickey E, Klaus B, Madwed J, Moriak M, Moss N, Pargellis C, Pav S, Proto A, Swinamer A, Tong L, Torcellini C.** 2002. Pyrazole urea-based inhibitors of p38 MAP kinase: from lead compound to clinical candidate. J. Med. Chem. **45:**2994-3008.

141. **Liu Q, Hofmann PA.** 2004. Protein phosphatase 2a-mediated cross-talk between p38 MAPK and ERK in apoptosis of cardiac myocytes. Am. Journal of Physiology - Heart and Circulatory Physiology **286:**2204-2212.

142. **Waskiewicz AJ, Flynn A, Proud CG, Cooper JA.** 1997. Mitogen-activated protein kinases activate the serine/threonine kinases Mnk1 and Mnk2. EMBO **16:**1909-1920.

143. **Deak M, Clifton AD, Lucocq JM, Alessi DR.** 1998. Mitogen- and stess-activated protein kinase-1 (Msk1) is directly activated by MAPK and SAPK2/p38, and may mediate activation of CREB. EMBO **17:**4426-4441.

144. **Ahn NG.** 2009. PORE-ing over ERK substrates. Nat Struc Mol Biol. **16:**1004-1005.

145. **Lee T, Hoofnagle AN, Kabuyama Y, Stroud J, Min X, Goldsmith EJ, Chen L, Resing KA, Ahn NG.** 2004. Docking motif interactions in MAP kinases revealed by hydrogen exchange mass spectrometry. Mol Cell **14:**43-55.

146. **Faustino RS, Maddaford TG, Pierce GN.** 2011. Mitogen activated protein kinase at the nuclear pore complex. J. Cell. Mol. Med **15:**928-937.

147. **Jones MS, Lukashov VV, Ganac RD, Schnurr DP.** 2007. Discovery of a novel human picornavirus in a stool sample from a pediatric patient presenting with fever of unknown origin. J. Clin. Microbiol. **45:**2144-2150.

148. **Her L-S, Lund E, Dahlberg JE.** 1997. Inhibition of Ran guanosine triphosphatase-dependent nuclear transport by the matrix protein of vesicular stomatitis virus. Science **276:**1845-1848.

149. **Faria PA, Chakraborty P, Levay A, Barber GN, Ezelle HJ, Enninga J, Arana C, van Deursen J, Fontoura BM.** 2005. VSV disrupts the Rae1/mrnp41 mRNA nuclear export pathway. Mol Cell **17:**93-102.

150. **Ricour C, Borghese F, Sorgeloos F, Hato SV, van Kuppeveld FJ, Michiels T.** 2009. Random mutagenesis defines a domain of Theiler's virus leader protein that is essential for antagonism of nucleocytoplasmic trafficking and cytokine gene expression. J.Virol. **83:**11223-11232.

151. **Le Sage V, Mouland AJ.** 2013. Viral subversion of the nuclear pore complex. Viruses **5:**2019-2042.

152. **Ricour C, Delhaye S, Hato SV, Olenyik TD, Michel B, van Kuppeveld FJ, Gustin KE, Michiels T.** 2009. Inhibition of mRNA export and dimerization of interferon regulatory factor 3 by Theiler's virus leader protein. J.Gen.Virol **90:**177-186.

153. **Fagerlund R, Kinnuen L, Kohler M, Julkunen I, Melen K.** 2005. NF-kappa B is transported into the nucleus by importin alpha3 and importin alpha4. J. Biol. Chem. **280:**15942-15951.

154. **Kumar KP, McBride KM, Weaver BK, Dingwall C, Reich NC.** 2000. Regulated nuclear-cytoplasmic localization of interferon Regulatory Factor 3, a subunit of double stranded RNA-Activaed Factor 1. Mol and Cell Biol. **20:**4159-4168.

155. **McBride KM, Banninger G, C. M, Reich NC.** 2002. Regulated nuclear import of the STAT1 transcription factor by direct binding of importin-alpha. EMBO **21:**1754-1763.

156. **Kataoka N, Bachorik JL, Dreyfuss G.** 1999. Transportin-SR, a nuclear import receptor for SR proteins. J. Cell Biol. **145:**1145-1152.

157. **Pollard VW, Michael WM, Nakielny S, Siomi MC, Wang F, Dreyfuss G.** 1996. A novel receptor-mediated nuclear protein import pathway. Cell **86:**985-994.

158. **Wen W, Meinkotht JL, Tsein RY, Taylor SS.** 1995. Identification of a signal for rapid export of proteins from the nucleus. Cell **82:**463-473.

159. **Cohen P, Holmes CFB, Tsukitani Y.** 1990. Okadaic acid: a new probe for the study of cellular regulation. Trends Biochem Sci **15:**92-102.

160. **Ho DT, Shayan H, Murphy TH.** 1997. Okadaic acid induces hyperphosphorylation of tau independently of mitogen-activated protein kinase activation. J. Neurochem. **68:**106-111.

161. **Adam EJH, Adam SA.** 1994. Identification of cytosolic factors required for nuclear location sequence-mediated binding to the nuclear envelope. J. Cell Biol. **125:**547-555.

162. **Gorlich D, Vogel F, Mills AD, Hartmann E, Laskey RA.** 1995. Distinct functions for the two importin subunits in nuclear protein import. Nature **377:**246-248.

163. **Moroianu J, Hijikata M, Blobel G, Radu A.** 1995. Mammalian karyopherin alpha 1 beta and alpha 2 beta heterodimers; alpha 1 or alpha 2 subunit binds nuclear localization signal and beta subunit interacts with peptide repeat-containing nucleoporins. Proc Natl Acad Sci U S A **92:**6532-6536.

164. **Hedley ML, Amrein H, Maniatis T.** 1995. An amino acid sequence motif sufficient for subnuclear localization of an arginine/serine-rich splicing factor. Proc Natl Acad Sci U S A **92:**11524-11528.

165. **Lai MC, Lin RI, Tarn WY.** 2001. Transportin-SR2 mediates nuclear import of phosphorylated SR proteins. Proc Natl Acad Sci U S A **98:**10154-10159.

166. **Fischer U, Huber J, Boelens WC, Mattaj IW, Luhrmann R.** 1995. The HIV-1 Rev activation domain is a nuclear export signal that accesses an export pathway used by specific cellular RNAs. Cell **82:**475-483.

167. **Zehorai E, Yao Z, Plotnikov A, Seger R.** 2010. The subcellular localiation of MEK and ERK--a novel translocation signal (NTS) paves a way to the nucleus. Mol Cell Endocrinol. **314:**213-220.

168. **Yaseen NR, Blobel G.** 1997. Cloning and characterization of human karyopherin β3. Proc Natl Acad Sci U S A **94:**4451-4456.

169. **Sheehy AM, Gaddis NC, Choi JD, Malim MH.** 2002. Isolation of a human gene that inhibits HIV-1 infection as is supressed by the viral Vif protein. Nature **418:**646-650.

170. **Mili S, Shu HJ, Zhao Y, Pinol-Roma S.** 2001. Distinct RNP complexes of shuttling hnRNP proteins with pre-mRNA and mRNA: Candidate intermediates in formation and export of mRNA. Mol. Cell Biol. **21:**7307-7319.

171. **Hahn H, Palmenberg AC.** 1995. Encephalomyocarditis viruses with short poly(C) tracts are more virulent than their Mengo virus counterparts. J.Virol. **69:**2697-2699.

172. **Nakielny S, Dreyfuss G.** 1999. Transport of proteins and RNAs in and out of nucleus. Cell **99:**677-690.

173. **Cornilescu CC, Porter FW, Zhao Q, Palmenberg AC, Markley JL.** 2008. NMR structure of the Mengovirus leader protein zinc-finger domain. FEBS Letters **582:**896-900.

174. **Hutten S, Kehlenbach RH.** 2006. Nup214 is required for CRM1-dependent nuclear protein export in vivo. Mol and Cell Biol. **26:**6772-6785.

175. **Wu ZM, Jiang Q, Clarke PR, Zhang C.** 2013. Phosphorylation of Crm1 by CDK1-cyclin-B promotes Ran-dependent mitotic spindle assembly. Journal of Cell Science **126:**3417-3228.

176. **Hamamoto T, Seto H, Beppu T.** 1983. Leptomycins A and B, new antifungal antibiotics. II. Structure and elucidation. The Journal of Antibiotics **36:**646-650.

177. **Sun Q, Carrasco YP, Hu Y, Guo X, Mirzaei H, Macmillan J, Chook YM.** 2012. Nuclear export inhibition through covalent conjugation and hydrolysis of Leptomycin B by CRM1. PNAS **110:**1303-1308.

178. **Guttler T, Madl T, Neumann P, Deichsel D, Corsini L, Monecke T, Ficner R, Sattler M, Gorlich D.** 2010. NES consensus redefined by structures of PKI-type and Rev-type nuclear export signals bound to CRM1. Nat Struct Mol Biol. **17:**1367-1376.

179. **Atasheva S, Fish A, Fornerod M, Frolova EI.** 2010. Venezuelan equine Encephalitis virus capsid protein forms a tetrameric complex with CRM1 and importin alpha/beta that obstructs nuclear pore complex function. J.Virol. **84:**4158-4171.

180. **Rajani KR, Pettit Kneller EL, McKenzie MO, Horita DA, Chou JW, Lyles DS.** 2012. Complexes of vesicular stomatitis virus matrix protein with host Rae1 and Nup98 involved in inhibition of host transcription. PLoS Pathog. **8:**e1002929.

181. **Park N, Katikaneni P, Skern T, Gustin KE.** 2008. Differential targeting of nuclear pore complex protein in poliovirus-infected cells. J.Virol. **82:**1647-1655.

182. **Park N, Skern T, Gustin KE.** 2010. Specific cleavge of the nuclear pore complex protein Nup62 by a viral protease. J. Biol. Chem. **285:**28796-28805.

183. **Hato SV, Sorgeloos F, Ricour C, Zoll J, Melchers WJ, Michiels T, Kuppeveld FJv.** 2010. Differential IFN-alpha/beta production suppressing capacities of the leader proteins of mengovirus and food-and-mouth disease virus. Cell Microbiol **12:**310-317.

184. **Davies SP, Reddy H, Caivano M, Cohen P.** 2000. Specificity and mechanism of action of some commonly used protein kinase inhibitors. Biochem J **351:**95-105.

185. **Macaulay C, Meier E, Forbes DJ.** 1995. Differential mitotic phosphorylation of proteins of the nuclear pore complex. J Biol Chem **270:**254-262.

186. **Sorgeloos F, Vertommen D, Rider M, Michiels T.** 2014. Modulation of downstream effectors of the Ras/ERK MAPK pathway by Theiler's virus leader protein.

187. **de Souza CA, Osmani AH, Hashmi SB, Osmani SA.** 2004. Partial Nuclear Pore Complex Disassembly during Closed Mitosis in Aspergillus nidulans. Curr Biol **14:**1973-1984.

188. **Lusk CP, Waller DD, Makhnevych T, Dienemann A, Whiteway M, Thomas DY, Wozniak RW.** 2007. Nup53p is a target of two mitotic kinases, Cdk1p and Hrr25p. Traffic **8:**647-660.

189. **Pelech S.** 2006. Dimerization in protein kinase signaling. J Biol. **5:**12.

190. **Adachi M, Fukuda M, Nishida E.** 2000. Nuclear export of MAP kinase (ERK) involves a MAP kinase kinase (MEK)-dependent active transport mechanism. J Cel Biol. **148:**849-856.

191. **Catalanotti F, Reyes G, Jesenberger V, Galabova-Kovacs G, de Matos Simoes R, Carugo O, Baccarini M.** 2009. A Mek1–Mek2 heterodimer determines the strength and duration of the Erk signal. Nat Struc Mol Biol. **16:**294-303.

192. **Lidke DS, Huang F, Post JN, Rieger B, Wilsbacher J, THomas JK, Pouyssegur J, Jovin TM, Lenormand P.** 2010. ERK nuclear translocation is dimerization-independent but controlled by the rate of phosphorylation. J Biol Chem **285:**3092-3102.

193. **Khokhlatchev AV, Canagarajah B, Wilsbacher J, Robinson M, Atkinson M, Goldsmith E, Cobb MH.** 1998. Phosphorylation of the MAP kinase ERK2 promotes its homodimerization and nuclear translocation. Cell **93:**605-615.

194. **Roux PP, Richards SA, Blenis J.** 2003. Phosphorylation of p90 ribosomal S6 kinase (RSK) regulates extracellular signal-regulated kinase docking and RSK activity Mol and Cell Biol. **23:**4796-4804.

195. **Richards SA, Fu J, Romanelli A, Shimamura A, Blenis J.** 1999. Ribosomal S6 kinase 1 (RSK1) activation requires signals dependent on and independent of the MAP kinase ERK. Curr Biol **9:**810-820.

196. **Yarbrough ML, Mata MA, Sakthivel R, Fontoura BM.** 2014. Viral subversion of nucleocytoplasmic trafficking. Traffic **15:**127-140.

197. **Amanchy R, Periaswamy B, Mathivanan S, Reddy R, Tattikota SG, Pandey A.** 2007. A curated compendium of phosphorylation motifs. Nature biotechnology **25:**285-286.

198. **Gnad F, Gunawardena J, Mann M.** 2011. PHOSIDA 2011: the posttranslational modification database. Nucleic acids research **39:**D253-D260.